KH98-1 leg.2 Cruise Report

Natural earthquakes in Solomon Arc Region

Shinji Yoneshima *et al.* ← みんなの名前 を書く。

Ocean Research Institute University of Tokyo

1. Solomon Island Arc region

The Solomon Island Arc region (SIA) has a peculiar techtonic feature which cannot be seen in other subduction zones. SIA lies between two oceanic plates: the North Pacific Plate, and India-Australia plate (Figure 1). The North Pacific plate is underlain by the Ontong Java Plateau (OJP) which is the largest plateau in the world. OJP is considered to have begun colliding with SIA about 12 to 10 Ma , and now the collision is still going on. After the beginning of the collision, active subduction zone transferred from that of between OJP and SIA to that of between the India-Australia plate and SIA about 10 Ma. This reversal of active subduction zone resulted in the uplifting of the New Georgia islands group accompanied in the the late Cenozoic. Then, the Woodlark Basin (WLB) was formed prior to 5 Ma, then began spreading southward the New Britain Trench (Taylor, 1987), and is now subducting into the New Britain-San Cristobal subduction zone. It is considered that before the collision of OJP, the Kia-Korigole-Kaipito (KKK) fault zone was once considered to be an active subduction zone between SIA and North-Pacific plate in the early Tertiary (Stanton,1961; Ramsay, 1978, 1982). In the following subsection, we summarize the seismicity of natural earthquakes which can be seen from the global seismological network.

2. Seismicity in SIA

In the SIA region, a large number of natural earthquakes occur especially in the New Briatin Trench subduction zone. Figure 2 shows the NEIC seismicity map from 1990 to 1997. More than 2,000 earthquakes occured during this period in SIA. The radius of circles and the color indicate the scale of magnitude and depth, respectively. This hypocenter map seems to be concistent with the geological techtonics as mentioned above: many events along the subduction between the Solomon Sea plate and SIA, clear hypocenters accompanied with the spreading of the

WLB, some events between India-Australia plate and SIA, and inactive seismicity between OJP and SIA. In this report, we noticed the variety of the seismicity in SIA According to the change of seismicity, we thus devided SIA into five segments and named them Seg. A, B, C, D, and E(Figure 3). In the following, we describe the detail of each segments.

Seg A is consisted of main part of the New Britain island, where west portion of the Solomon Sea plate is in convergence. The cross sectional view of of this segment is shown in Figure 4. The New Britain trench is marked by inversed triangle (shown as NBT). The ratio of Vertical to Horizontal is 1 : 1. The subducting of the Solomon Sea plate is clearly seen. Moreover, the Double Seismic Zone (DSZ) extends from 60 to 170 km depth southward of the NBT (Mcguire and Weins, 1995). Generally, DSZ extends from about several tens of kilometers to one hundred and several tens of kilometers depth, and its upper plane dominates the earthquakes type of down dip compression, and lower plane down dip extension. Although the cause of DSZ has not vailed yet, there are mainly three hypotheses about the existance of DSZ. First, the plate unbending model (Kawakatsu, 1986). Second, Compositional anormally in the lithosphere (Abers, 1992). The last is the phase transformation in the crust (Comte and Suarex, 1994). Moreover, taking a look at focal mechanisms of Harvard CMT catalogue (Figure 5), the focal mechanisms seems to be consistent with the strike of NBT in spite of the oblique subduction. In the outer rise region, the earthquakes of reverse fault type seems to dominate in the shallow depth. Therefore, this region may be approximately an active subduction zone.

Seg. B is the region consisted of Bougainville and West portion of Choiseul Island where the highest seismicity is seen. As shown in seg. A, Solomon Sea plate collides with SIA in seg. B. Despite oblique subduction, the type of earthquakes is dominated by trench-parallel strikes which is also seen in seg. A. Although the seismicity in the outer rise region of this segment seems to be lower than seg. A, large normal fault event occured which cannot seen in seg. A. Moreover, the axis of NBT seems to be turning toward the Solomon Sea. Thus, unclear aspect of subducting slab cannot be seen in the cross sectional view of this segment (Figure 6). In this figure, the Kilinailau trench and the New Britain trench are also shown with filled inverse triangle in Figure 6. In this figure the existance of deep earthquakes is identified

from 400 to 500 km depth. These deep events cannot be constrained which part of plate boundary causes: the North Pacific plate and SIA, or Solomon Sea plate and SIA. Though DSZ does not reported in this segment, there are a lot of earthquakes which are the uniform strike around 50 km depth (Figure 5). One of our main purposes in this OBS study is to investigate whether DSZ exists or not. Along the Kilinailau trench, earthquakes are hardly seen.

Seg. C is the lowest seismicity region because this segment locates at the boundary between Solomon Sea plate and India-Australia plate. The boundary is the Woodlark basin. There occurs some earthquakes which are consistent with plate techtonics in the Woodlark basin: normal fault type event at spreading center, right or left-lateral events at transform fault. The cross sectional view is shown in Figure 7. It is intersting to study seg. C where sudden descending of seismicity occurs compared to seg. B.

Seg. D is consisted of the Santa Isabel, east portion of the New Georgia group, Guadalcanal, and main poriotn of the Malaita island. In this section, we so far did not mentioned the collision of OJP well, because seldom earthquakes are seen in Kilinailau trench or NST except in this segment. Figure 8 shows the cross sectional view of this segment. Filled inverse triangle shows the trench axis. This figure shows the clear plate boundary between the North Pacific plate and SIA until about 200 km depth. However, there is a room for discussing whether the North Pacific plate is on subducting or not. Miura *et al.* (1998) indicated the possibility of the delamination, by investigating the remarkable thickness of sedimentary layer, which is induced from the velocity strucrure model by using OBSs in 1995. Moreover, the seismicity in the shallower part of this segment is much less earthquakes along the plate boundary between the North Pacific plate and SIA if earthquakes around 30 km depth, which does not determined well, are ignored. Then, the focal mechanisms dominates the normal fault type at 50 km depth in Figure 5. The strikes of these events are consistent with that of NST. On the other hand, the aspect of subducting India-Australia plate cannot be seen in Figure 8. The reason why earthquakes along this plate boundary occur restricted in this segment is still unvailed.

Seg. E is the region consisted of a little portion of the Malaita, and the San Cristobal island. There are no earthquakes deeper than 160 km depth. In seg. D and

seg. E, India-Australia plate does not seems to be subducting (Figure 9).

Thus, the seismological characteristics changes drastically due to each segments. Noticable change of seismicity is that of NBT and SCT. The contrasts are: number of earthquakes, the existance of deep earthquakes, active side of the plate boundary. Seg. C is the important segment because the drastic change of the seismicity takes place there.

3. Observation of small-to-moderate earthquakes

In order to study the state of plate boundary, it is very important to investigate small-to-moderate earthquakes, especially when it comes to the study of plate boundaries. The importance of studying plate boundaries has been recognized widely, because focal mechanisms occured along there would represent the stress state of plate boundaries. Hence, some noticable observation are reported about active subduction zones: Double Seismic Zone, Seismic Gap, and so on. These investigation have made by using not only large earthquakes but also small-to-moderate earthquakes. However, because of the sparse distribution of local seismological stations, there are much less research on natural earthquakes occred around SIA region compared to other subduction zones except large earthquakes. Therefore, in order to understand the subduction system in SIA, it is very important to study small-to-moderate earthquakes accompanied with subducting of oceanic plate by using Ocean Bottom Seismometers (OBSs). An OBS has an advantage of not being restricted by geographical feature such as ocean, where it is hardly possible to observe without specified equipemaent. Thus it is expected that OBSs can acquire the data of small-to-moderate earthquakes , even microearthquakes in SIA.

4. The purpose of the OBS survey

In the world-famous subduction zones, for example, Aleutian, Chili, Japan and so on, the aspect of subducting slab has been studied well by investigating precise hypocenter locations and focal mechanisms of small-to-moderate earthquakes generated along the plate boundary and various types of subduction are reported. In order to unvail these defferences in inter-subduction features, it is very important to research every active subduction zones including the SIA region. However, because of

difficulties in observing natural earthquakes, precise studies in this region have not made enough.. Therefore, the purpose of OBS survay is to study the techtonic feature of collision between OJP and SIA, and the subducting slab of the Solomon Sea plate. Then we would like to compare with world-famous subduction zones noticing whether double seismic zone , seismic gap, are found or not..

5. Deployment of OBSs

In order to determine hypocenters, good station converage is required, OBSs surrounding hypocenter as many as possible. Since, we focus on the subducting the Solomon Sea plate and west side of colliding OJP with SIAOJP, we deployed OBSs onto 2 sites: site A; three OBSs north of Choiseul island, and site B; six OBSs south-east of Bougainville island. Arrengement of OBSs is listed in Table 1 and the map shown in figure 3. OBSs in site A is consisted of ones developed by Earthquake Research Institute University of Tokyo (ERI type), and site B consisted of ones by Tohoku University (Tohoku Univ. type). In this report, we donot mention about the precise description of each OBSs (see Araki et al., this cruise report)

Figure Captions

Figure 1: Techtonic map of Solomon Island Arc region.

Figure 2: Seimicity map of the SIA region. NEIC hypocenter data from 1990 to 1997 is used. The scale of magnitude and depth are shown each bottom and right side of the figure respectively.

Figure 3: Seismicity map devided into five segments.

Figure 4: Cross sectional view of the seismicity map in seg. A. The aspct of subducting slab is clearly seen. Hypocenters about 30 km depth is a unreliable solutions which have not determined with good RMS. There is no vertical exaggration in this figure. Right side of the view correspond to NBT, which marked with filled-inverse triangle.

Figure 5: Focal mechanisms of Harvard CMT solutions. Filled and open area of focal mechanisms stands for compressional and tensional area, respectively. Focal mechanisms are projected to the Schmidt net in the lower sphere. The data are used from 1977 to 1994, Earthquakes are larger than M5.

Figure 6: Cross sectional view of seg. B. The display of the figure is as same as Figure 5. NBT as shown as filled inverse triangle. The complicated aspect of this cross sectional view is due to the turning of trench axis toward Solomon Sea.

Figure 7: Cross sectional view of seg. C. SCT stands for the San Cristobal Trench.

Figure 8: Cross sectional view of seg. D. Obvious plate boundary between the North Pacific plate and SIA inseen at 200km depth. Sparse earthquakes at SCT side.

Figure 9: Cross sectional view of seg. E.

Table 1: List of OBSs. Details description are reported Araki et al (1998).

REFERENCES

Patricia A. Cooper and Brian Taylor , Polarity reversal in the Solomon Islands arc, *Nature,* **314**, 428-430.

Slanton, R. L.,1961, Explanatory notes to accompany a first geological map of Santa Isabel, British Solomon Islands Protectorate, *Overseas Geology and Mineral Resources,* **8** , 127-149.

Ramsay, W. R. H., 1978, Field, mineralogical and strucrual observations on some basement rocks, southeast Choiseul Solomon Islands, *Bulletin of the Australian Society of Exporation Geophysicists*, **9**, 107-110.

Ramsa, W. R. H., 1982, Crustal strain phenomena in the Solomon Islands, constrains from field evidence, and relationship to the India-Pacific plates boundary, *Tectonophysics*, **87**, 109-126.

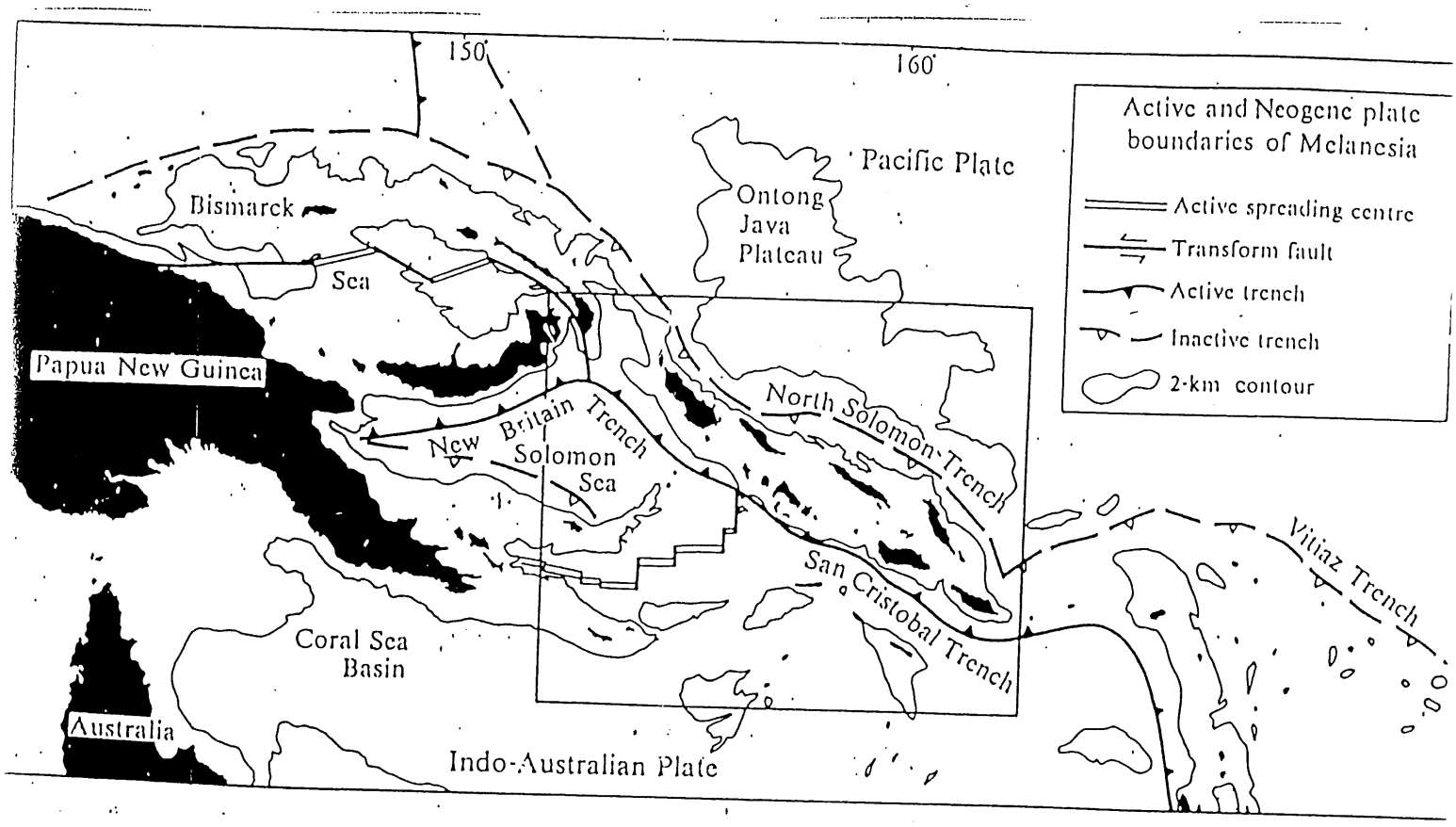

From Cooper and Taylor (1985)

Figure. 1

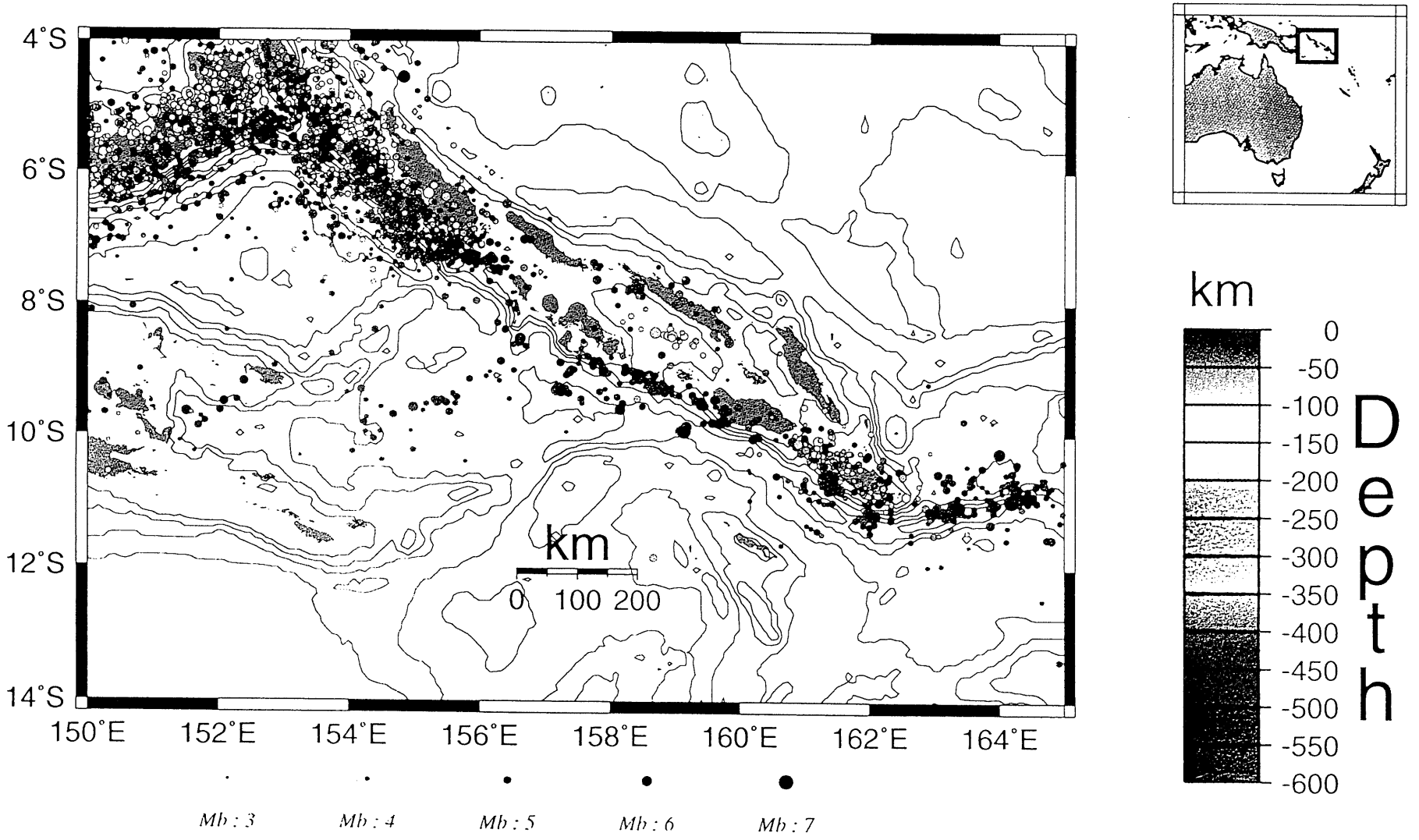
NEIC Hypocenters (1990/1/1 - 1997/10/21)
4°S
6°S
8°S
10°S
12°S
14°S
150°E
152°E
154°E
156°E
158°E
160°E
162°E
164°E
km
0 100 200
Mb : 3
Mb : 4
Mb : 5
Mb : 6
Mb : 7
km
0
-50
-100
-150
-200
-250
-300
-350
-400
-450
-500
-550
-600
Depth

Figure 2

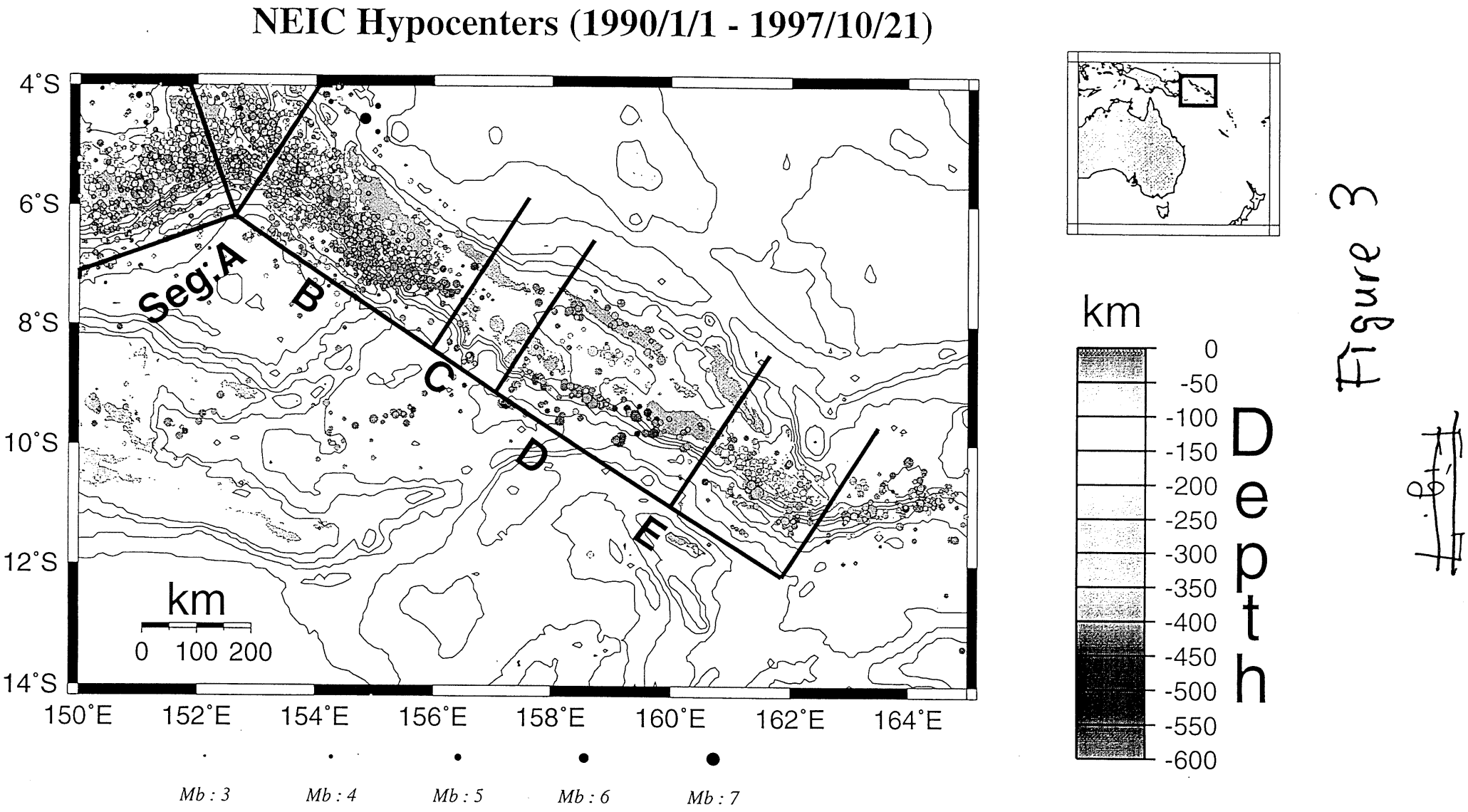
NEIC Hypocenters (1990/1/1 - 1997/10/21)
4°S
6°S
8°S
10°S
12°S
14°S
150°E
152°E
154°E
156°E
158°E
160°E
162°E
164°E
Seg.A
B
C
D
E
km
0 100 200
Mb : 3
Mb : 4
Mb : 5
Mb : 6
Mb : 7
km
0
-50
-100
-150
-200
-250
-300
-350
-400
-450
-500
-550
-600
Depth

Figure 3

~~Fig. 8~~

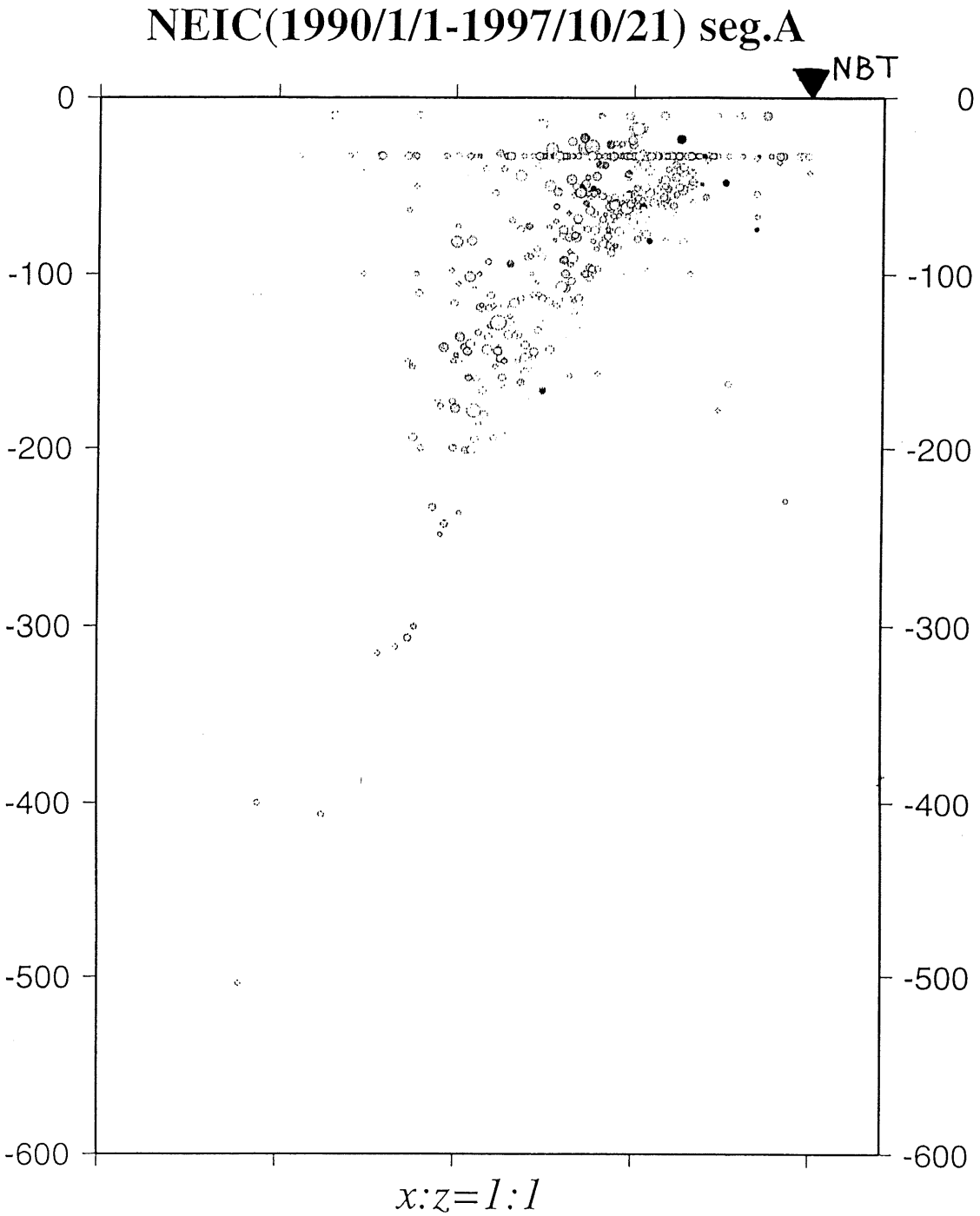

Figure 4 Seg. A

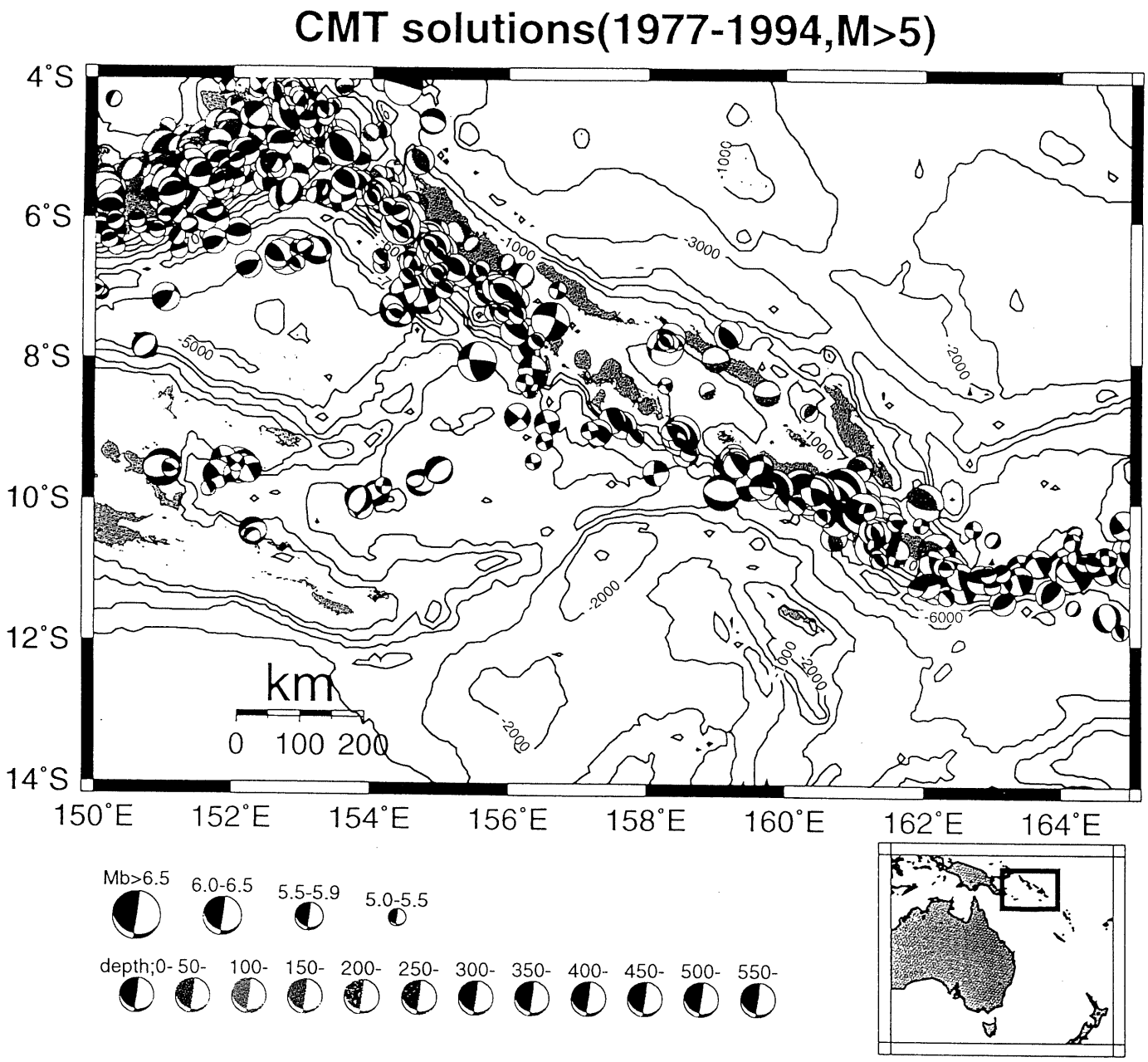
CMT solutions(1977-1994,M>5)
4°S
6°S
8°S
10°S
12°S
14°S
150°E
152°E
154°E
156°E
158°E
160°E
162°E
164°E
-1000
-3000
-5000
-2000
-6000
km
0 100 200
Mb>6.5
6.0-6.5
5.5-5.9
5.0-5.5
depth;0- 50- 100- 150- 200- 250- 300- 350- 400- 450- 500- 550-

Figure 5

Fig. 10

NEIC(1990/1/1-1997/10/21) Cross Sections

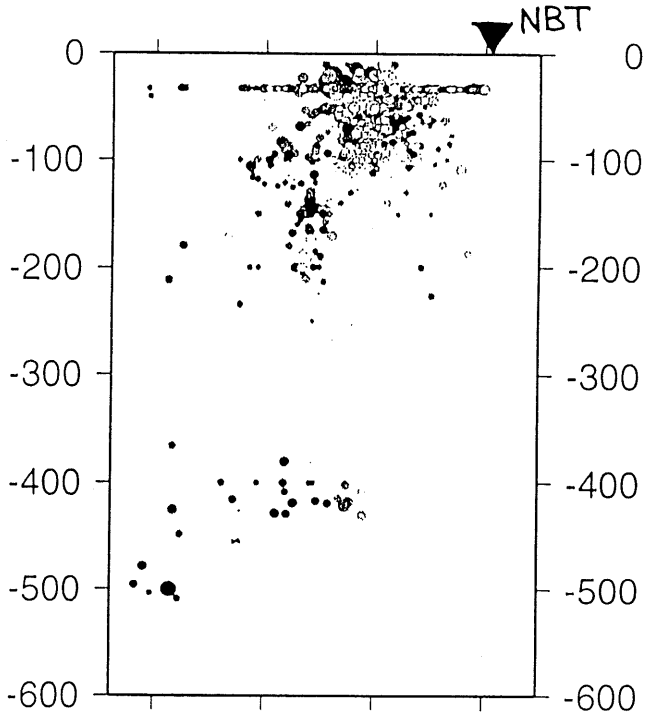

Figure 6 Seg.B

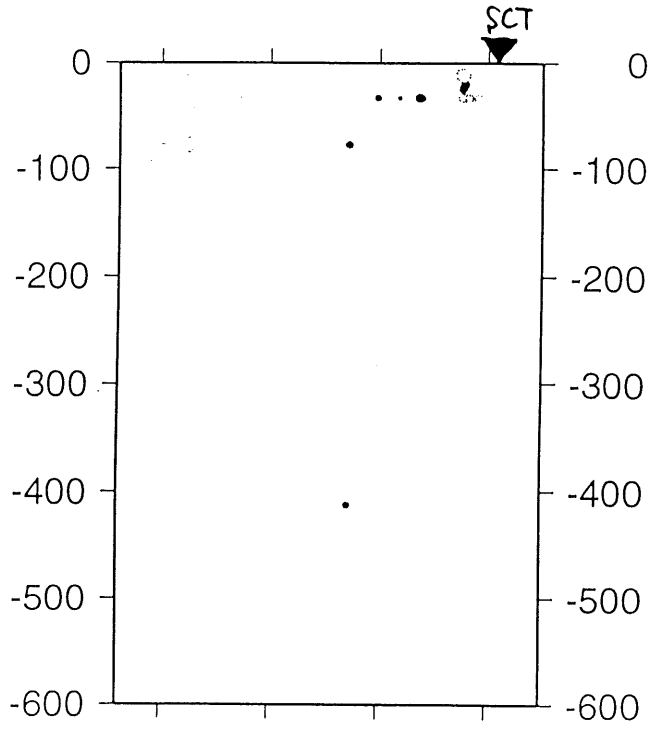

Figure 7 Seg.C

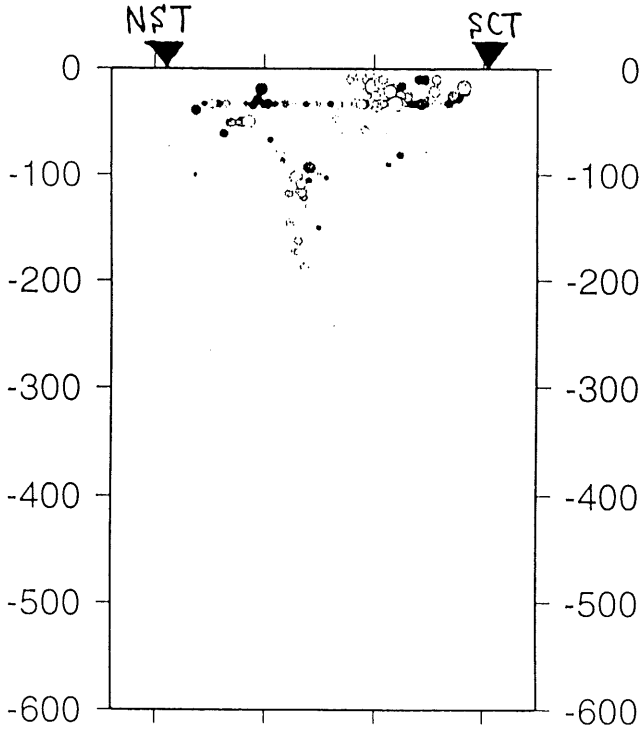

Figure 8 Seg.D X : Z = 1 : 1

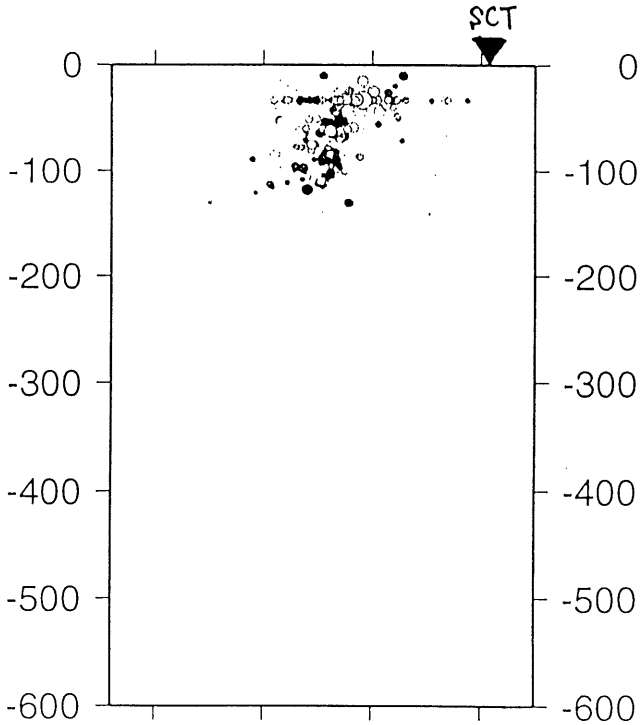

Figure 9 Seg.E

KH98-1 CRUISE REPORT LEG 2: MAGNETIC AND GRAVITY DATA

Garrett Ito and Loren Kroenke
School of Ocean and Earth Science and Technology, University of Hawaii

Kimihiro Mochizuki
The Ocean Research Institute, University of Tokyo

1. Introduction and Objectives

The tectonic setting in which the Ontong Java Plateau (OJP) formed has important reprocussions on the evolution of the Pacific Ocean basin yet remains poorly understood. Recent analysis of the regional gravity and geomagnetic field has led *Winterer and Nakanishi* [1998] to propose that Ontong Java erupted at an Early Cretaceous spreading center system. Other models, however, do not require a near-ridge origin and attribute the voluminous volcanism to the surfacing a giant head of an initiating mantle plume [e.g. *Mahoney and Bercovici*, 1994]. Another controversy deals with the age and duration of volcanic events. Formation of the Ontong Java by two major magmatic events (ie. ~122 and ~90 Ma, *Mahoney et al.*, 1993; *Tejada et al.*, 1996]) suggests very high eruption rates, consistent with a plume head origin. Long-lived volcanism throughout the period of 122-90 Ma, on the other hand, would suggest much lower eruption rates [*Ito and Clift*, 1998] and thus would indicate a more steady-state mantle source [e.g. *Mahoney*, 1987].

To address the above problems we completed geomagnetic and marine gravity surveys of the Ontong Java and the surrounding Stewart and Nauru Basins during Leg 2 of the KH98-1 expedition. The objectives of the magnetic survey is to reveal magnetic isochrons, which are necessary to determining the age and geometry of seafloor spreading. Gravity data, combined with bathymetric and seismic velocity data, is needed to constrain deep crustal structure of volcanic edifices, which reflects the thermo-mechanical state of the lithosphere at the time of volcanic loading and/or crustal faulting. Our surveys include a SW-NE crossing of Ontong Java's eastern salient, the intervening Stewart Basin, an E-W transect from the Nauru Basin on to the shallowest crest of the main plateau, and a SSW-NNE transect from the center of the plateau to the NE edge of the plateau.

2. Magnetic Data

2.1 Acquisition

Magnetic data was measured by the shipboard proton precession magnetometer and recorded at 30 s intervals. Magnetometer readings were combined with the ship's logs of time (GMT), navigation, and depth and was then recorded on PC floppy diskettes as well as printed on paper. Magnetic data was collected continuously when the

magnetometer was deployed. The magnetometer was removed from the water only during deployment of the multi-channel seismic equipment and during the OBS retrieval.

2.2 Preliminary Observations

A question of particular interest that the magnetic data can best address is whether or not the Stewart Basin formed due to NNE-SSW rifting of Ontong Java's eastern salient, or alternatively, if the basin formed by NW-SE seafloor spreading with the two lobes of the eastern salient forming along fracture zones [*Winterer and Nakanishi,* 1998]. We crossed the Stewart Basin nearly perpendicularly to the two arms of the eastern salient, which is an ideal orientation to test the NNE-SSW rifting hypothesis. After correcting for the regional magnetic field gradient along our ship track we observed magnetic field oscillations of amplitudes 100-700 nt and over wavelengths of ~100 km (Fig. 1). High amplitude negative magnetic anomalies lie over the north and south boundaries of the Stewart Basin near the margins of the two eastern salient lobes. A local positive anomaly is evident over a small volcanic feature in the center of the basin. Further analysis to filter short wavelength noise, to remove the effects of topography, and to correct for diurnal and latitudinal variations may be necessary before any seafloor-spreading related magnetic anomalies can be identified.

3. Gravity Data

3.1 Acquisition and Data Quality

The Surface Ship Gravimeter NIPR-ORI measured absolute gravity that was recorded on magnetic tape and the HP computer hard drives at 60 s intervals. Also recorded with the raw data was the free-air gravity anomaly (FAA), obtained by applying to the raw gravity, an Eotvos and free-air correction. The free-air gravity anomalies show varying quality. High frequency (~60 s period) scatter in FAA by +/-1-3 mGal characterizes all of the measurements and are most likely associated in navigation errors which yield 60-s period errors in ship speed (Fig. 2). These errors can easily be removed either by filtering the FAA or, more appropriately, by filtering the navigation data and reapplying Eotvos corrections to the raw data.

An additional check of measurement accuracy can be made by comparing readings at locations where survey lines cross. Crossings occured at 4 points as well as a ~150-km long profile where two survey lines over-lapped. Discrepancies at the crossing points ranged between 0.5-5 mGal; < 5 mGal cross-over errors are most desirable for modern shipboard gravity measurements. The largest cross-over discrepancies (~5 mGal) occured along the two over-lapping lines (Fig. 2) located on the shallowest portion of the

main plateau where we deployed the OBS. These cross-over descrepancies will need to be considered in future detailed studies of the regional gravity field. We note, however, this preliminary analysis did not correct for time-dependent drift in the gravimeter.

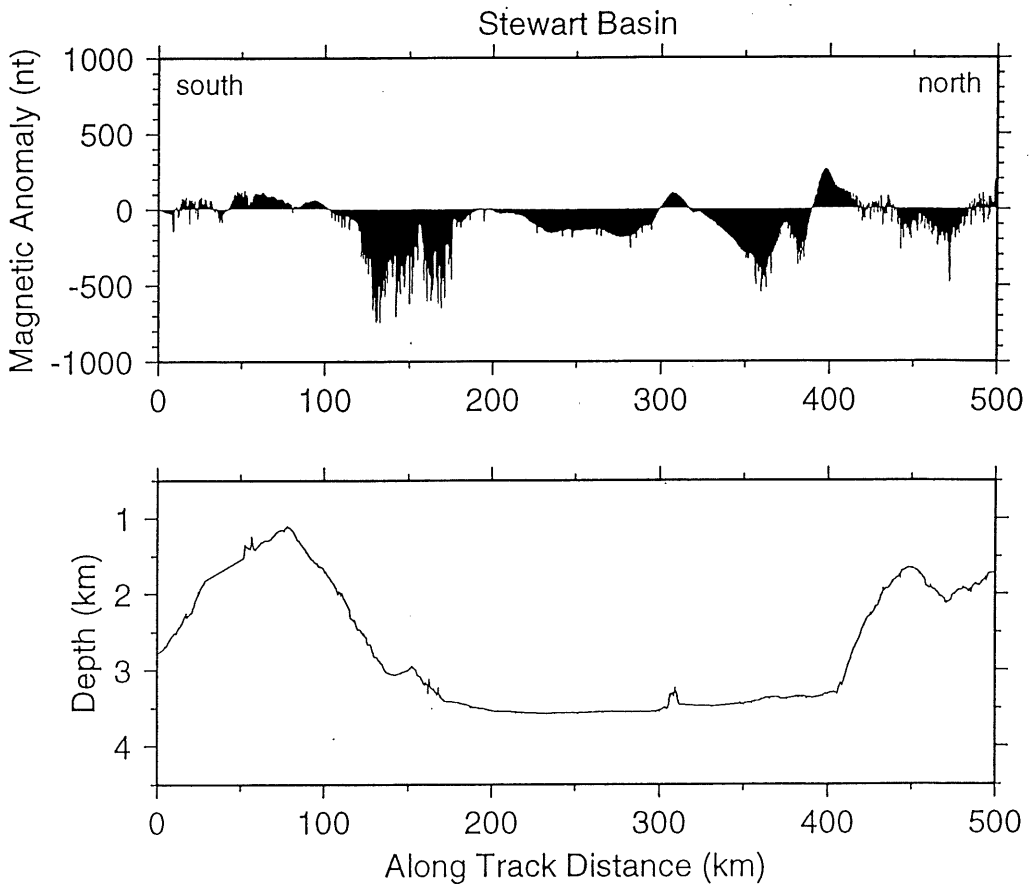

Fig. 1 Observed magnetic field (top) and seafloor topography (bottom) variations over the Stewart Basin and the two lobes of Ontong Java's eastern salient.

3.2 Preliminary Observations and Analysis

In general, broad wavlength (>200 mGal) variations in the shipboard free-air gravity are consistent with the the satellite-derived gravity of *Sandwell and Smith* [1997]. At shorter wavelengths (~40-50 km), the satellite gravity show ~10 mGal differences that most likely reflect errors associated with satellite track spacing. Shipboard measurements reveal short wavelength (<20 km) anomalies (~10 mGal) unresolved by the satellite data.

Free-air gravity from the Nauru Basin over the main portion of the plateau, is characterized by small amplitude (<~40 mGal) broad wavelength variations. Preliminary analysis indicate that these observations are consistent with findings of *Gladczendo et al.* [1997] that the main OJP plateau is in isostatic equilibrium (consistent with formation on

young lithosphere) with a thick, high-density, lower crust.

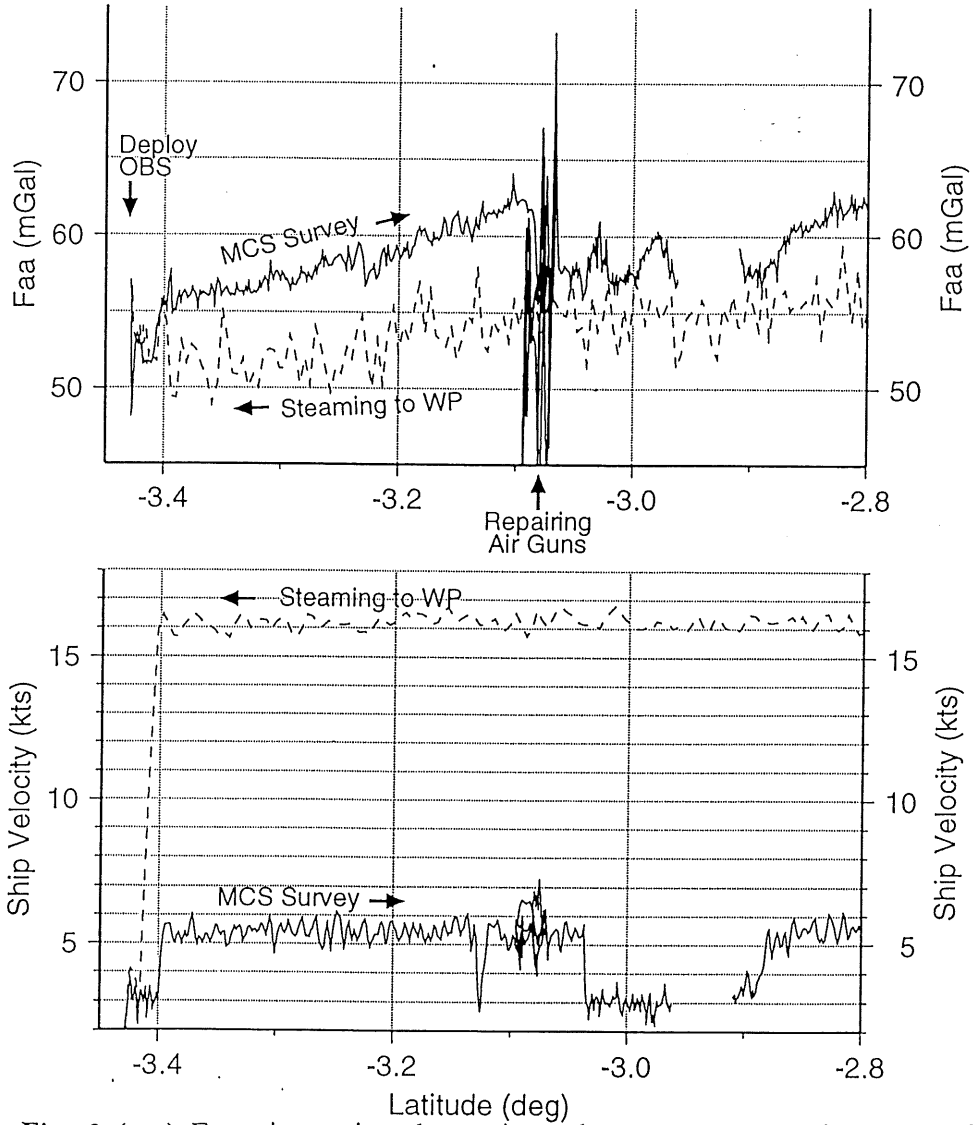

Fig. 2 (top) Free-air gravity observations along two over-lapping survey lines. The dashed line was taken as we steamed south toward our OBS deployment site. We then traveled north along the same line for our MCS survey. The high amplitude variations near 3.7 S can be disgarded and is due to repeated loops of the ship done to repair the airguns. (bottom) Ship speed along the two survey lines.

Along our survey of the eastern salient and Stewart Basin we observe significantly higher amplitude variations. The largest variations of >100 mGal are observed at our crossing of the Solomon Trench and on to the southern lobe of the eastern OJP salient. These high amplitude anomalies most likely reflects flexural uplift associated with the subduction of the Pacific Plate. From the Stewart Basin to the northern lobe of the eastern salient, FAA varies by ~70 mGal; whereas on the Nauru-Basin side of the

northern lobe, variations increase to almost ~90 mGal (Fig. 3). This increase in FAA between the Stewart and Nauru Basins most likely reflects lateral variations in crustal compensation of the northern lobe of the OJP salient.

The crust-mantle interface (Moho) beneath a volcanic edifice bends downward into the mantle with a curvature that is controlled by the effective elastic strength of the underlying lithospheric plate. Zero elastic strength predicts the greatest down-warping of the Moho and corresponds to Airy isostastic compensation; infinite elastic strength predicts a flat Moho and is the case in which all seafloor topography is supported by the elastic plate. Because gravity anomalies reflect Moho structure (in addition to seafloor topography), shipboard gravity and bathymetry can therefore be used to constrain the effective strength and thus thermal age of the lithosphere at the time of volcano loading. We thus forward modeled the free-air gravity assuming that the 2D bathymetry (shipboard and gridded bathymetry) was compensated by a lithosphere of uniform elastic thickness T_e. The method used assumes laterally uniform crustal density and solves for the flexure of an elastic plate as well as the combined gravity field from seafloor and Moho topography using a standard spectral method [e.g. *Watts,* 1978].

Fig. 3 (top) shows results of calculations assuming a thin (T_e = 3 km) and thick (T_e = 15 km) elastic plate. The thin elastic plate model predicts Moho to extend deep into the mantle. This large downward flexture of the Moho contributes a large negative gravity signal that reduces the positive contribution from seafloor topography. The low amplitude gravity anomalies predicted by this thin plate model are consistent with the observed anomalies on the south side of this lobe of the eastern salient; however, they underpredict FAA on the Nauru Basin side. In contrast, the thick elastic plate model predicts less downward flexure of the Moho and therefore larger amplitude FAA values (~70 mGal). The predicted amplitudes are consistent with the observations near the Nauru Basin but are too high to explain the observations on the south side of the plateau. These findings suggest that the southern portion of this lobe of the eastern salient may have formed when the underlying plate was young and weak, but the northern side formed after the plate cooled with age and strengthened.

To further test this hypothesis, we simulated a two-stage loading history. We first modeled compensation of topography of the southern side of the eastern salient lobe with a thin (T_e = 3 km) elastic plate. We then added the gravitational effects due to compensation of topography on the north side assuming a thick elastic plate. We found that the best fit to the observed gravity was obtained if the topography to the north added no additional flexure to the original Moho, or equivalently, the second stage of volcanism loaded an elastic plate of infinite thickness (Fig. 3, bottom). These preliminary results

indicate that volcanic lineations on the Nauru Basin side of the eastern salient most likely formed on lithosphere significantly older (>30 m.y.) than the Stewart Basin side of the of the eastern salient. Such results are in consistent with *Winterer and Nakahishi*'s [1998] hypothesis that the Nauru Basin volcanic lineations formed at or near a ridge crest. Further analysis of the effects of laterally varying crustal density is necessary to more rigorously test the sensitivity of this type of modeling to elastic plate thickness.

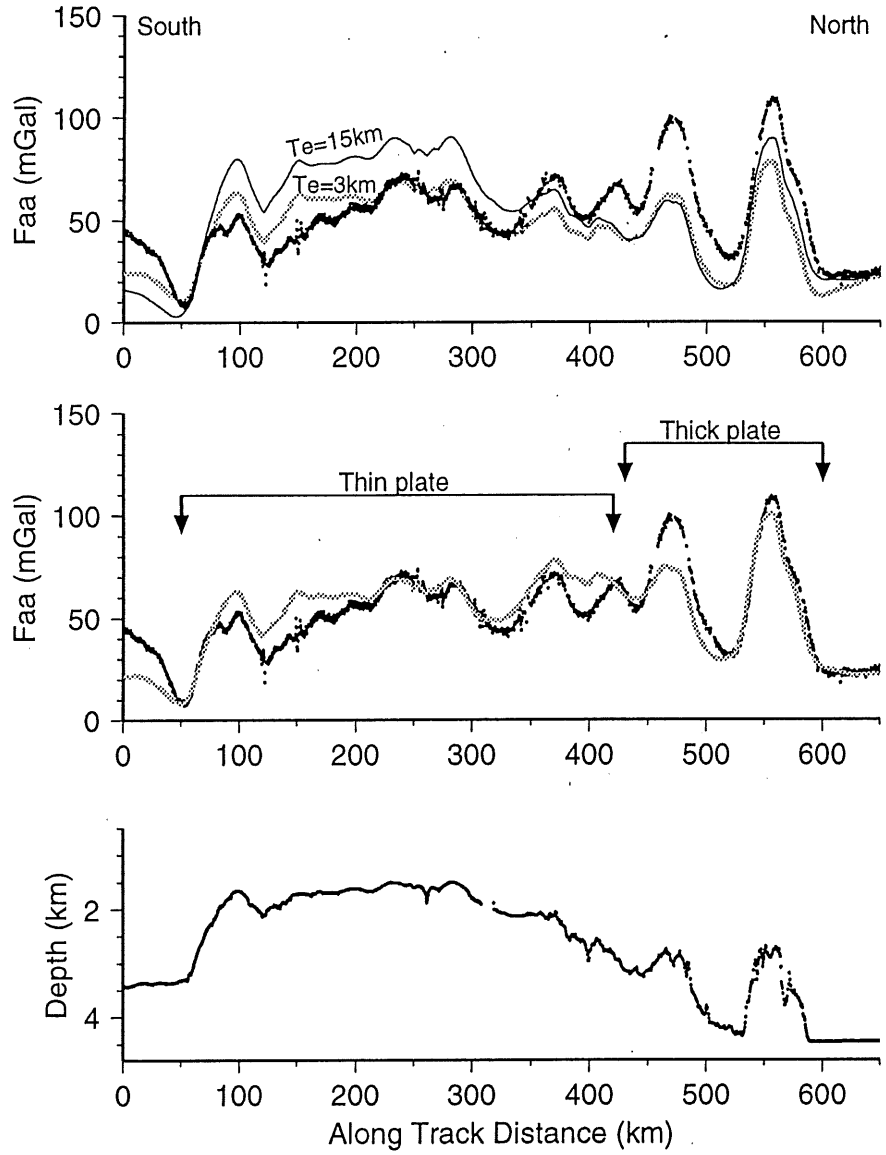

Fig. 3 (top) Observed (dots) free-air gravity anomaly across the northern lobe of the eastern salient is compared with model predictions of a thin (gray line) and thick (thin solid line) elastic plate. (middle) Observed anomaly is compared with a predictions in which the bathymetry to the south formed on a thin elastic plate and the bathymetry to the north loaded a thick elastic plate. (bottom) Bathymetry from the Stewart Basin in the south (left) to the Nauru Basin in the north (right).

4. References

Bercovici, D. and J. Mahoney, Double flood basalts and plume head separation at the 660-thermal boundary layer, *Geology*, 24, 551-554, 1996.

Gladczenko, T.P., M.F. Coffin, and O. Eldholm, Crustal structure of the Ontong Java Plateau: Modeling of new gravity and existing seismic data, *J. Geophys. Res., 102*, 22,711-22,729, 1997.

Ito., G. and P.D. Clift, Subsidence and growth of Pacific Cretaceous plateaus, submitted to *Earth. Planet. Sci. Lett.*, 1998.

Mahoney, J.J., An isotopic survey of Pacific oceanic plateaus: Implications for their nature and origin, in: Seamounts, Islands, and Atolls, P. Fryer, B. Keating, R. Batiza, and G. W. Boehlert, edgs., pp. 207-220, AGU Washington D. C., 1987.

Mahoney, J.J., M. Storey, R.A. Duncan et al., Geochemistry and age of the Ontong Java Plateau, in : The Mesozoic Pacific, M. Pringle, W. Sager, W. Sliter, and S. Stein, eds., pp. 223-261, Washington D. C., 1993.

Sandwell, D.T. and W. H.F. Smith, Marine gravity anomalies from Geosat and ERS satellite altimetry, *J. Geophys. Res., 102,* 10,039-10,054, 1997.

Tejada, M.L.G., J.J. Mahoney, R.A. Duncan, and M.P. Hawkins, Age and geochemistry of basement and alkalic rocks of Malaita and Santa Isabel, Solomon Islands, southern margin of Ontong Java Plateau, *J. Petrol, 37*, 361-394, 1996.

Winterer, E.L., and M. Nakanishi, Evidence for a plume-augmented, abandoned, Early Cretaceous spreading center on Ontong Java Plateau, submitted to *J. Geophys. Res.*, 1998.

Watts, A. B., An analysis of isostasy in the world's oceans, 1. Hawaiian-Emperor seamount chain, *J. Geophys. Res., 83*, 5989-6004, 1978.

Extra Figures

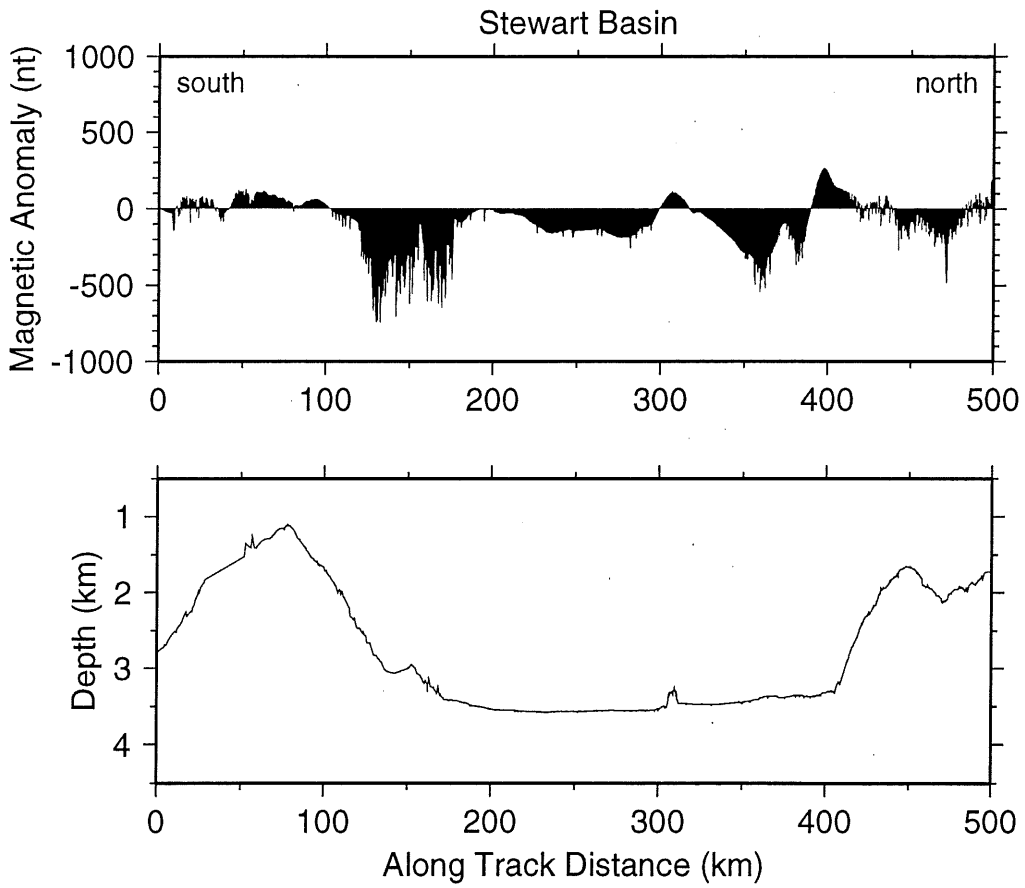

Fig. 1

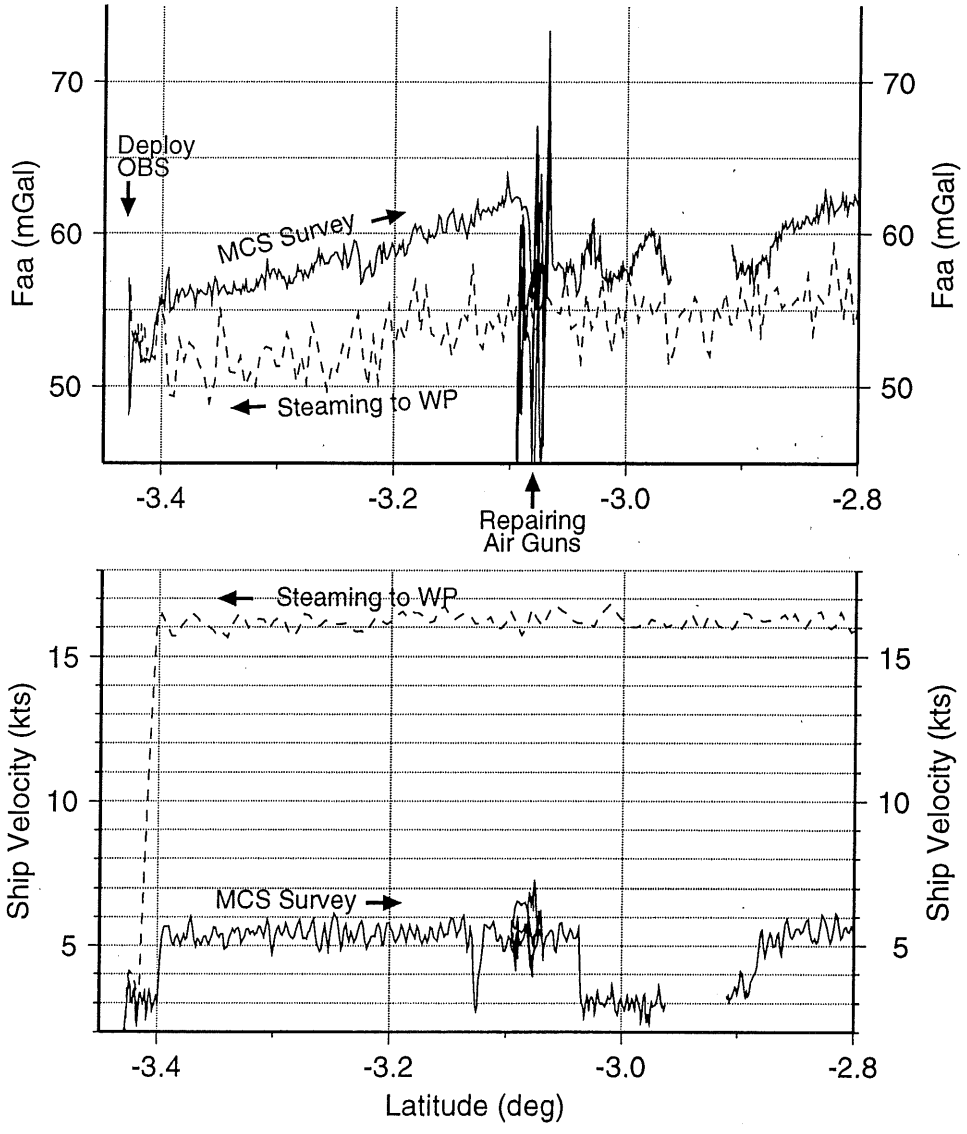
70
60
50
Faa (mGal)
Deploy
OBS
MCS Survey
Steaming to WP
-3.4
-3.2
-3.0
-2.8
Repairing
Air Guns
Steaming to WP
15
10
5
Ship Velocity (kts)
MCS Survey
Latitude (deg)

Fig. 2

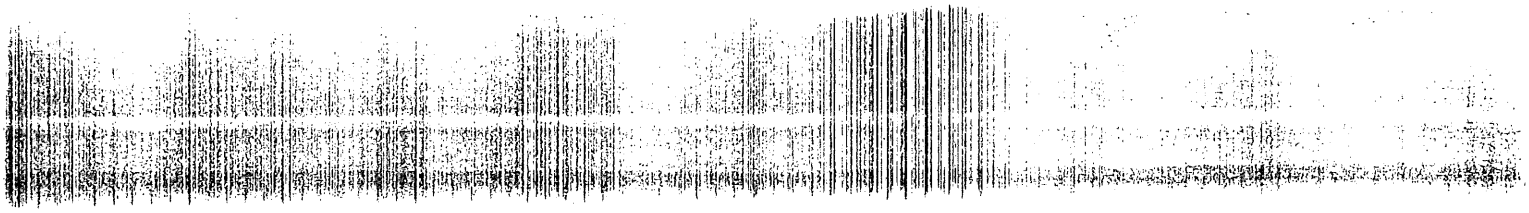

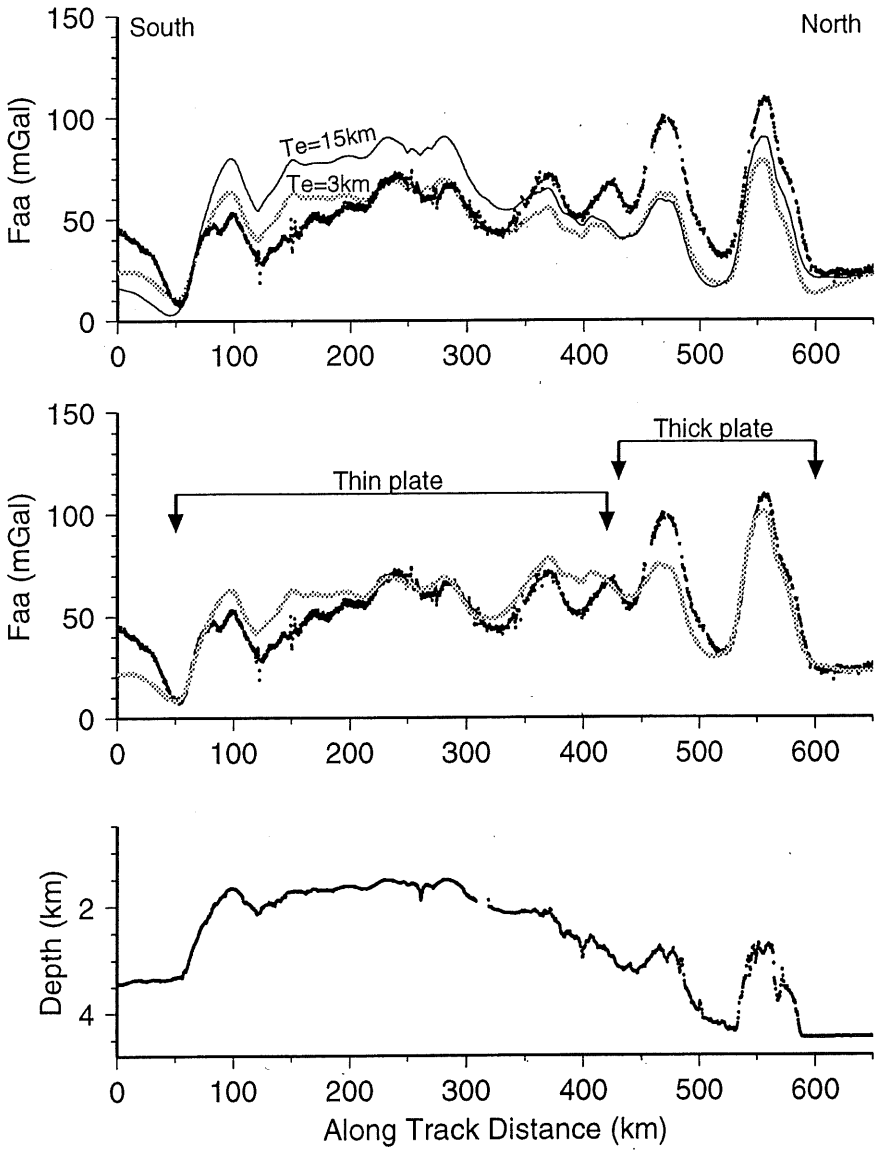
South
North
Te=15km
Te=3km
Faa (mGal)
Thin plate
Thick plate
Depth (km)
Along Track Distance (km)

Fig. 3

KH98-1 Leg 2 Seismic Line Summary

Line	*Area*	*Length*	*Shot Interval*	*Record Length*	*Streamer*	*Source*	*Sonobuoys*
101	Eastern Salient	149 km	10 s	8 s	24-channel, 300 m ITI	4.5 liters	0
102	Eastern Salient	96 km	10 s	8 s	24-channel, 300 m ITI	4.5 liters	0
103	Eastern Salient	27 km	10 s	8 s	24-channel, 300 m ITI	4.5 liters	0
201	Nauru Basin	41 km	20 s	16 s	24-channel, 300 m ITI	57 liters	1
301	Gun Tests	2 km	20 s	16 s	48-channel, 1200 m ITI	37 liters	0
401	Nauru-OJP	550 km	20 s	16 s	48-channel, 1200 m ITI	17-57 liters	11
402	Nauru-OJP	29 km	20 s	16 s	48-channel, 1200 m ITI	37-54 liters	1
403	Nauru-OJP	438 km	20 s	16 s	48-channel, 1200 m ITI	37-57 liters	12
404	Nauru-OJP	260 km	20 s	16 s	48-channel, 1200 m ITI	40-57 liters	2
501	OJP	364 km	20 s	16 s	48-channel, 1200 m ITI	20-57 liters	5
601	OJP	152 km	20 s	16 s	48-channel, 1200 m ITI	37-57 liters	5

48-CHANNEL SEISMIC OPERATIONS

Mark Wiederspahn[1], Millard Coffin[1], Kimihiro Mochizuki[2], Eiichiro Araki[2], and Masanao Shinohara[3]

[1]Institute for Geophysics, The University of Texas at Austin
[2]Ocean Research Institute, University of Tokyo
[3]Department of Earth Sciences, Chiba University

INTRODUCTION

This section describes the 48-channel seismic reflection system used during KH98-1 Leg 2, and significant observations thereof. This section is primarily a technical description; other sections address scientific aspects of the seismic data. We collected ≈27,000 shotpoints (50+ Gbytes) of 48-channel data during the cruise.

DESCRIPTION OF EQUIPMENT

The cable reel on *Hakuho Maru* was located on the port side afterdeck ≈20 m forward from the stern. The rubber coated drum is 1.2 m diameter by 1.6 m wide, and it is driven by an electrically powered hydraulic motor system. An Innovative Technology Inc. ST-5 48-channel, 1200 m active length cable was loaded on the reel before Leg 1. The ITI cable is a solid, 3 cm diameter, reinforced, floatation cable with bulbous hydrophones every 5 m. Inside each molded bulb, a flat, pressure sensitive, plastic sheet is coiled around an axially positioned aluminum cylinder. Each group consists of 5 such phones, yielding a 25 meter active channel. The outboard phone bulb of each channel is labeled with the channel number within the section (1E-24E) for the individual 600 m

active cable sections. Each group has a single preamplifier located inside the cylinder of the near offset bulb, powered by 12 volt batteries in the recording room. The cable used consisted of two 600 m active sections plus a 185 m leader, 12 m trailer, and 100 m tail rope and 0.25 m diameter tailbuoy ("Norwegian buoy"). The cable was towed directly off the reel, to minimize sharp radius turns as much as possible, straight back to a narrow 10 cm diameter stern roller with side rollers on the port quarter rail. Tow height at the stern was ≈3 meters above the water. Plastic chafing gear (≈1 cm thick) around the area exposed to the roller served to minimize the bend radius.

There are 5 bird coil bulbs per 24-channel section, at equal spacing along the section, midway between phones. Five Syntron Multitrak depth control units ("birds"), each with compass, temperature sensor, and wing angle feedback, were installed in equal intervals along the two sections. Bird bulbs have no black and white wires visible in the clear part of the bulb, but otherwise look exactly like phones. They were not labeled; some had red vinyl tape on them for identification.

The inboard end of the leader has an amphibious connector, and the deck cable connected to it led up one level and ≈20 m forward into Laboratory 3, where it was connected to an OYO ST-5 breakout box, the OYO DAS-1 recorder, and two 48 amp-hour, 12 volt lead acid batteries.

Bolt 1500C air guns with 1000 in^3 and 1200 in^3 barrels and I/O SS8 shuttle motion detectors were towed at equal offset behind the stern from deck level, ≈2 m above the water. Up to three guns were deployed simultaneously. Each could be retrieved and launched independently with little change in the tow characteristics of the other two. The two center guns were retrieved using stainless wire rope from winches at the top of the stern A-frame. The third

starboard gun was retrieved with ≈2.5 cm rope using a snatch block on a hanger outboard of the A-frame, about halfway up, and a capstan. Depth could be adjusted by changing the tow length or the ship speed. Guns depths could not be determined directly, and in contrast to standard air gun deployment techniques for MCS work, no floats were used.

Up to 2000 psi air from two LMF-200 compressors located in the winch room below the afterdeck supplied air via permanent piping to a valve box forward of the reel. Flexible hose led aft across the entire deck, a safety issue on the well-traveled fantail, to each gun tow point. Except for a short test period, the guns were fired at 1600-1700 psi throughout KH98-1 Leg 2, significantly below the nominal 2000 psi usually used in air gun reflection seismology. According to the manufacturer, operating the 1500C air guns at less than 2000 psi results in overall reduced energy into the water as well as power loss at higher frequencies., thus skewing the air guns' peak energy output toward lower frequencies.

The air guns were fired from a countdown timer derived from the ORI master OBS timing clock with auxiliary logic and level converters. The start signal derived from this chain was routed to a True Time GPS clock, which provided a sub-ms accuracy time stamp for each start. The start signal was routed to all analog recorders, the OYO digital recorder, and a relay box which triggered two IO Auto Sync I WG (lines 101-404) or IO Auto Sync I "AG" (lines 501-601). Important differences in characteristics of the two kinds of boxes only became apparent midway through KH98-1 Leg 2. Each introduces some additional delay between the start time and the actual acoustic pulse, with the goal of adjusting some measured signal to a common aiming point. This was 90 ms for the WG box, and 50 ms for the AG box.

One or more seismic channels from the ST5 breakout box were routed via a differential preamplifier, then single ended gain and bandpass filter, to the ship's EPC 9800 , or the UTIG EPC 3212 graphic recorders. We fed sonobuoy signals from an ICOM 8500 radio receiver into the OYO auxiliary channel, as well as displaying them on the UTIG EPC 3212 recorder.

CABLE OPERATIONS

UTIG purchased 3 rolls of lead sheet ("lead dampcourse" of 300 mm x 20 k x 6 m dimensions), rolls of 0.4 mm x 5 cm plastic tape, and tie wraps at BBC Hardware and Ideal Electrical Suppliers in Cairns to ballast the cable, which as manufactured has significant positive buoyancy in water. The cable was run out in large loops on the aft and starboard deck in port, and 528 g weights attached every other phone, according to specifications supplied to UTIG by the manufacturer, beginning with the two tail channels. After weighting the two tail channels, we floated them alongside the ship to determine their approximate buoyancy. Although the Cairns harbor water was less salty than water over the Ontong Java Plateau observed during KH98-1 Leg 1, temperatures were about the same. This test convinced us that the predicted amount of weight would be too great, so we adjusted the calculated amount by half on all other channels, putting 264 g weights on every other phone. This plan was followed for the rest of the cable, except where a mistake was made in the pattern, in channel 8 of the outboard section. We weighted channels with a bird bulb, which are slightly heavier than birdless channels, the same as birdless channels. Two tie wraps on the front end of the tape wrap were used to keep the plastic tape from unwinding in the water stream, instead of tying off the plastic tape. These were much faster to install, but probably less secure than tying off the tape. About half seemed to loosen during each deployment. We

were unsure if the thinner tape we purchased in Cairns—no friction ("bulldog") tape could be located—would tie well.

Once tested at sea, we found the cable to be slightly positively buoyant. At 3-5 kts through the water, wing angles averaged <4°, except at the ends. The greater the tow speed, the more correction was needed by the head and tail birds. To reduce this effect, we put more weight on the leader, adding ≈8.5 kg. This reduced but did not eliminate the problem. The 1st bird was always at full dive (-14°), which should generate ≈35 pounds of downward force at 5 kts. Except for this, the birds maintained the 10 m set depth most of the time with small angles. Following seas with a 2+ m swell caused some instability in the bird feedback scheme. Generally, with the slow dynamics of the 48-channel cable, we found 30 s non-averaged updates to be quite stable. We placed the nearest bird in full down wing angle on one occasion because it tended to oscillate, as we also observed with the 24-channel cable.

Tow noise was not quantitatively evaluated, but the cable seemed to be quieter than a similar ITI cable used aboard RVIB *Nathaniel B. Palmer* 9507. In particular, high velocity noise coherent across many channels was absent from this cable. The weather was better during KH98-1 Leg 2, and tow speed generally lower, so a direct comparison is difficult. Some noise characterization will be done as part of MCS processing at UTIG.

Channels 30, 42, and 48 were faulty at some times. The far offset, channel 48, could have been power starved; ITI suggested that 36 volts might be needed to power the cable to full signal/noise at the far channels, where voltage drop would be greatest. We saw no direct evidence of this need. The channel 48 problem looked more like a broken wire or a bad sensor. If the center tap were not well attached to the battery half voltage point, the outboard 12 or 14

channels only would latch with no signal. ITI says this effect is characteristic of the OYO response if common mode voltage is too great.

A spare 600 m cable section (ITI sn 974002) of the same construction was stored on a wooden reel; it was neither ballasted nor tested during KH98-1 Leg 2. One of us (M. Wiederspahn) had participated, however, in a test of the spare section and the outboard section (ITI sn 974001) used during KH98-1 Leg 2 undertaken from Galveston on 22 December 1997. The inboard section (ITI sn 974003) used during KH98-1 Leg 2 had not been field tested in Galveston or elsewhere prior to the cruise.

Safety problems could be considerable in high seas in manually lifting the birds over the stern rail when deploying and retrieving the streamer. A gently curved ramp over the rail might permit a single person to handle this task, and securely capture the cable as well to limit its movement.

In one instance during KH98-1 Leg 2, the head of an ITI streamer section was observed being secured during towing by figure eighting around the port aft mooring bollards. As the diameter of the figure eights was well below that recommended by the manufacturer for winding the streamer—the diameter of the wooden reels on which the streamer sections were shipped is a good guide to the minimum recommended diameter for winding the streamer—extreme care should be used to avoid such practice in the future, thus minimizing the chance of wire breakage inside the cable. Additional guidelines for care and preservation of the ITI cable are given in the manuals supplied by the manufacturer.

We deployed the cable at ≈3 kts through the water, and retrieved it at ≈1.5 kts. This seemed to provide enough tension to wind the cable on the drum gently but securely.

CABLE LAYOUT

```
B  = bird location, with no collar
BC = bird location, with collars installed
Bn = bird location, with programmable bird ID we used

w = 8.8 x 15 cm 20 kg/m**2 lead weight = 264 g
W = 8.8 x 30 cm 20 kg/m**2 lead weight = 528 g
(note: cable circumference is ≈9.4 cm)

p = hydrophone bulb
X = patch over small hole in cable jacket, channel 2, outboard

leader marked with black marker at drum wrap intervals, 3.78 m.
15 each 8.8 x 30 cm 528 g weights at 5 m interval at the outboard end.
```

Inboard section, sn 974003

	connector	
1	B3 p w p w p w p w p	1
2	p w p p w p p	2
3	w p p w p p w p	3
4	p w p p w p p	4
5	w p p w p p w p	5
6	p w p p w p p	6
7	BC p p w p p w p	7
8	p w p p w p p	8
9	w p p w p p w p	9
10	p w p p w p p	10
11	w p p w p p w p	11
12	p w p p w p p	12
13	B4 p p w p p w p	13
14	p w p p w p p	14
15	w p p w p p w p	15
16	p w p p w p p	16
17	w p p w p p w p	17
18	p w p p w p p	18
19	B p p w p p w p	19
20	p w p p w p p	20
21	w p p w p p w p	21
22	p w p p w p p	22
23	w p p w p p w p	23
24	p w p p w p p	24
	B	B7
	connector	connector

Outboard section, sn 974001

	connector	
1	B5 p p w p p w p	25
2	p w p X p w p p	26
3	w p p w p p w p	27
4	p w p p w p p	29
5	w p p w p p w p	29
6	p w p p w p p	30
7	BC p p w p p w p	31
8	w p p w p p w p	32
9	p w p p w p p	33
10	w p p w p p w p	34
11	p w p p w p p	35
12	w p p w p p w p	36
13	B6 p w p p w p p	37
14	w p p w p p w p	38
15	p w p p w p p	39
16	w p p w p p w p	40
17	p w p p w p p	41
18	w p p w p p w p	42
19	BC p w p p w p p	43
20	w p p w p p w p	44
21	p w p p w p p	45
22	w p p w p p w p	46
23	p W p p W p p	47
24	W p p W p p W p	48

connector
tail section with swivel
tail rope with buoy

AIR GUN OPERATIONS

The air guns were towed from the deck on stainless wire rope with a slant distance from deck to gun port of 27.3 m. Each gun could be retrieved individually for repairs and redeployed without changing ship speed (at least in good weather), or altering the tow points of the guns still firing. However, the tow points were close enough together so that several snarls developed in quartering seas. As the depth of each gun was not well controlled, surfacing times of the three bubbles differed at least sometimes by 0.5 to 1 s. Often the guns towed so they fired within a meter or so of each other, even though the tow points were 3-5 m apart.

Generally, our tow speed was 3.5-5.5 kts through the water. The longest line (400) was shot at the slower speed due to a strong accompanying current, and this probably limited wear and tear on the hose bundles and guns.

Gun bundles should contain rugged hydrophones (blast phones), as is standard in MCS operations, to unambiguously monitor the firing time of each gun in case there is doubt about the correct working of the I/O SS8 shuttle motion detector. Not having phones available in the harnesses available for monitoring made detection of the gun mis-timing much more difficult, and logging of such problems for treatment in subsequent data processing impossible. In addition, a storage oscilloscope or other display device should be part of the air gun quality control package so that every gun phone can be monitored simultaneously for every shot, and logged. Ideally, such gun phone data should be recorded for all shots as well.

SYSTEM TIMING AND AIR GUN ELECTRONICS

The OBS master clock provided a stable, accurate 1 Hz signal to the countdown timer, which then sent the master start signal either directly to buffer and level converters to distribute to all the recording devices, or routed it through a PC based software randomizer (designed, constructed, tested, and installed during the first few days of KH98-1 Leg 2) which delayed the trigger by 0 to 0.5 s for all devices. We shot all the data with the randomizer enabled. This randomized start signal time was logged by the True Time clock, and closed a relay, with a delay of 10 ms, which caused the AutoSync gun fire boxes to output a pulse of high voltage which fired the solenoids in the air guns.

Use of the AutoSync I WG gun controllers caused significant air gun mis-timing during lines 101-404. The WG model, which is intended to fire water guns, differs in several important ways from the airgun ("AG") AutoSync model, even when the WG is internally jumpered for airgun operation. The most important is that the WG misses the initial shuttle motion, and instead, synchronizes the shuttle return. The actual gun peak pressure point is ≈465 ms after start, rather than the expected 500 ms after start. This was measured by looking at the raw shuttle motion signal. The jitter was anywhere from a few ms to 20 ms, the latter when the trigger picked a different part of the waveform (probably the inductive kick when the solenoid pulse turned off).

Other differences between WG and AG models include:

1) WG waits 32-40 ms after shot before trigger possible, AG waits 8 ms;
2) WG charges to 60 v, AG to 110 v;
3) WG fires 60 ms pulse, AG 40 ms pulse;
4) WG aims at 90 ms, AG at 50 ms;
5) WG has 3 v sensor detect with filter, AG has 0.5 v detect, no filter.

Thus, because air guns and water guns function in fundamentally different ways, the AutoSync I WG controllers should only be used for synchronization

of water guns, and the AutoSync "AG" controllers should only be used for synchronization of air guns.

Recording

We used the OYO DAS-1 without any significant problems. It is tricky to configure initially, but once set up in a particular configuration, is quite reliable. All problems resulted from a configuration change, or switching between two different production modes. We were able to record 16 seconds of data every 20 seconds without problem to an HP 1533 DAT drive internal to the OYO. The output to tape overlaps the start of the next shot by 2 or 3 s. We carefully tested this by injecting known data for each shot (before shooting began), and verifying the content on tape, and believe the OYO worked as expected. About 6 shots were missed at each tape change, with one shot being buffered in memory during the transition. For example, if 100 shots/tape were recorded, tape 2 would have shot 101, then shot 107, 108, etc. on it.

On occasion, the shot header was not recorded on the first shot of the first tape of a line. This seemed to be a function of configuration, but we never learned the exact cause(s).

The OYO time drifts significantly; this must be monitored and logged to permit correction of the shot time of the raw seismic data so it can be merged with the navigation. We did so at the end of each line.

Overdriving the AUX input causes data glitches on all seismic channels, coincident with the direct wave arrival on the AUX input. Interestingly, this glitch was observed on the analog EPC monitor attached to the breakout box.

The cable depths, wing angles, and compass readings from each bird are logged by the Syntron controller. We experienced significant problems with data loss due to inexperience with the program. Not recording is altogether too easy with the Syntron software, potentially causing problems with subsequent MCS data processing. The first half of line 401 seems not to have been saved, or was saved and then erased by operator error. The bird interrogation was set to occur 18 s after start. At the start of line 403 the trigger was disconnected and a default cycle occurred during a recording window, inductively coupling the bird commands into all the seismic channels across the display until the problem was corrected.

The EPC 9800 worked quite well as a single channel monitor. We generally ran it at a 4 second sweep, with varying non-zero delay from channel 5 at a ≈200 m offset from the guns.

NAVIGATION

We recorded the ship's "system" filtered position, from connector J106 of the JRC data LAN as the only available real-time navigation. The initial ship velocity estimates from this source at one minute time intervals look quite variable. Raw GPS fixes from Leica/Magnavox 9212 receivers at 5 second intervals may have been recorded by the ship's logging system and will be extracted post-cruise from the master log tapes. Raw GPS from the OBS group GPS Trimble VX6 receiver were also recorded each second. The antenna for this receiver was poorly located beneath a large ship's mast, so may have biases due to invisible satellites or multipath from time to time.

We recorded the Truetime GPS clock output to obtain the time of each shot. On other cruises, this might not be available, and one would have to trust the OYO

time to interpolate navigation in locating each shot. Since the OYO does not output, nor can it input, either time, file number, or shot, some unique label needs to be common to the navigation and the seismic data.

It would be extremely useful to have raw GPS available, or to have someone on the ship who understands the system filter characteristics so navigation quality control can be accomplished during the cruise. This especially affects gravity quality, but also MCS shot navigation.

We were unsuccessful in determining the location of the guns relative to the streamer or stern. From geometry, we expected the gun to 1st active section distance to be ≈110 m. From travel time calculations of the direct wave traveling down the cable, the distance seems to have been ≈75 m. We can't reconcile such a large error or find a timing error which could cause this. However, while doing the moveout analysis for the stacks, an airgun-1st channel offset of 110 m and a water velocity of 1505-1510 m/s resulted in a flat water bottom. This will be further investigated post-cruise.

From tow angle and other geometry, we think that the guns were ≈12 m deep, but this too is ambiguous. We will look for ghost notches in the spectrum of recorded data to see if we can determine gun depth. Use of floats for the air guns would eliminate ambiguity in gun depths.

We produced raw stacked sections on the ship for selected areas of interest for ≈20 hours of shooting. We estimated the average velocity by plotting WGS-84 great circle distance from the lines' endpoints vs. each minute of time. We used 50 m bins, giving a fold of 30+ for a standard simple marine sort. Velocities were estimated by examining moved out gathers.

TABLE OF GEOMETRY AND TIMING

nav antenna to stern	58 m	(from ship's plans, frame 82)
obs gps antenna to stern	17 m	(from ship's plans, frame 27)
gun slant range stern to gun	27.3 m	(from gun tech report)
stern to gun offset	18 m	(? see discussion)
gun depth	12 m	(? see discussion)
stern to center first active	123 m	(? see discussion)
gun to center first active	105 m	(? see discussion)

Autosync WG start to pressure peak	465 ms nominal; much jitter
Autosync AG start to pressure peak	460 ms; jitter ~3 ms

48 CHANNEL LINE SUMMARY

line	day.hrmn	file	tape
301	46.0345	570	8
	46.0517	842	8
401	46.0517	843	8
	47.2238	8259	15
402	47.2345	8438	15
	48.0430	9296	16
403	48.0501	9391	16
	49.1421	15383	21
404	49.1423	1	22
	59.2017	3578	23
501	51.1122	1	27
	53.0100	6767	32

601	53.1516	1	33
	54.0420	2324	35

Institute for Geophysics, The University of Texas at Austin

KH98-1 Leg 2 Seismic Reflection Line Log

Line	101
Vessel	R/V Hakuho Maru
Area	Ontong Java Plateau—Eastern Salient
Survey Number	KH98-1 Leg 2

Line Information	Time (UTC)	Shot Point	Tape Number
Acquisition Start	43.1602	571	1
Acquisition Stop	44.0118	3894	4

Line Details	Start of Line (FSP)	End of Line (LSP)
Wind Direction/Speed		
Feather Angle	Hdg=31°	Hdg=33°
Water Depth	3478	1976
Primary Navigation	GPS	GPS
Latitude	5°59.87′S	4°54.00′S
Longitude	163°37.15′E	164°18.06′E
Source Volume	4.5 l	4.5 l
Bad Traces		

Underway Geophysical Data	
SeaBeam	Center Beam Only
12 kHz Echo Sounder/Transducer Depth	
3.5 kHz Echo Sounder/Transducer Depth	Yes/
Gravity	Yes
Magnetics	Yes
Magnetometer Distance from Stern	

Comments

Institute for Geophysics, The University of Texas at Austin

KH98-1 LEG 2 SEISMIC ACQUISITION RECORDING PARAMETERS

Line	101
Sample Interval	2.0 ms
Sample Length	8.0 s
Trace Length	12.5 m
Seismic Traces on Tape	24
Seismic Channels	24
Gun Sensors	0
Sonobuoy Channels	0
Low Cut Filter	3 Hz
High Cut Filter	125 Hz
First Group Offset (source midpoint to first group)	
Energy Source Offset (stern to source midpoint)	≈10 m (get precise #)
Tow Leader Length	≈300 m (get precise #)
Shot Interval	10 s
Shot Spacing	variable
Ship Speed	nominal 8 kts
Vessel	R/V *Hakuho Maru*
Area	Ontong Java Plateau
Survey Number	KH98-1 Leg 2
Number of Airguns	1
Volume of Airguns	4.5 l
Total Source Volume	4.5 l
Airgun Pressure	1800 psi
Gun Fire Time	465 ms
Firing Randomizer Limits	500 ms (±250 ms)
Number of Birds	2
Location(s) of Birds	before channels 1, 13
Cable Depth	10 m
Gun Depth	≈ 5 m
Tail Rope Length	
GPS Antenna to Stern Distance	58 m

Institute for Geophysics, The University of Texas at Austin

KH98-1 LEG 2 SEISMIC REFLECTION LINE LOG

Line	102
Vessel	R/V Hakuho Maru
Area	Ontong Java Plateau—Eastern Salient
Survey Number	KH98-1 Leg 2

LINE INFORMATION	Time (UTC)	Shot Point	Tape Number
Acquisition Start	44.0329	4664	5
Acquisition Stop	44.0936	6864	5

LINE DETAILS	Start of Line (FSP)	End of Line (LSP)
Wind Direction/Speed		
Feather Angle	Hdg=302°	Hdg=302°
Water Depth	1706	1571
Primary Navigation	GPS	GPS
Latitude	5°05.71′S	4°39.02′S
Longitude	164°25.26′E	163°40.72′E
Source Volume	4.5 l	4.5 l
Bad Traces		

UNDERWAY GEOPHYSICAL DATA	
SeaBeam	Center Beam Only
12 kHz Echo Sounder/Transducer Depth	
3.5 kHz Echo Sounder/Transducer Depth	Yes/
Gravity	Yes
Magnetics	Yes
Magnetometer Distance from Stern	

COMMENTS

Institute for Geophysics, The University of Texas at Austin

KH98-1 LEG 2 SEISMIC ACQUISITION RECORDING PARAMETERS

Line	102
Sample Interval	2.0 ms
Sample Length	8.0 s
Trace Length	12.5 m
Seismic Traces on Tape	24
Seismic Channels	24
Gun Sensors	0
Sonobuoy Channels	0
Low Cut Filter	3 Hz
High Cut Filter	125 Hz
First Group Offset (source midpoint to first group)	
Energy Source Offset (stern to source midpoint)	≈10 m (get precise #)
Tow Leader Length	≈300 m (get precise #)
Shot Interval	10 s
Shot Spacing	variable
Ship Speed	nominal 8 kts
Vessel	R/V *Hakuho Maru*
Area	Ontong Java Plateau
Survey Number	KH98-1 Leg 2
Number of Airguns	1
Volume of Airguns	4.5 l
Total Source Volume	4.5 l
Airgun Pressure	1800 psi
Gun Fire Time	465 ms
Firing Randomizer Limits	500 ms (±250 ms)
Number of Birds	2
Location(s) of Birds	before channels 1, 13
Cable Depth	10 m
Gun Depth	≈ 5 m
Tail Rope Length	
GPS Antenna to Stern Distance	58 m

Institute for Geophysics, The University of Texas at Austin

KH98-1 Leg 2 Seismic Reflection Line Log

Line	103
Vessel	R/V Hakuho Maru
Area	Ontong Java Plateau—Eastern Salient
Survey Number	KH98-1 Leg 2

Line Information	Time (UTC)	Shot Point	Tape Number
Acquisition Start	44.1116	7460	5
Acquisition Stop	44.1300	8084	6

Line Details	Start of Line (FSP)	End of Line (LSP)
Wind Direction/Speed		
Feather Angle	Hdg=30°	Hdg=33°
Water Depth	1585	1819
Primary Navigation	GPS	GPS
Latitude	4°48.26′S	4°35.78′S
Longitude	163°46.09′E	163°53.53′E
Source Volume	4.5 l	4.5 l
Bad Traces		

Underway Geophysical Data	
SeaBeam	Center Beam Only
12 kHz Echo Sounder/Transducer Depth	
3.5 kHz Echo Sounder/Transducer Depth	Yes/
Gravity	Yes
Magnetics	Yes
Magnetometer Distance from Stern	

Comments

KH98-1 LEG 2 SEISMIC ACQUISITION RECORDING PARAMETERS

Line	103
Sample Interval	2.0 ms
Sample Length	8.0 s
Trace Length	12.5 m
Seismic Traces on Tape	24
Seismic Channels	24
Gun Sensors	0
Sonobuoy Channels	0
Low Cut Filter	3 Hz
High Cut Filter	125 Hz
First Group Offset (source midpoint to first group)	
Energy Source Offset (stern to source midpoint)	≈10 m (get precise #)
Tow Leader Length	≈300 m (get precise #)
Shot Interval	10 s
Shot Spacing	variable
Ship Speed	nominal 8 kts
Vessel	R/V *Hakuho Maru*
Area	Ontong Java Plateau
Survey Number	KH98-1 Leg 2
Number of Airguns	1
Volume of Airguns	4.5 l
Total Source Volume	4.5 l
Airgun Pressure	1800 psi
Gun Fire Time (initial firing delay)	465 ms
Firing Randomizer Limits	500 ms (±250 ms)
Number of Birds	2
Location(s) of Birds	before channels 1, 13
Cable Depth	10 m
Gun Depth	≈ 5 m
Tail Rope Length	
GPS Antenna to Stern Distance	58 m

Institute for Geophysics, The University of Texas at Austin

KH98-1 Leg 2 Seismic Reflection Line Log

Line	201
Vessel	R/V Hakuho Maru
Area	Nauru Basin
Survey Number	KH98-1 Leg 2

Line Information	Time (UTC)	Shot Point	Tape Number
Acquisition Start	45.0406	1	7
Acquisition Stop	45.1000	1023	7

Line Details	Start of Line (FSP)	End of Line (LSP)
Wind Direction/Speed	62°/7 kts	65°/7 kts
Feather Angle	Crs=28°, Hdg=46°	
Water Depth	4434 m	4430 m
Primary Navigation	GPS	GPS
Latitude	1°33.13'S	1°13.65'S
Longitude	165°23.76'E	165°34.43'E
Bad Traces	1, 10, 24	1, 10, 24

Underway Geophysical Data	
SeaBeam	Center Beam Only
12 kHz Echo Sounder/Transducer Depth	
3.5 kHz Echo Sounder/Transducer Depth	Yes/
Gravity	Yes
Magnetics	Yes
Magnetometer Distance from Stern	

Comments

Airgun Summary
45.041720-45.043600: 1 x 20 l, 1 x 17 l, 1 x 20 l @ 1600 psi
45.043600-45.080523: 1 x 20 l, 1 x 17 l, 1 x 20 l @ 1500 psi
45.080523-45.100000: 1 x 20 l, 1 x 17 l, 1 x 20 l @ 1800 psi

Institute for Geophysics, The University of Texas at Austin

KH98-1 Leg 2 Seismic Acquisition Recording Parameters

Line	201
Sample Interval	2.0 ms
Sample Length	16 s
Trace Length	12.5 m
Seismic Traces on Tape	24
Seismic Channels	24
Gun Sensors	0
Sonobuoy Channels	1
Low Cut Filter	3 Hz
High Cut Filter	125 Hz
First Group Offset (source midpoint to first group)	
Energy Source Offset (stern to source midpoint)	
Tow Leader Length	
Shot Interval	20 s
Shot Spacing	variable
Ship Speed	nominal 5 kts
Vessel	R/V *Hakuho Maru*
Area	Nauru Basin
Survey Number	KH98-1 Leg 2
Number of Airguns	3
Volume of Airguns	2 x 20 l, 1 x 17 l
Total Source Volume	57 l
Airgun Pressure	1500-1800 psi
Gun Fire Time (initial firing delay)	465 ms
Firing Randomizer Limits	500 ms (±250 ms)
Number of Birds	2
Location(s) of Birds	before channels 1, 13
Cable Depth	10 m
Gun Depth	≈10 m
Tail Rope Length	
GPS Antenna to Stern Distance	58.4 m

Institute for Geophysics, The University of Texas at Austin

KH98-1 LEG 2 SEISMIC REFLECTION LINE LOG

Line	301
Vessel	R/V Hakuho Maru
Area	Ontong Java Plateau
Survey Number	KH98-1 Leg 2

LINE INFORMATION	Time (UTC)	Shot Point	Tape Number
Acquisition Start	46.0345	570	8
Acquisition Stop	46.0517	842	8

LINE DETAILS	Start of Line (FSP)	End of Line (LSP)
Wind Direction/Speed		
Feather Angle	Hdg=99°	Hdg=262°
Water Depth	4335 m	4338 m
Primary Navigation	GPS	GPS
Latitude	0°27.20′N	0°26.14′N
Longitude	166°15.78′E	166°15.77′E
Bad Traces		

UNDERWAY GEOPHYSICAL DATA	
SeaBeam	Center Beam Only
12 kHz Echo Sounder/Transducer Depth	
3.5 kHz Echo Sounder/Transducer Depth	Yes/
Gravity	Yes
Magnetics	Yes
Magnetometer Distance from Stern	

COMMENTS—Gun tests - no useful information.

Airgun Summary
46.0345-46.034700: 1 x 1200 in^3, 1 x 1000 in^3 @ 1500 psi
46.034700-46.051721: 1 x 1200 in^3, 1 x 1000 in^3 @ 1600 psi

Institute for Geophysics, The University of Texas at Austin

KH98-1 LEG 2 SEISMIC ACQUISITION RECORDING PARAMETERS

Line	301
Sample Interval	2.0 ms
Sample Length	16 s
Trace Length	25 m
Seismic Traces on Tape	50
Seismic Channels	48
Gun Sensors	0
Sonobuoy Channels	1
Low Cut Filter	3 Hz
High Cut Filter	125 Hz
First Group Offset (source midpoint to first group)	calculate (105.5 field)
Energy Source Offset (stern to source midpoint)	20 m
Tow Leader Length (stern to first group midpoint)	115 m
Shot Interval	20 s
Shot Spacing	variable
Ship Speed	nominal 5 kts
Vessel	R/V *Hakuho Maru*
Area	Ontong Java Plateau
Survey Number	KH98-1 Leg 2
Number of Airguns	2
Volume of Airguns	1 x 1200 in^3, 1 x 1000 in^3
Total Source Volume	2200 in^3
Airgun Pressure	1500-1600 psi
Gun Fire Time	465 ms
Firing Randomizer Limits	500 ms (±250 ms)
Number of Birds	5
Location(s) of Birds	pre-1, 13, 25, 37; post-48
Cable Depth	10 m
Gun Depth	≈10 m
Tail Rope Length (+ 12 m trailer)	100 m
GPS Antenna to Stern Distance	58 m

Gun tests - no useful MCS data.

Institute for Geophysics, The University of Texas at Austin

KH98-1 Leg 2 Seismic Reflection Line Log

Line	401
Vessel	R/V Hakuho Maru
Area	Ontong Java Plateau
Survey Number	KH98-1 Leg 2

Line Information	Time (UTC)	Shot Point	Tape Number
Acquisition Start	46.0517	843	8
Acquisition Stop	47.2238	8259-8349*	15

Line Details	Start of Line (FSP)	End of Line (LSP)
Wind Direction/Speed	120/8 m/s	
Feather Angle	261.5/258.7	
Water Depth	4338	3543
Primary Navigation	GPS	GPS
Latitude	0°26.12′N	0°24.43′S
Longitude	166°15.77′E	161°23.10′E
Bad Traces		

Underway Geophysical Data	
SeaBeam	Center Beam Only
12 kHz Echo Sounder/Transducer Depth	
3.5 kHz Echo Sounder/Transducer Depth	Yes/
Gravity	Yes
Magnetics	Yes
Magnetometer Distance from Stern	

Comments

*use time

Gun Summary

46.051721-47.043200: 1 x 1200 in³, 1 x 1000 in³ @ 1600 psi
47.043200-47.043240: 1 x 1200 in³, 1 x 1000 in³, 1 x 1200 in³ @ 1600 psi
47.043240-47.051620: 1 x 1200 in³, 1 x 1000 in³ @ 1600 psi
47.051620-47.052820: 1 x 1200 in³, 1 x 1000 in³, 1 x 1000 in³ @ 1600 psi
47.052820-47.222600: 1 x 1200 in³, 1 x 1000 in³ @ 1600 psi
47.222600-47.223820: 1 x 1200 in³, 1 x 1000 in³, 1 x 1000 in³ @ 1650 psi
47.223820 (end): 1 x 1000 in³ @ 1650 psi

Institute for Geophysics, The University of Texas at Austin

KH98-1 LEG 2 SEISMIC ACQUISITION RECORDING PARAMETERS

Line	401
Sample Interval	2.0 ms
Sample Length	16 s
Trace Length	12.5 m
Seismic Traces on Tape	50
Seismic Channels	48
Gun Sensors	2
Sonobuoy Channels	1
Low Cut Filter	3 Hz
High Cut Filter	125 Hz
First Group Offset (source midpoint to first group)	calculate (105.5 m field)
Energy Source Offset (stern to source midpoint)	20 m
Tow Leader Length (stern to first group midpoint)	115 m
Shot Interval	20 s
Shot Spacing	variable
Ship Speed	nominal 5 kts
Vessel	R/V *Hakuho Maru*
Area	Ontong Java Plateau
Survey Number	KH98-1 Leg 2
Number of Airguns	variable
Volume of Airguns	variable
Total Source Volume	1000 in^3-3400 in^3
Airgun Pressure	1600-1650 psi
Gun Fire Time	465 ms
Firing Randomizer Limits	500 ms (±250 ms)
Number of Birds	5
Location(s) of Birds	pre-1, 13, 25, 37; post-48
Cable Depth	10 m
Gun Depth	≈10 m
Tail Rope Length	100 m
GPS Antenna to Stern Distance	58 m

Institute for Geophysics, The University of Texas at Austin

KH98-1 Leg 2 Seismic Reflection Line Log

Line	402
Vessel	R/V Hakuho Maru
Area	Ontong Java Plateau
Survey Number	KH98-1 Leg 2

Line Information	Time (UTC)	Shot Point	Tape Number
Acquisition Start	47.2345	>8438 (use time)	15
Acquisition Stop	48.0430	9296	16

Line Details	Start of Line (FSP)	End of Line (LSP)
Wind Direction/Speed	45°/10 kts	
Feather Angle	Hdg=79°	Hdg=78°
Water Depth	3459	3648
Primary Navigation	GPS	GPS
Latitude	0°26.27'S	0°24.11'S
Longitude	161°15.76'E	161°31.43'E
Bad Traces		

Underway Geophysical Data	
SeaBeam	Center Beam Only
12 kHz Echo Sounder/Transducer Depth	
3.5 kHz Echo Sounder/Transducer Depth	Yes/
Gravity	Yes
Magnetics	Yes
Magnetometer Distance from Stern	

Comments

Airgun Summary

47.234520-48.021000: 1 x 1200 in^3, 1 x 1000 in^3, 1 x 1000 in^3 @ 1650 psi
48.021000-48.035700: 1 x 1200 in^3, 1 x 1000 in^3 @ 1600 psi
48.035700-48.041040: 1 x 1200 in^3, 1 x 1000 in^3, 1 x 1000 in^3 @ 1600 psi
48.041040-48.043000: 1 x 1200 in^3, 1 x 1000 in^3 @ 1700 psi

Institute for Geophysics, The University of Texas at Austin

KH98-1 LEG 2 SEISMIC ACQUISITION RECORDING PARAMETERS

Line	402
Sample Interval	2.0 ms
Sample Length	16 s
Trace Length	12.5 m
Seismic Traces on Tape	50
Seismic Channels	48
Gun Sensors	3
Sonobuoy Channels	1
Low Cut Filter	3 Hz
High Cut Filter	125 Hz
First Group Offset (source midpoint to first group)	calculate (105.5 field)
Energy Source Offset (stern to source midpoint)	20 m
Tow Leader Length (stern to first group midpoint)	115 m
Shot Interval	20 s
Shot Spacing	variable
Ship Speed	nominal 5 kts
Vessel	R/V *Hakuho Maru*
Area	Ontong Java Plateau
Survey Number	KH98-1 Leg 2
Number of Airguns	variable
Volume of Airguns	variable
Total Source Volume	2200 in^3-3200 in^3
Airgun Pressure	1600-1700 psi
Gun Fire Time	465 ms
Firing Randomizer Limits	500 ms (±250 ms)
Number of Birds	5
Location(s) of Birds	pre-1, 13, 25, 37; post-48
Cable Depth	10 m
Gun Depth	≈10 m
Tail Rope Length	100 m
GPS Antenna to Stern Distance	58 m

Institute for Geophysics, The University of Texas at Austin

KH98-1 LEG 2 SEISMIC REFLECTION LINE LOG

Line	403
Vessel	R/V Hakuho Maru
Area	Ontong Java Plateau
Survey Number	KH98-1 Leg 2

LINE INFORMATION	Time (UTC)	Shot Point	Tape Number
Acquisition Start	48.0501	9391	16
Acquisition Stop	49.1421	15383	21

LINE DETAILS	Start of Line (FSP)	End of Line (LSP)
Wind Direction/Speed	20°/5.7 kts	
Feather Angle	Hdg=263°	Hdg=254°
Water Depth	3118	1871
Primary Navigation	GPS	GPS
Latitude	0°23.29′S	1°04.47°S
Longitude	161°29.33′E	157°36.40′E
Bad Traces		

UNDERWAY GEOPHYSICAL DATA	
SeaBeam	Center Beam Only
12 kHz Echo Sounder/Transducer Depth	
3.5 kHz Echo Sounder/Transducer Depth	Yes/
Gravity	Yes
Magnetics	Yes
Magnetometer Distance from Stern	

COMMENTS

Airgun Summary

48.050152-48.1310: 1 x 1200 in^3, 1 x 1000 in^3, 1 x 1000 in^3 @ 1700 psi
48.1310-48.152400: 1 x 1200 in^3, 1 x 1000 in^3 @ 1700 psi
48.152400-48.1730: 1 x 1200 in^3, 1 x 1000 in^3, 1 x 1200 in^3 @ 1700 psi
48.1730-48.1902: frequent changes of combination
48.1902-49.1421: 1 x 1200 in^3, 1 x 1000 in^3, 1 x 1200 in^3 @ 1700 psi

Institute for Geophysics, The University of Texas at Austin

KH98-1 LEG 2 SEISMIC ACQUISITION RECORDING PARAMETERS

Line	403
Sample Interval	2.0 ms
Sample Length	16 s
Trace Length	12.5 m
Seismic Traces on Tape	50
Seismic Channels	48
Gun Sensors	3
Sonobuoy Channels	1
Low Cut Filter	3 Hz
High Cut Filter	125 Hz
First Group Offset (source midpoint to first group)	calculate (105.5 field)
Energy Source Offset (stern to source midpoint)	20 m
Tow Leader Length (stern to first group midpoint)	115 m
Shot Interval	20 s
Shot Spacing	variable
Ship Speed	nominal 5 kts
Vessel	R/V *Hakuho Maru*
Area	Ontong Java Plateau
Survey Number	KH98-1 Leg 2
Number of Airguns	variable
Volume of Airguns	variable
Total Source Volume	2200 in^3-3400 in^3
Airgun Pressure	1700 psi
Gun Fire Time	465 ms
Firing Randomizer Limits	500 ms (±250 ms)
Number of Birds	5
Location(s) of Birds	pre-1, 13, 25, 37; post-48
Cable Depth	10 m
Gun Depth	≈10 m
Tail Rope Length	100 m
GPS Antenna to Stern Distance	58 m

Institute for Geophysics, The University of Texas at Austin

KH98-1 Leg 2 Seismic Reflection Line Log

Line	404
Vessel	R/V Hakuho Maru
Area	Ontong Java Plateau
Survey Number	KH98-1 Leg 2

Line Information	Time (UTC)	Shot Point	Tape Number
Acquisition Start	49.1423	1	22
Acquisition Stop	50.1017	3578	25

Line Details	Start of Line (FSP)	End of Line (LSP)
Wind Direction/Speed		38°/4.4 kts
Feather Angle	Hdg=254°	Crs=260°, Hdg=257°
Water Depth	1871 m	2147 m
Primary Navigation	GPS	GPS
Latitude	1°04.47'S	1°28.16'S
Longitude	157°36.40'E	155°18.13'E
Bad Traces		

Underway Geophysical Data	
SeaBeam	Center Beam Only
12 kHz Echo Sounder/Transducer Depth	
3.5 kHz Echo Sounder/Transducer Depth	Yes/
Gravity	Yes
Magnetics	Yes
Magnetometer Distance from Stern	

Comments

Airgun Summary

49.142340-50.003320: 1 x 1200 in^3, 1 x 1000 in^3, 1 x 1200 in^3 @ 1700 psi
50.003320-50.003940: 1 x 1200 in^3, 1 x 1200 in^3 @ 1700 psi
50.003940-50.101743: 1 x 1200 in^3, 1 x 1000 in^3, 1 x 1200 in^3 @ 1700 psi

Institute for Geophysics, The University of Texas at Austin

KH98-1 LEG 2 SEISMIC ACQUISITION RECORDING PARAMETERS

Line	404
Sample Interval	2.0 ms
Sample Length	16 s
Trace Length	12.5 m
Seismic Traces on Tape	50
Seismic Channels	48
Gun Sensors	3
Sonobuoy Channels	1
Low Cut Filter	3 Hz
High Cut Filter	125 Hz
First Group Offset (source midpoint to first group)	calculate (105.5 field)
Energy Source Offset (stern to source midpoint)	20 m
Tow Leader Length (stern to first group midpoint)	115 m
Shot Interval	20 s
Shot Spacing	variable
Ship Speed	nominal 5 kts
Vessel	R/V *Hakuho Maru*
Area	Ontong Java Plateau
Survey Number	KH98-1 Leg 2
Number of Airguns	variable
Volume of Airguns	variable
Total Source Volume	2400 in^3-3400 in^3
Airgun Pressure	1700 l
Gun Fire Time	465 ms
Firing Randomizer Limits	500 ms (±250 ms)
Number of Birds	5
Location(s) of Birds	pre-1, 13, 25, 37; post-48
Cable Depth	10 m
Gun Depth	≈10 m
Tail Rope Length	100 m
GPS Antenna to Stern Distance	58 m

52.010120-52.010820: 1 x 1200 in^3 @ 1650 psi
52.010820-52.010900: 1 x 1000 in^3, 1 x 1200 in^3 @ 1650 psi
52.010900-52.040240: 1 x 1200 in^3, 1 x 1000 in^3, 1 x 1200 in^3 @ 1700 psi
52.040240-52.053620: 1 x 1200 in^3, 1 x 1200 in^3 @ 1700 psi
52.053620-52.053900: 1 x 1200 in^3 @ 1650 psi
52.053900-52.053940: 1 x 1200 in^3, 1 x 1200 in^3 @ 1650 psi
52.053940-52.133420: 1 x 1200 in^3, 1 x 1000 in^3, 1 x 1200 in^3 @ 1700 psi
52.133420-52.150000: 1 x 1200 in^3, 1 x 1200 in^3 @ 1700 psi
52.150000-52.1606: 1 x 1200 in^3, 1 x 1000 in^3, 1 x 1200 in^3 @ 1650 psi
52.1606-52.171340: 1 x 1000 in^3, 1 x 1200 in^3 @ 1600 psi
52.171340-53.010000: 1 x 1200 in^3, 1 x 1000 in^3, 1 x 1200 in^3 @ 1650-1700 psi

Check channel 30: dead at start, appears active @ 51.2315

Institute for Geophysics, The University of Texas at Austin

KH98-1 LEG 2 SEISMIC ACQUISITION RECORDING PARAMETERS

Line	501
Sample Interval	2.0 ms
Sample Length	16 s
Trace Length	12.5 m
Seismic Traces on Tape	50
Seismic Channels	48
Gun Sensors	3
Sonobuoy Channels	1
Low Cut Filter	3 Hz
High Cut Filter	125 Hz
First Group Offset (source midpoint to first group)	calculate (105.5 field)
Energy Source Offset (stern to source midpoint)	20 m
Tow Leader Length (stern to first group midpoint)	115 m
Shot Interval	20 s
Shot Spacing	variable
Ship Speed	nominal 5 kts
Vessel	R/V *Hakuho Maru*
Area	Ontong Java Plateau
Survey Number	KH98-1 Leg 2
Number of Airguns	variable
Volume of Airguns	variable
Total Source Volume	1200 in^3-3400 in^3
Airgun Pressure	1600-1700 psi
Gun Fire Time	460 ms
Firing Randomizer Limits	500 ms (±250 ms)
Number of Birds	5
Location(s) of Birds	pre-1, 13, 25, 37; post-48
Cable Depth	10 m
Gun Depth	≈10 m
Tail Rope Length	100 m
GPS Antenna to Stern Distance	58 m

Institute for Geophysics, The University of Texas at Austin

KH98-1 Leg 2 Seismic Reflection Line Log

Line	601
Vessel	R/V Hakuho Maru
Area	Ontong Java Plateau
Survey Number	KH98-1 Leg 2

Line Information	Time (UTC)	Shot Point	Tape Number
Acquisition Start	53.1516	1	33
Acquisition Stop	54.0420	2324	35

Line Details	Start of Line (FSP)	End of Line (LSP)
Wind Direction/Speed	59°/6.6 kts	
Feather Angle	198°	
Water Depth	2213	
Primary Navigation	GPS	GPS
Latitude	0°10.9851'S	1°24.30'S
Longitude	158°39.645'E	158°02.40'E
Bad Traces		

Underway Geophysical Data	
SeaBeam	Center Beam Only
12 kHz Echo Sounder/Transducer Depth	
3.5 kHz Echo Sounder/Transducer Depth	Yes/
Gravity	Yes
Magnetics	Yes
Magnetometer Distance from Stern	

Comments

Airgun Summary

53.151600-53.1532: 1 x 1200 in^3, 1 x 1000 in^3, 1 x 1200 in^3 @ 1100 psi
53.1532-53.160000: 1 x 1200 in^3, 1 x 1000 in^3 @ 1100 psi
53.160000-53.161200: no guns
53.161200-53.170820: 1 x 1200 in^3, 1 x 1000 in^3 @ 1600 psi
53.170820-54.025920: 1 x 1200 in^3, 1 x 1000 in^3, 1 x 1200 in^3 @ 1650 psi
54.025920-54.042040: 1 x 1000 in^3, 1 x 1200 in^3 @ 1700 psi

Institute for Geophysics, The University of Texas at Austin

KH98-1 LEG 2 SEISMIC ACQUISITION RECORDING PARAMETERS

Line	601
Sample Interval	2.0 ms
Sample Length	16 s
Trace Length	12.5 m
Seismic Traces on Tape	50
Seismic Channels	48
Gun Sensors	3
Sonobuoy Channels	1
Low Cut Filter	3 Hz
High Cut Filter	125 Hz
First Group Offset (source midpoint to first group)	calculate (105.5 field)
Energy Source Offset (stern to source midpoint)	20 m
Tow Leader Length (stern to first group midpoint)	115 m
Shot Interval	20 s
Shot Spacing	variable
Ship Speed	nominal 5 kts
Vessel	R/V *Hakuho Maru*
Area	Ontong Java Plateau
Survey Number	KH98-1 Leg 2
Number of Airguns	variable
Volume of Airguns	variable
Total Source Volume	2200 in^3-3400 in^3
Airgun Pressure	1100-1700 psi
Gun Fire Time	460 ms
Firing Randomizer Limits	500 ms (±250 ms)
Number of Birds	5
Location(s) of Birds	pre-1, 13, 25, 37; post-48
Cable Depth	10 m
Gun Depth	≈10 m
Tail Rope Length	100 m
GPS Antenna to Stern Distance	58 m

KH98-1 Leg 2 Seismic Line Summary

Line	*Area*	*Length*	*Shot Interval*	*Record Length*	*Streamer*	*Source*	*Sonobuoys*
101	Eastern Salient	149 km	10 s	8 s	24-channel, 300 m ITI	4.5 liters	0
102	Eastern Salient	96 km	10 s	8 s	24-channel, 300 m ITI	4.5 liters	0
103	Eastern Salient	27 km	10 s	8 s	24-channel, 300 m ITI	4.5 liters	0
201	Nauru Basin	41 km	20 s	16 s	24-channel, 300 m ITI	3400 in^3	1
301	Gun Tests	2 km	20 s	16 s	48-channel, 1200 m ITI	2200 in^3	0
401	Nauru-OJP	550 km	20 s	16 s	48-channel, 1200 m ITI	1000-3400 in^3	11
402	Nauru-OJP	29 km	20 s	16 s	48-channel, 1200 m ITI	2200-3200 in^3	1
403	Nauru-OJP	438 km	20 s	16 s	48-channel, 1200 m ITI	2200-3400 in^3	12
404	Nauru-OJP	260 km	20 s	16 s	48-channel, 1200 m ITI	2400-3400 in^3	2
501	OJP	364 km	20 s	16 s	48-channel, 1200 m ITI	1200-3400 in^3	5
601	OJP	152 km	20 s	16 s	48-channel, 1200 m ITI	2200-3400 in^3	5

SONOBUOY WIDE-ANGLE SEISMIC VELOCITY ACQUISITION PROGRAM

Olav Eldholm, Lewis J. Abrams, Millard F. Coffin and Mark Wiederspahn

Objectives

The sonobuoy program comprised two parts:

1. Velocity measurements for ODP site survey in Nauru Basin, in particular to investigate whether the acoustic basement reflector represents oceanic basement or sills/flows overlying sediments and "real" oceanic basement. The program was operated by the University of North Carolina-University of Rhode Island group.
2. Velocity measurements on the Ontong Java Plateau and its adjacent Nauru Basin to:
   - determine the velocity structure in the sediments and upper crystalline crust,
   - provide interval velocties for processing of the MCS lines.

   The program was operated by the University of Texas-University of Oslo group.

Five commercial sonobuoys provided by University of North Carolina – Wilmington were available for the Nauru Basin survey (#1-5, Fig. 1, Table 1), and 40 sonobuoys provided by University of Oslo for the Greater Ontong Java Plateau survey (#6-43, Fig. 1, Table 1).

Technical specifications

The University of North Carolina sonobuoys were type AN/SSQ-57A produced by Sparton Electronics, and the University of Oslo military surplus sonobuoys included 38, AN/SSQ-57A and 2 AN/SSQ-41,41A. The sonobuoys operate in the 160-172 MHz frequency range.

The sonobuoy receiving system, provided by University of North Carolina, included a custom-built 2 m dual Yagi antenna mounted at the ships aft mast about 23 m above sea level, and an ICOM-R8500 communications receiver. The signals were fed to the receiver via a 55 m long LMR-400 coaxial cable. The system was installed and tested during the port stay in Cairns.

The radio recorder output was connected to UTIG's Ithaco 481 amplifier operated at 0, -6, -12 dB, and its output was was recorded on the OYO digital recording system's auxiliary channel. The direct wave overdrove the auxiliary channel input at 0 and –6 dB causing coherent noise on all seismic channels.

The analog signal was displayed using a UTIG system. The signal from the amplifier was routed through another 481 amplifier and a Rockland bandpass filter for display on an EPC graphics recorder. Typically, 52dB gain was required. The filter was always set to 100 Hz, 6dB/octave low pass only.

Operation

Of the five commercial sonobuoys, one sank and two got tangled in the streamer and magnetometer cable. The military ones, all of 1984 and older vintage, indeed proved very reliable. Only two did not function properly: one did not surface, and another floated but had no carrier signal. In addition, three buoys were used for testing purposes. Thus, a total of 35 sonobuoy profiles were recorded (Table 1)

SB#2 was recorded along the 24-channel MCS line 200. All other sonobuoy profiles were recorded along the 48-channel MCS lines, while profiling at 5-7 knots over the sea floor. Shot intervals were 20 s., record length 16 s., and sampling interval 2 ms. The signal source varied from one to three 17 and 20 l airguns, operating at ±1600 psi.

Few profiles were affected by major sea floor and/or sub-sea floor topography, and the arrivals of the direct wave through the water document that the vessel maintained a remarkably constant speed with respect to the sonobuoy. On the other hand, westward moving surface currents reaching up to 2.5 knots, show that the assumption of a fixed sonobuoy position relative to the sea floor does not apply.

Profile locations (Fig. 1, Table 1)

MCS line 200

One profile, SB#2, in the Nauru Basin.

Nauru Basin-Ontong Java Plateau Transect (MCS line 400, including a 210-km-long E-W OBS line)

Approximately evenly spaced profiles, SB#5-30, from the Nauru Basin to the OBS line. In addition, one profile SB#31, in the center of the OBS line; and one profile, SB#32, west of OBS 10.

Line 500 (a 210-km-long N-S OBS line)

One profile, SB#35, south of OBS 9; another profile, SB#36, in the center; and two profiles, SB#37-38, north of OBS 1.

Line 600 (DSDP Site 289-Transect tie line)

Five profiles, SB#39-43.

Preliminary results

All profiles have recorded well-defined reflection hyperbolas from intra-sedimentary layers and top acoustic basement, thus providing input for reliable determination of interval velocities within the sedimentary column.

The quality of refracted arrivals improves considerably westward along the Nauru Basin-Ontong Java Plateau Transect. In the Nauru Basin few and relatively poorly defined refractors are observed in the analog records, although shipboard playback of the digital data showed the potential for considerable improvement by digital processing.

The profiles on the Ontong Java Plateau summit and flanks commonly show a series of refracted arrivals. In particular, the profiles on the main plateau reveal a consistent pattern of P-wave refractors, including:

- arrivals from deeper, high-velocity, sedimentary layers.
- strong arrivals from top acoustic basement, and in some profiles converted S-waves.
- weak but, in many profiles persistent, sub-basement arrivals.
- indications of pre-critical, sub-acoustic basement reflection hyperbolas.

Planned processing and data reduction

Preliminary velocities will be determined from the analog records for profiles in the vicinity of proposed ODP drill site locations.

The digital profiles have been copied from the MCS-tapes to a separate sonobuoy tape. At UTIG, the Ontong Java Plateau and adjacent Nauru Basin profiles will be transformed into travel time-range plots, then reduced and interpreted in conjunction with the interpretation of the MCS profiles. The ODP site survey profiles in the Nauru Basin will be analyzed at the University of North Carolina – Wilmington.

SB #	MCS line\ tape\record # \Julian day	Time Z	Lat. start	Long. start	Water depth, m	Comments
1	201\7\302\45	0659-0700			4442	Hit streamer
2	201\7\350-1023\45	0615-1000	165.451	-1.4575	4442-4430	
3	401\8\-\46					No carrier
4	401\9\1717\46	1009			4367	Hit mag.cable
5	401\9-10\1911-2389\46	1114-1354	165.5891	0.3298	4381-4297	
6	401\10\2432-2983\46	1407-1711	165.2730	0.2731	4396-4388	
7	401\10\3003-3519\46	1718-2010	164.9116	0.2168	4391-4370	
8	401\11\3534-4008\46	2015-2253	164.5683	0.1566	4388-4409	
9	401\11\4063\47	2312-0130	164.2223	0.0950	4413-4457	
10	401\12\4653-4710\47	0228-0246			4459-4460	No audio
11	401\12\4710-5158\47	0247-0516	163.7813	0.0183	4450-4450	
12	401\12\5247-5723\47	0546-0825	163.4150	-0.0475	4454-4465	
13	401\13\5727-\47	0826-1100	163.0895	-0.1053	4465-4457	
14	401\13-14\6301-6731\47	1137-1400	162.6843	-0.1768	4451-4422	
15	401\14\6742-7268\47	1404-1700	162.3865	-0.2298	4422-	
16	401\14\7292-7776\47	1708-1949	162.0196	-0.2948	4383-3960	
17	401\15\7797-8218\47	1956-2216	161.6898	-0.3536	3942-3555	
18	402\15-16\8536-\48	0017-	161.2946	-0.4323	3449-	
19	403\16\9417-9889\48	0510-0748	161.4718	-0.3913	3594-3254	
20	403\17\9967-10258\48	0813-0951	161.1090	-0.4560	3253-3052	
21	403\17\10271-10555\48	0955-1130	160.9130	-0.4911	3043-2930	
22	403\17-18\10625-11135\48	1153-1444	160.6891	-0.5300	2922-2918	
23	403\18\11305-\48	1540-1806	160.2570	-0.6078	2914-2765	
24	403\18\11758-12261\48	1811-2059	159.9570	-0.6603	2765-2532	
25	403\19\12332-\48	2122-2330	159.5781	-0.7273	2489-2441	
26	403\19-20\12767-13210\48	2347-0215	159.2915	-0.7783	2407-2244	
27	403\20\13222-13675\49	0219-0451	158.9951	-0.8305	2245-2161	
28	403\20\13691\14242\49	0455-0800	158.6923	-0.8838	2157-2049	
29	403\20\14255-14604\49	0804-1000	158.3330	-0.9468	2056-2004	
30	403\21\14691-\49	1029-1300	158.0565	-0.9958	2004-1996	
31	404\23\1166-1637\49	2053-2330	156.8546	-1.2033	1848-1902	
32	404\24-25\2965-3524\50	0653-1000	155.6945	-1.3998	2106-2136	
33	-\26\1-\51	0555-			1713-	Guntest
34	501\27\177-\51	1220-				No carrier
35	501\27\187-711\51	1224-1520	157.1295	-2.7645	1711-1663	
36	501\30\3469-4067\52	0641-1000	156.8643	-1.2270	1844-1865	
37	501\32\5679-6061\52	1857-2105	156.6771	-0.1560	2012-2008	
38	501\32\6071-6497\52	2108-2330	156.6453	-0.0363	2010-2081	
39	601\33\230-597\53	1648-1845	158.6026	-0.3127	2192-2225	
40	601\33\607-957\53	1848-2045	158.5040	-0.4993	2220-2146	
41	601\33-34\977-1363\53	2050-2300	158.4060	-0.6900	2141-2068	
42	601\34\1505-1931\53	2347-0210	158.2630	-0.9663	2035-1968	
43	601\34\1946-2324\54	0214-0420	158.1445	-1.1991	1971-1963	

Table 1. Sonobuoy profile parameters.

Fig. 1. Location of sonobuoy profiles (small black circles) recorded during KH98-1 Leg 2 (Table 1). Solid lines show MCS profiles, triangles are OBS locations and large circles mark DSDP/ODP sites.

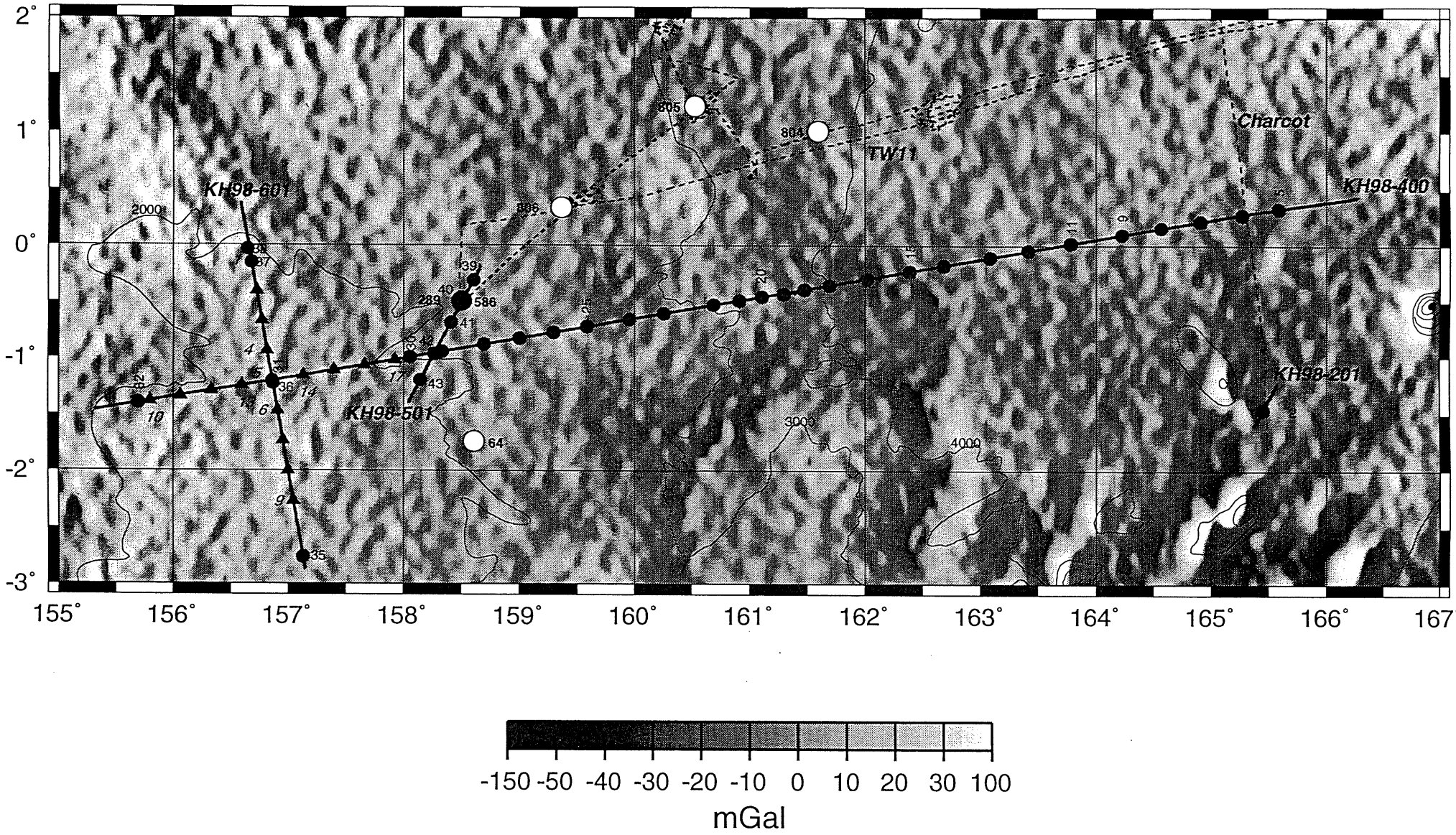

SONOBUOY WIDE-ANGLE SEISMIC VELOCITY ACQUISITION PROGRAM

Olav Eldholm, Lewis J. Abrams, Millard F. Coffin and Mark Wiederspahn

Objectives

The sonobuoy program comprised two parts:

1. Velocity measurements for ODP site survey in Nauru Basin, in particular to investigate whether the acoustic basement reflector represents oceanic basement or sills/flows overlying sediments and "real" oceanic basement. The program was operated by the University of North Carolina-University of Rhode Island group.
2. Velocity measurements on the Ontong Java Plateau and its adjacent Nauru Basin to:
   - determine the velocity structure in the sediments and upper crystalline crust,
   - provide interval velocties for processing of the MCS lines.

   The program was operated by the University of Texas-University of Oslo group.

Five commercial sonobuoys provided by University of North Carolina – Wilmington were available for the Nauru Basin survey (#1-5, Fig. 1, Table 1), and 40 sonobuoys provided by University of Oslo for the Greater Ontong Java Plateau survey (#6-43, Fig. 1, Table 1).

Technical specifications

The University of North Carolina sonobuoys were type AN/SSQ-57A produced by Sparton Electronics, and the University of Oslo military surplus sonobuoys included 38, AN/SSQ-57A and 2 AN/SSQ-41,41A. The sonobuoys operate in the 160-172 MHz frequency range.

The sonobuoy receiving system, provided by University of North Carolina, included a custom-built 2 m dual Yagi antenna mounted at the ships aft mast about 23 m above sea level, and an ICOM-R8500 communications receiver. The signals were fed to the receiver via a 55 m long LMR-400 coaxial cable. The system was installed and tested during the port stay in Cairns.

The radio recorder output was connected to UTIG's Ithaco 481 amplifier operated at 0, -6, -12 dB, and its output was was recorded on the OYO digital recording system's auxiliary channel. The direct wave overdrove the auxiliary channel input at 0 and –6 dB causing coherent noise on all seismic channels.

The analog signal was displayed using a UTIG system. The signal from the amplifier was routed through another 481 amplifier and a Rockland bandpass filter for display on an EPC graphics recorder. Typically, 52dB gain was required. The filter was always set to 100 Hz, 6dB/octave low pass only.

Operation

Of the five commercial sonobuoys, one sank and two got tangled in the streamer and magnetometer cable. The military ones, all of 1984 and older vintage, indeed proved very reliable. Only two did not function properly: one did not surface, and another floated but had no carrier signal. In addition, three buoys were used for testing purposes. Thus, a total of 35 sonobuoy profiles were recorded (Table 1)

SB#2 was recorded along the 24-channel MCS line 200. All other sonobuoy profiles were recorded along the 48-channel MCS lines, while profiling at 5-7 knots over the sea floor. Shot intervals were 20 s., record length 16 s., and sampling interval 2 ms. The signal source varied from one to three 17 and 20 l airguns, operating at ±1600 psi.

Few profiles were affected by major sea floor and/or sub-sea floor topography, and the arrivals of the direct wave through the water document that the vessel maintained a remarkably constant speed with respect to the sonobuoy. On the other hand, westward moving surface currents reaching up to 2.5 knots, show that the assumption of a fixed sonobuoy position relative to the sea floor does not apply.

Profile locations (Fig. 1, Table 1)
MCS line 200
One profile, SB#2, in the Nauru Basin.
Nauru Basin-Ontong Java Plateau Transect (MCS line 400, including a 210-km-long E-W OBS line)
Approximately evenly spaced profiles, SB#5-30, from the Nauru Basin to the OBS line. In addition, one profile SB#31, in the center of the OBS line; and one profile, SB#32, west of OBS 10.
Line 500 (a 210-km-long N-S OBS line)
One profile, SB#35, south of OBS 9; another profile, SB#36, in the center; and two profiles, SB#37-38, north of OBS 1.
Line 600 (DSDP Site 289-Transect tie line)
Five profiles, SB#39-43.

Preliminary results
All profiles have recorded well-defined reflection hyperbolas from intra-sedimentary layers and top acoustic basement, thus providing input for reliable determination of interval velocities within the sedimentary column.

The quality of refracted arrivals improves considerably westward along the Nauru Basin-Ontong Java Plateau Transect. In the Nauru Basin few and relatively poorly defined refractors are observed in the analog records, although shipboard playback of the digital data showed the potential for considerable improvement by digital processing.

The profiles on the Ontong Java Plateau summit and flanks commonly show a series of refracted arrivals. In particular, the profiles on the main plateau reveal a consistent pattern of P-wave refractors, including:
- arrivals from deeper, high-velocity, sedimentary layers.
- strong arrivals from top acoustic basement, and in some profiles converted S-waves.
- weak but, in many profiles persistent, sub-basement arrivals.
- indications of pre-critical, sub-acoustic basement reflection hyperbolas.

Planned processing and data reduction
Preliminary velocities will be determined from the analog records for profiles in the vicinity of proposed ODP drill site locations.

The digital profiles have been copied from the MCS-tapes to a separate sonobuoy tape. At UTIG, the Ontong Java Plateau and adjacent Nauru Basin profiles will be transformed into travel time-range plots, then reduced and interpreted in conjunction with the interpretation of the MCS profiles. The ODP site survey profiles in the Nauru Basin will be analyzed at the University of North Carolina – Wilmington.

SB #	MCS line\ tape\record # \Julian day	Time Z	Lat. start	Long. start	Water depth, m	Comments
1	201\7\302\45	0659-0700			4442	Hit streamer
2	201\7\350-1023\45	0615-1000	165.451	-1.4575	4442-4430	
3	401\8\-\46					No carrier
4	401\9\1717\46	1009			4367	Hit mag.cable
5	401\9-10\1911-2389\46	1114-1354	165.5891	0.3298	4381-4297	
6	401\10\2432-2983\46	1407-1711	165.2730	0.2731	4396-4388	
7	401\10\3003-3519\46	1718-2010	164.9116	0.2168	4391-4370	
8	401\11\3534-4008\46	2015-2253	164.5683	0.1566	4388-4409	
9	401\11\4063\47	2312-0130	164.2223	0.0950	4413-4457	
10	401\12\4653-4710\47	0228-0246			4459-4460	No audio
11	401\12\4710-5158\47	0247-0516	163.7813	0.0183	4450-4450	
12	401\12\5247-5723\47	0546-0825	163.4150	-0.0475	4454-4465	
13	401\13\5727-\47	0826-1100	163.0895	-0.1053	4465-4457	
14	401\13-14\6301-6731\47	1137-1400	162.6843	-0.1768	4451-4422	
15	401\14\6742-7268\47	1404-1700	162.3865	-0.2298	4422-	
16	401\14\7292-7776\47	1708-1949	162.0196	-0.2948	4383-3960	
17	401\15\7797-8218\47	1956-2216	161.6898	-0.3536	3942-3555	
18	402\15-16\8536-\48	0017-	161.2946	-0.4323	3449-	
19	403\16\9417-9889\48	0510-0748	161.4718	-0.3913	3594-3254	
20	403\17\9967-10258\48	0813-0951	161.1090	-0.4560	3253-3052	
21	403\17\10271-10555\48	0955-1130	160.9130	-0.4911	3043-2930	
22	403\17-18\10625-11135\48	1153-1444	160.6891	-0.5300	2922-2918	
23	403\18\11305-\48	1540-1806	160.2570	-0.6078	2914-2765	
24	403\18\11758-12261\48	1811-2059	159.9570	-0.6603	2765-2532	
25	403\19\12332-\48	2122-2330	159.5781	-0.7273	2489-2441	
26	403\19-20\12767-13210\48	2347-0215	159.2915	-0.7783	2407-2244	
27	403\20\13222-13675\49	0219-0451	158.9951	-0.8305	2245-2161	
28	403\20\13691\14242\49	0455-0800	158.6923	-0.8838	2157-2049	
29	403\20\14255-14604\49	0804-1000	158.3330	-0.9468	2056-2004	
30	403\21\14691-\49	1029-1300	158.0565	-0.9958	2004-1996	
31	404\23\1166-1637\49	2053-2330	156.8546	-1.2033	1848-1902	
32	404\24-25\2965-3524\50	0653-1000	155.6945	-1.3998	2106-2136	
33	-\26\1-\51	0555-			1713-	Guntest
34	501\27\177-\51	1220-				No carrier
35	501\27\187-711\51	1224-1520	157.1295	-2.7645	1711-1663	
36	501\30\3469-4067\52	0641-1000	156.8643	-1.2270	1844-1865	
37	501\32\5679-6061\52	1857-2105	156.6771	-0.1560	2012-2008	
38	501\32\6071-6497\52	2108-2330	156.6453	-0.0363	2010-2081	
39	601\33\230-597\53	1648-1845	158.6026	-0.3127	2192-2225	
40	601\33\607-957\53	1848-2045	158.5040	-0.4993	2220-2146	
41	601\33-34\977-1363\53	2050-2300	158.4060	-0.6900	2141-2068	
42	601\34\1505-1931\53	2347-0210	158.2630	-0.9663	2035-1968	
43	601\34\1946-2324\54	0214-0420	158.1445	-1.1991	1971-1963	

Table 1. Sonobuoy profile parameters.

Fig. 1. Location of sonobuoy profiles (small black circles) recorded during KH98-1 Leg 2 (Table 1). Solid lines show MCS profiles, triangles are OBS locations and large circles mark DSDP/ODP sites.

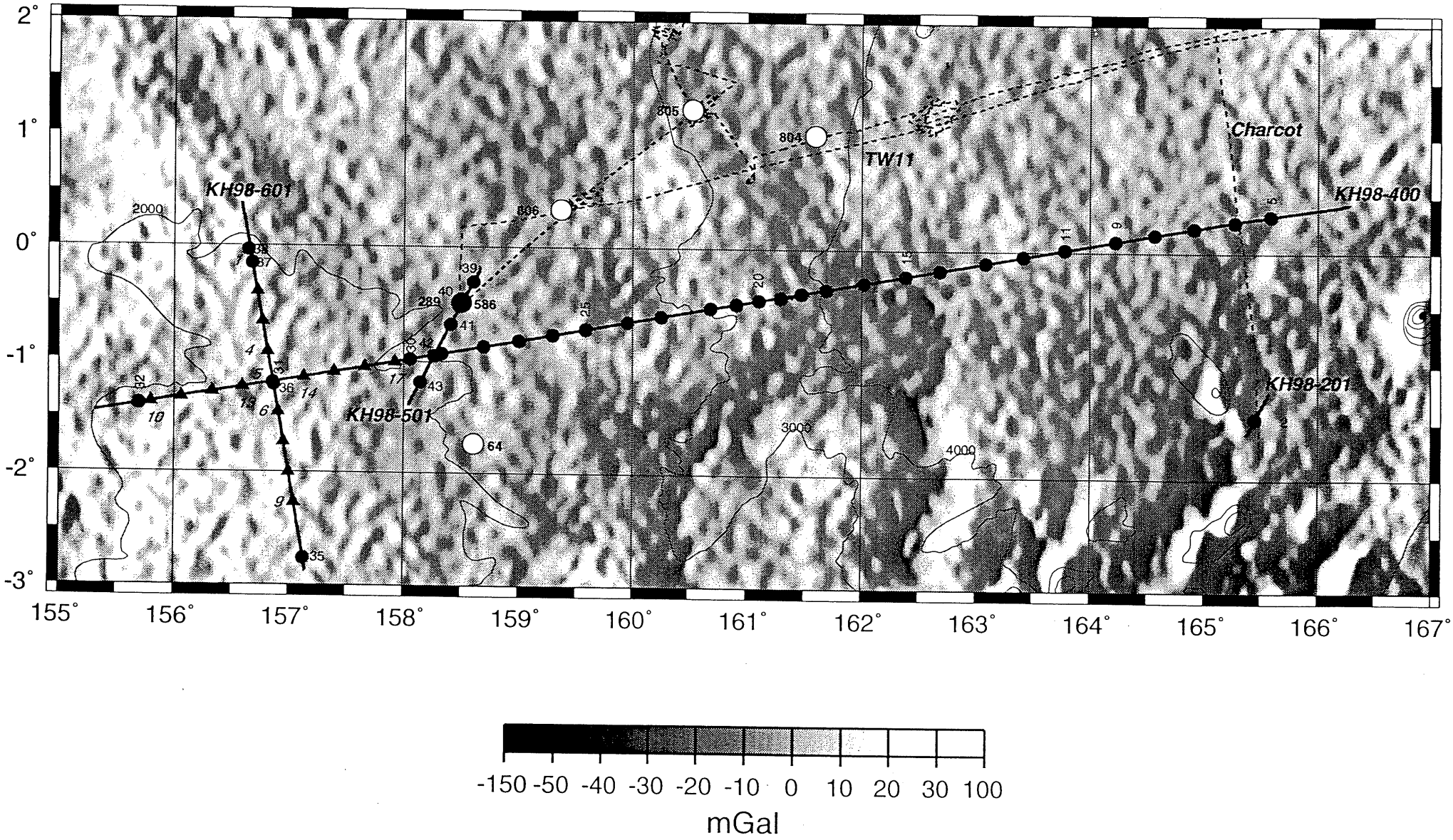

STRUCTURE AND STRATIGRAPHY OF THE OJP-NAURU BASIN TRANSECT AND NORTH-CENTRAL OJP: MCS AND SONOBUOY STUDY

Millard Coffin[1], Kimihiro Mochizuki[2], Mark Wiederspahn[1], Tadeusz Gladczenko[3], and Olav Eldholm[3]

[1]Institute for Geophysics, The University of Texas at Austin
[2]Ocean Research Institute, University of Tokyo
[3]Dept. of Geology, University of Oslo

INTRODUCTION

Episodic, voluminous, mafic magmatism has emplaced large igneous provinces (LIPs)—continental flood basalts, volcanic passive margins, and oceanic plateaus—worldwide. Many such provinces form rapidly by processes not clearly related to plate tectonics. The size and distribution of oceanic plateaus, broad regions of anomalously thick crust, demonstrate that their emplacements are major global geological events (e.g., Coffin & Eldholm, 1994). At present, ~6% of the Earth's heat flux is represented by LIP emplacement (Davies, 1988; Sleep, 1990), although in parts of the Early Cretaceous, perhaps 50% of the total flux originated at LIPs, especially via the two giant oceanic plateaus—Ontong Java (OJP) and Kerguelen. The geodynamic processes that have resulted in LIP formation on Earth, Venus, Mars, and the Moon are poorly understood (Head & Coffin, 1997), yet have enormous significance for increasing our knowledge of solid earth circulation and of links between the solid earth and the environment. LIPs may form in response to rising mantle plumes ("plume heads"), originating in either the upper or the lower mantle, causing huge mantle melting events. Other theories suggest more continuous emplacement, e.g., the long-lived igneous activity at Iceland (e.g., Coffin & Gahagan, 1995), which apparently originates entirely in the upper mantle.

Oceanic plateaus, by virtue of their predominant structural setting on oceanic lithosphere, offer the best potential for providing needed boundary conditions for

improved geophysical, petrologic, and geochemical modeling of LIP emplacement. No oceanic plateau, however, is well-characterized by seismic imaging, and only one drill hole (ODP Site 807, OJP) has penetrated >100 m into oceanic plateau basement. As a result, no unambiguous genesis for this class of LIP has yet been hypothesized. Critically-needed geophysical constraints from plateaus include: 1) sedimentary and igneous stratigraphic relationships, and 2) crustal velocity information.

ONTONG JAVA PLATEAU

The OJP encompasses 1.86 x 10^6 km^2 of the western equatorial Pacific. The plateau's southern margins, bounded by trenches, mark where it is colliding with the Solomon Islands arc (Fig. 1). Towards the trenches, crust and sediment become progressively more folded and reverse-faulted (Kroenke, 1984). In fact, Malaita and northern Santa Isabel islands appear to be exhumed sections of the OJP thrust above sea level in Pliocene time (Kroenke, 1972; Stanton & Ramsay, 1975; and Hughes & Turner, 1977; Tejada et al., 1996). Unfortunately, basalt sections on those islands (Saunders et al., 1993; Mahoney et al., 1993; Tejada et al., 1996; Neal et al., 1997) provide no insight into deeper plateau structure because of the complex structure of the islands and the absence of intrusive rock.

The western flank of OJP is block-faulted (sheared?) down into the Lyra Basin. On the northern margin, seamounts presumably younger than OJP crust separate the plateau from the East Mariana Basin. The northern and western margins are also incised by submarine canyons (Kroenke, 1972), making clear seismic transitions difficult. In contrast, the north-central region is characterized by a uniform layer of stratified sediment ~1 s thick overlying relatively smooth acoustic basement. Only local sediment slumping and sliding is evident (Kroenke, 1972; Berger & Johnson, 1976). Acoustic basement deepens gradually toward the Nauru Basin, overlain in places by what appears seismically to be a continuously deposited, undisturbed pelagic carbonate section; sediment thickness decreases systematically with increasing water depth. Existing SCS data, in general, resolve little or no intra-

basement structure, and in many places true igneous basement is difficult to identify unambiguously (Kroenke, 1972; Hussong et al., 1979; Hagen et al., 1993; Mosher et al., 1993). New, unpublished deep MCS data from the southernmost plateau highlight difficulties in identifying igneous basement solely on the basis of seismic reflection character. Until detailed velocity analyses were performed on these EW9511 data, the top of sequence OJ2 was interpreted to be acoustic and probably igneous basement. The new analyses demonstrate, however, that igneous basement lies beneath sequence OJ2 (Phinney et al., 1996; Coffin et al., 1996). ODP results suggest that OJP was emplaced below sea level (Tarduno, 1992; Mahoney et al., 1993; Saunders et al., 1993; Neal et al., 1997), which is not predicted by any emplacement model. This contrasts with the Kerguelen Plateau, where numerous dipping reflection sequences, angular unconformities between basement and overlying sediment, and ODP results indicate subaerial emplacement and erosion (Coffin et al., 1990; Coffin, 1992).

OBJECTIVES

The objectives of MCS and sonobuoys studies of the Ontong Java Plateau and adjacent Nauru Basin are to:

Image the seismic stratigraphy and structure of the OJP's upper crust, including the transition from thick crust of the central OJP to thinner, oceanic crust of the Nauru Basin, to discern their relative geologic histories. Reflection geometries document stratigraphic relationships of basalt and sediment between the OJP and Nauru Basin, show faulting patterns in the upper crust, and reveal intrabasement layering which will be used to estimate individual flow unit thicknesses and address the question of how basalt of two different ages at the three extant basement drill sites on the plateau are related. These are all constraints for developing and testing models for OJP emplacement.

Provide an improved suite of candidate ODP drill sites on OJP. OJP basement drilling has been and continues to be highly ranked by JOIDES, but seismic data of the type and quality required for siting ODP basement holes are sparse. MCS data with velocity control are critical for such siting, as a recent MCS line on the southernmost plateau demonstrates (see below). The R/V *Hakuho Maru* MCS data are the first acquired on the thick central OJP, and the one existing SCS OJP-Nauru Basin water gun transect is significantly augmented by a new MCS profile. Drilling will provide essential calibration of petrology, geochemistry, and timing, additional key inputs for refinement of LIP emplacement models.

OJP is ideal for a seismic study of an oceanic plateau for many reasons: 1) It is the largest known igneous province on Earth, more than twice as voluminous as the second largest, Kerguelen (Coffin & Eldholm, 1994), and thus has the greatest potential to contribute to understanding the mantle dynamics which account for LIP formation as well as to help investigations of the environmental effects of LIP emplacement; 2) Its NE flank slopes gently into the adjacent Nauru Basin, unlike all other flanks of the plateau and the flanks of most other plateaus in general, which are usually dominated by faults, seamount chains, or large slumps. Such an apparently uncomplicated crustal transition simplifies tracing crustal structure from plateau to basin, a critical goal for model discrimination (see Fig. 2); 3) OJP's northern half is characterized by smooth acoustic basement, mantled by a uniform blanket of pelagic carbonates (Kroenke, 1972), making it ideal for seismic imaging; 4) Depth over higher parts of the northern plateau is typically ~3 s two-way travel time, which allows a minimum of 1.5-2 s of intracrustal imaging without interference from sea-floor multiples. Furthermore, smooth OJP sea floor, unlike the rough bathymetry characterizing most oceanic plateaus, facilitates removal of multiples by pre-stack deconvolution, f-k filtering and stacking; 5) Basement samples from 3 sites (Fig. 1), the most of any plateau except Kerguelen, provide data for studies of the upper crust; 6) The Nauru Basin, unlike the East Mariana, Lyra, and most oceanic basins adjacent to plateaus in general, is well-characterized by available MCS data. Digital SCS profiles on the OJP already tie to MCS data in the

Nauru Basin (Shipley et al., 1993), which bodes well for more sophisticated seismic comparisons between plateau and basin crustal structure (e.g., Mosher et al., 1993); 7) OJP is generally characterized by low ambient seismic noise levels (Furumoto et al., 1976) and benign equatorial weather, both optimal conditions under which to conduct seismic studies. As shown by the digital seismic coverage (Fig. 1), however, the southern and eastern portions of OJP are essentially unexplored by modern seismic techniques.

The KH98-1 geophysical investigation of the OJP, the archetypal and largest oceanic plateau, thus aims to elucidate its stratigraphic and structural relationships with the Nauru Basin, a well-studied adjacent deep ocean basin, as well as its whole crustal velocities. UTIG's role in these investigations has been to help plan the scientific program of R/V *Hakuho Maru* marine geophysical cruise Legs 1 and 2; to participate on Legs 1 (P. Mann) and 2 (M. Coffin, M. Wiederspahn); to provide technical expertise on streamer balancing, deployment, towing, and retrieval; to provide technical expertise on airgun synchronization; to provide technical expertise on navigation processing; to install and test a sonobuoy data acquisition system; to oversee quality control during MCS data acquisition; to process and interpret multichannel seismic (MCS) and sonobuoy data acquired during the cruise; and to work as part of the scientific team integrating and interpreting MCS, sonobuoy, ocean bottom seismometer (OBS), and other geophysical data. This work continues the UTIG-ORI collaborative research initiated in 1994 with "U.S.-Japan Marine Geophysical Study of the Solomon Island Arc-Ontong Java Plateau Convergent Zone, Southwest Pacific Ocean" (Mann et al., 1996). Results of the investigation should comprise a benchmark for oceanic LIPs, and will be used to improve geodynamic models of LIP formation.

Testable Emplacement Models for Large Igneous Provinces

Large mafic igneous events occur in a variety of tectonic settings, both continental and oceanic. Various mechanisms have been proposed to account for sudden,

voluminous magmatism—decompression melting in anomalously hot mantle at seafloor spreading centers or active rift margins (Morgan, 1981; White & McKenzie, 1989); impingement of the 'head' of a rising mantle plume (Morgan, 1981; Richards et al., 1989; Campbell & Griffiths, 1990); and extensive melting due to hydrated mantle lithosphere (e.g., Gallagher & Hawkesworth, 1992). OJP genesis has been variously ascribed to a plume head model (Richards et al., 1989; 1991; Duncan & Richards, 1991; Mahoney & Spencer, 1991; Mahoney et al., 1993), a double-event variant of that model (Bercovici & Mahoney, 1994), and an age-progressive model, by which OJP formed over a long period from a mantle plume centered on the Pacific-Phoenix spreading ridge, a tectonic setting similar to Iceland (Hussong et al., 1979; Mahoney & Spencer, 1991; Nakanishi et al., 1992; Nakanishi & Winterer, 1996; Winterer & Nakanishi, submitted). Some evidence suggests that it formed at the initiation of a hotspot track (Louisville Ridge) (Duncan & Richards, 1989; 1991; Mahoney et al., 1993). Existing data, however, do not reveal whether OJP was initiated at or near a mid-ocean ridge or in an isolated intraplate setting (Coffin & Gahagan, 1995).

Although only one numerical modeling effort has been undertaken to describe the emplacement of OJP specifically (Farnetani et al., 1996), the two general models outlined in the previous paragraph—"plume head" and "age-progressive"—form likely end members of the spectrum of scenarios resulting in the formation of OJP. The two general models predict differing stratigraphic relationships (Fig. 2), crustal structures (Fig. 2), and geochronologies (Fig. 2) for OJP and its adjacent ocean basins (summarized in Table 1), and the OJP numerical model (Farnetani et al., 1996) makes specific, testable velocity predictions. Existing geochronologic, crustal structure, and single-channel seismic (SCS) reflection data (discussed later) are not sufficient to distinguish between the two end member models, or to test the numerical model. Sedimentary and igneous stratigraphic relationships observed on MCS data at the Caribbean flood basalt province's margins, i.e., older sediment underlying flood basalts (Bowland & Rosencrantz, 1988), are similar to those predicted by the plume head model for OJP (Fig. 2 - left). In contrast, the age-

progressive model (Fig. 2 - right) predicts no sediment underlying flood basalts, and an unbroken edifice of plateau volcanics formed continuously at a spreading center over a long period of time, similar to the Greenland-Iceland-Faeroe Ridge (Bott, 1983; Thiede & Eldholm, 1983). The plume head model predicts many thick (>8-10 m) basalt flows, as observed on the Vøring volcanic margin, and resultant continuous reflections (Planke & Eldholm, 1994). A single, 28 m-thick flow has been sampled, at ODP Site 807 (Fig. 1) on the OJP (Kroenke, Berger, Janacek et al., 1991). In contrast, the age-progressive (Iceland) model predicts mostly thin (~1 m), discontinuous flows (Thordarson & Self, 1993), although thicker flows occur in places. The age-progressive model predicts that OJP should have a relatively well-organized tectonic fabric, similar to Iceland or crust created at a mid-ocean ridge, i.e., ridge-parallel normal faults and perpendicular fracture zones. The plume head model predicts no such pattern. Processed *Hakuho Maru* refraction and reflection work should reveal the internal structure of the plateau, critical information for discriminating between these emplacement mechanisms. As tempting as it may be to emphasize geodynamic hypothesis-testing, it is possible that all proposed models for OJP are wrong. Therefore, the new seismic data were collected both to test some, but clearly not all, of the models' predictions discussed above, and to provide a much more comprehensive geophysical picture of the largely unexplored OJP, as a prelude to further drilling.

DATA AND METHODS-UTIG COMPONENT

The R/V *Hakuho Maru* cruise to the Ontong Java Plateau, consisting of two legs, took place from 16 January to 27 February 1998 (Tokyo-Cairns-Pohnpei). Much of Leg 2 was devoted to investigating the structure and stratigraphy of sediment and igneous rock along an OJP-Nauru Basin transect using MCS and sonobuoy data.

MCS Data Acquisition

MCS and sonobuoy data image thick OJP crust on the central plateau, the structural transition between the central plateau and the Nauru Basin, and oceanic crust of the

Nauru Basin. Existing bathymetric and satellite-derived gravity control was sufficient to avoid rough topography along OJP's edges. Results of recent and ongoing work on OJP's optimal targets for ODP (Kroenke et al., 1997); tectonic framework (e.g., Nakanishi & Winterer, submitted); crustal structure (e.g., Gladczenko et al., 1997); geodynamics (e.g., Farnetani et al., 1996); and vertical tectonic history (e.g., Neal et al., 1997) were incorporated into plans for seismic imaging. We have also tied DSDP Site 289 with a proposed ODP site (OJ3*) on the central OJP.

Digital MCS data were acquired aboard R/V *Hakuho Maru* using a 1,200 m, 48-trace, 25-m group interval solid streamer, and between one and four large airguns (2 x 1037 in^3 and 2 x 1220 in^3) in various combinations. All MCS data are suitable for shot gather f-k filtering to remove seafloor multiples. To supplement the MCS data, wide angle reflection/refraction data were collected coincidentally using 35 sonobuoys along ≈1500 km of track, and 17 (16 recovered) OBSs along 420 km of track (see "A Study of the Crust and Upper Mantle Structure of OJP by OBSs," by Araki et al.). Approximately 2000 km of MCS data, including coincident OBS recording, were acquired using a randomized 20 s shot interval and 16 s record length.

OJP-Nauru Basin Transect (Line 400)

Overview

A ≈1220 km long transect oriented ~E-W extends from well-defined oceanic crust of the Nauru Basin across the flank of OJP onto the crest of the north-central OJP (Fig. 3). The Nauru Basin end of the line crosses a N-S *Charcot* MCS line (Shipley et al., 1993) which images the top of Aptian flood basalts and the top of Tithonian-Berriasian oceanic crust, and ties to DSDP Site 462 in the northern Nauru Basin (Fig. 1). Near its western end, the transect ties to DSDP Site 289 on the north-central OJP via KH98-1 line 601. Water depths range from ≈4450 m in the Nauru Basin to ≈1650 m on the crest of the Ontong Java Plateau.

Nauru Basin

Sediment. In general, sediment thins from the center of the Nauru Basin towards its boundary with the OJP, which is defined by an inflection point in slope between the flat Nauru Basin abyssal plain seafloor and the gentle slope of the northeastern OJP flank (Fig. 4). The boundary is also marked by several small normal faults with apparent easterly dips. Sediment thickness along line 400 varies from ≥1.1 s twt near the intersection of line 401 and the *Charcot* profile (Figs. 1, 3) to near nil near the basin's bathymetric boundary with OJP (Figs. 3, 4). Abyssal plain sediment along most of the Nauru Basin portion of the transect appears turbiditic.

Thick (≥1.1 s twt) sediment near the eastern end of the transect consists of at least two megasequences (Fig. 5). Flat-lying sediment, characterized by high frequency, high amplitude, and high continuity reflections, and thus probably turbidites, forms the upper megasequence, and onlaps the mounded surface of a hummocky lower megasequence which is characterized by moderate frequency, high amplitude, and moderate continuity reflections. Interpretation of the nearby *Charcot* data suggest that the top of the lower megasequence is Eocene chert (Shipley et al., 1993). Within the lower megasequence are high amplitude, low to medium frequency reflections which are probably volcanic horizons. The bottom of the sedimentary sequence cannot be unambiguously identified on the monitor seismic record; processed MCS data and sonobuoy results should reveal significantly more detail about the sedimentary section.

Basement Acoustic basement is observed at different levels in the Nauru Basin (Figs. 4, 5), consistent with Shipley et al.'s (1993) interpretation of *Charcot* data that subsequent to the formation of oceanic crust and deposition of abyssal sediment, the Nauru Basin was affected by substantial basaltic volcanism which is manifested as flows, sills, and dikes. A window into original oceanic crust of the Nauru Basin may lie near Line 401's intersection with the *Charcot* profile (Fig. 5). Basement is

difficult to identify unambiguously within the window, but is probably smoother than "typical" oceanic crust. Acoustic basement is much shallower on the flanks of the window, but no faulting is visible and the window presumably represents a small portion of the Nauru Basin which escaped magmatism following formation of oceanic crust. Near the Nauru Basin's boundary with OJP (Fig. 4), small basement faults bound small rifts (47.1230-47.1540).

OJP

Sediment Sediment thickness increases, in general, from near nil at the boundary of the OJP with the Nauru Basin towards OJP's crest, where a maximum of 1.2 s twt of sediment is observed. The increase in sediment thickness with decreasing water depth is consistent with the bulk of the sediment being carbonates; below the carbonate compensation depth, which has varied through time, no carbonate is preserved. No rise has developed at the boundary of the Nauru Basin and OJP.

Three major domains may be discerned in OJP's sedimentary record along the transect. From east to west, these are: 1) a lower slope, 2) an upper slope, and 3) the crest. Sediment on the lower slope is primarily undeformed pelagic drape, albeit with strong evidence for sediment reworking near the base of the slope (Fig. 4); sediment on the upper slope is deformed drape (Fig. 6); and sediment on the crest is mostly undeformed drape (Fig. 7). The OJP sedimentary section throughout the three major domains comprises at least two megasequences separated by an unconformity. Reflections are highly continuous, of high frequency, and of medium to high amplitude. Differential compaction is observed in places.

In the lower slope domain (Fig. 4), sediment thickness increases to 1 s twt as water depth decreases. Aside from disrupted reflections, indicating sediment reworking, near the base of the slope, parallel reflections are of high frequency, high amplitude, and low to moderate continuity.

In the upper slope domain (Fig. 6), from 48.1700 to 49.0015 (Fig. 3), parallel reflections are also of high frequency, high amplitude, and high continuity as well, but the sedimentary section is intensely folded, and in places faulted. In places, deformation appears to originate within basement; in others, no clear relationship exists. Deformation may result from gravity slides or slumps, or strike-slip or compressional basement deformation, or combinations thereof.

On the crest of the plateau (Fig. 7), sediment thickness ranges from 0.9 to 1.1 s twt. The deepest sedimentary sequence varies significantly in thickness (0.2-0.4 s twt), especially near the crest of the plateau, suggesting an active, and possibly shallow water (carbonate banks?) or subaerial, sedimentary regime.

Basement. Basement is relatively smooth in the lower slope (Fig. 4) and crestal domains (Fig. 7), and disrupted in the upper slope domain (Fig. 6), although some basement topography is visible in all domains in the form of small basement grabens and highs. In places, we observe intrabasement reflections in the three domains, but they are much more rare and less developed than those imaged on the Kerguelen Plateau and on volcanic margins.

Central OJP Profile (Line 501)

Overview

At the crest of the north-central OJP, N-S, ≈360 km long MCS/OBS/sonobuoy line 501 intersects the MCS/OBS/sonobuoy portion of line 404 (Fig. 8). Sediment thickness ranges from 0.95 to 1.05 s twt, and water depth ranges from 1650 to 2100 m along the profile.

Sediment. We observe at least two sedimentary megasequences along line 501. Individual reflections can be traced across the crest of OJP; reflections are typically parallel to subparallel, and of high continuity (Fig. 9). Reflection amplitudes are medium to high, and frequency is high. The sediment appears to be dominantly

pelagic drape; some differential compaction is observed. The seafloor is rough in places, suggesting a high energy sedimentary environment. Piercement structures penetrate the sedimentary section in places.

Basement

Acoustic basement is characterized by medium to high amplitude, moderately discontinuous reflections on the OJP's crest. Some intrabasement reflections which don't appear to be internal or seafloor multiples are observed.

DSDP Site 289 - Line 400 Profile (Line 600)

Overview:

A 150 km long profile was run from north of DSDP Site 289 to south of Line 400 (Fig. 10) to tie existing and proposed ODP sites on the eastern flank (OJ11) and crest (OJ3) of OJP. Sediment thickness ranges from 0.95 to 1.05 s twt, and water depth ranges from 1950 to 2200 meter along the line.

Sediment

Two sedimentary megasequences are observed along the profile. Sedimentary layers on the plateau appear continuous, parallel to subparallel, and of high frequency and amplitude on seismic monitor records. The sediment appears to be dominantly pelagic drape, with minor differential compaction interpreted in places. In the lower megasequence, disrupted reflections suggest sediment reworking.

Basement. The sediment-basement contact is generally smooth, although it is offset by small faults in places. Few intrabasement reflections are visible along the line. In most places they appear to be horizontal, but in a few locations they dip and terminate at relatively shallow depths.

MCS Data Processing

The MCS data will be processed on Sun workstations using CGG's interactive Geovecteur Plus software, in addition to other imaging software developed at UTIG. UTIG has utilized Geovecteur software since 1987. Geovecteur Plus allows interactive definition of seismic processing parameters and interpretation of velocities to be performed efficiently on small subsets of data. Potential seismic processing sequences are also tested interactively. Current seismic processing technology allows for a wide variety of 2D pre- and post-stack algorithms to be applied in combination as needed for the data being analyzed. Following processing using the selected algorithms, interactive display and interpretation of 2D sections is performed using GeoQuest software, again running on UTIG's local network of Sun computers.

UTIG has extensive experience in processing MCS data, including 240- and 120-channel data, both at sea and ashore. Portions of the EW9511 MCS data acquired over OJP in 1995, for example, were processed through brute stack and f-k, water velocity migration at sea using SIOSEIS. Detailed velocity analyses, determination of optimal deconvolution and multiple suppression techniques, and other pre- and post-stack processing of the data have required, and continue to require extensive efforts at UTIG using Geovecteur Plus. The large airguns used aboard R/V *Hakuho Maru* necessitate intensive work to determine optimal source deconvolution parameters. A minimum of 1.5-2.0 s of subbottom penetration above the first multiple was achieved on the central OJP, and more toward its flanks. MCS data in water depths of 0.5 to 5 s (two-way travel time) are commonly contaminated with water column multiples; these are difficult to attenuate because the sea surface reflection coefficient is –1 under ideal conditions. In reality, the problem is 3D, with energy traveling out of the acquisition plane, making reverberation prediction difficult. One approach to the multiple problem using a short streamer is basic prediction filtering, which exploits periodicities in multiple arrivals, and is best performed after plane wave decomposition. Once in the tau-p domain, the data are periodic for a 1D earth (as approximated by CDP gathering). After prediction

(OJ9) (Appendix C), which address primary objectives of an extant OJP drilling proposal, "Assessing the Origins, Age, and Post-Emplacement History of the Ontong Java Plateau through Basement Drilling," by Kroenke et al. (1997). OJ3 and OJ11 will examine basement age, composition, and emplacement environment of OJP, and OJ9 is a reference site on oceanic crust of the Nauru Basin.

WORK PLAN-UTIG COMPONENT AND ROLES OF INVESTIGATORS

The R/V *Hakuho Maru* MCS and sonobuoy (aside from three sonobuoys analyzed at UNC-Wilmington) data will be processed and interpreted at UTIG. ORI (Kimihiro Mochizuki) and University of Oslo (Eldholm and Gladczenko) scientists and students will visit UTIG to cooperate in these efforts. MCS and OBS data will be merged as processing and interpretation progress.

A. Taira, a marine geologist at ORI, is principal investigator for the 1998 R/V *Hakuho Maru* OJP research program (see I-1-9). **M. Coffin** will lead efforts in processing and interpreting MCS and sonobuoy data acquired during the cruise. **K. Suyehiro**, a seismologist at ORI, and **M. Nakahishi**, a seismologist at Chiba University, will manage OBS data acquisition and interpretation. **Coffin** and **Suyehiro**, who have worked together since 1994 as part of OCE-9301608, "U.S.-Japan Marine Geophysical Study of the Solomon Island Arc-Ontong Java Plateau Convergent Zone, Southwest Pacific Ocean," will work together (with students) to interpret the coincident MCS, sonobuoy, and OBS data. **O. Eldholm** and Ph.D. student **T. Gladczenko** from the University of Oslo, Norway will spend several months working on MCS data processing and interpretation at UTIG. In addition to Gladczenko, **Coffin** will supervise one or more University of Texas students on the project, and may co-supervise one or more ORI students as part of the project.

REFERENCES

Abrams, L. J., R.L. Larson, T.H. Shipley, and Y. Lancelot, Cretaceous volcanic sequences and Jurassic oceanic crust in the East Mariana and Pifagetta basins of the Western Pacific, i n The Mesozoic Pacific, AGU Monogr. 77, edited by M.S. Pringle, W.W. Sager, W. V. Sliter, and S. Stein, American Geophysical Union, Washington, D.C., 77-101, 1993.

Austin, J.A., Jr., P.L. Stoffa, J.D. Phillips, J. Oh, D.S. Sawyer, G.M. Purdy, E. Reiter, and J. Makris, Crustal structure of the Southeast Georgia embayment-Carolina trough: preliminary results of a composite seismic image of a continental suture (?) and a volcanic passive margin, Geology, 18, 1023-1027.

Baker, M.B. and E.M. Stolper, 1994, Determining the composition of high-pressure mantle melts using diamond aggregates, Geochim. Cosmochim. Acta, 58, 2811-2827.

Barruol, G. and D. Mainprice, 1993, 3-D seismic velocity calculated from lattice-preferred orientation and reflectivity of a lower crustal section—example of the Val Sesia section (Ivrea Zone, N Italy), Geophys. J. Int. 115, 1169-1188.

Bercovici, D., and Mahoney, J., Double flood basalts and plume head separation at the 660-kilometer discontinuity, Science, 266, 1367-1369, 1994.

Ben-Avraham, Z., A. Nur, D. Jones and A. Cox, Continental accretion and orogeny: From oceanic plateaus to allochthonous terranes, Science, 213, 47-54, 1981.

Berger, W., and T. Johnson, Deep-sea carbonates: Dissolution and mass wasting on Ontong Java Plateau, Science, 192, 785-787, 1976.

Bott, M.H.P., The crust beneath the Iceland-Faeroe Ridge, in Structure and Development of the Greenland-Scotland Ridge, edited by M.H.P. Bott, S. Saxov, M. Talwani, and J. Thiede, Plenum, New York, 63-75, 1983.

Bott, M.H.P., S. Saxov, M. Talwani, and J. Thiede, Structure and Development of the Greenland-Scotland Ridge, Plenum, New York, 685 pp., 1983.

Bowland, C.L., and E. Rosencrantz, Upper crustal structure of the western Columbian Basin, Caribbean Sea, Geol. Soc. America Bull., 100, 534-546, 1988.

Campbell, I.H., and R.W. Griffiths, Implications of mantle plume structure for the evolution of flood basalts, Earth Planet. Sci. Lett., 99, 79-93, 1990.

Campbell, I.H., R.W. Griffiths and R.I. Hill, Melting in an Archean mantle plume: heads its basalts, tails its komatites, Nature, 339, 697-699, 1989.

Cande, S.C., LaBrecque, J. L. et al., Magnetic lineations of the world's ocean basins, AAPG map series, 1989.

Caress, D.W., M.K McNutt, R.S. Detrick, & J.C. Mutter, Seismic imaging of hotspot-related crustal underplaing beneath the Marquesas Islands, Nature, 373, 600-603, 1995.

Carlson, R., N. Christensen, and R. Moore, Anomalous crustal structures in ocean basins: Continental fragments and oceanic plateaus, Earth Planet. Sci. Lett., 51, 171-180, 1980.

Carvalho, P.M., A.B. Weglein, and R.H. Stolt, Non-linear inverse scattering for multiple suppression: application to real data, Part I, SEG Expanded Abstracts, 1093–1095, 1992.

Charvis, P., S. Operto, L.K. Könnecke, M. Recq, Y. Hello, F. Houdry, P. Lebellegard, R. Louat, and F. Sage, Structure profonde du domaine nord du plateau de Kerguelen (océan Indien austral): résultats préliminaires de la campagne MD66/KeOBS, C.R. Acad. Sci. Paris, 316, 341-347, 1993.

Charvis, P., Recq, M., Operto, S., and Bréfort, D., Deep structure of the northern Kerguelen Plateau and hotspot-related activity, Geophys. J. Int., 122, 899-924, 1995.

Circum-Pacific Council, Plate-Tectonic Map of the Circum-Pacific Region, Northwest Quadrant, Amer. Assoc. Petrol. Geol., Tulsa, 1981.

Cloos, M., Lithospheric buoyancy and collisional orogenesis: subduction of oceanic plateaus, continental margins, island arcs, spreading ridges, and seamounts, Geol. Soc. America Bull., 105, 715-737, 1993.

Coffin, M.F., Emplacement and subsidence of Indian Ocean plateaus and submarine ridges, in Duncan, R.A., D.K. Rea, R.B. Kidd, U. von Rad, and J.K. Weissel, eds., Synthesis of Results from Scientific Drilling in the Indian Ocean, *Geophysical Monograph 70, American Geophysical Union*, (Washington, D.C.), 115-125, 1992.

Coffin, M. F., and O. Eldholm (eds.), Large Igneous Provinces, JOI/USSAC Workshop Report, 1991.

Coffin, M.F., and Eldholm, O., Scratching the surface: estimating dimensions of large igneous provinces, *Geology, 21*, 515-518, 1993.

Coffin, M.F., and Eldholm, O., Large igneous provinces: crustal structure, dimensions, and external consequences, *Reviews of Geophysics, 32*, 1-36, 1994.

Coffin, M.F., and Gahagan, L.M., Ontong Java and Kerguelen Plateaux: Cretaceous Icelands? J. Geol. Soc. London, 152, 1047-1052, 1995.

Coffin, M. F., M. Munschy, J. B. Colwell, R. Schlich, H. L. Davies, and Z. G. Li, Seismic stratigraphy of the Raggatt Basin, southern Kerguelan Plateau, Geol. Soc. America Bull., 102, 563-579, 1990.

Davies, G., Ocean bathymetry and mantle convection, 1, large-scale flow and hotspots, J. Geophys. Res., 93, 10467-10480, 1988.

Davies, H.L., S-s. Sun, F.A. Frey, I. Gautier, M.T. McCulloch, R.C. Price, Y. Bassias, C.T. Klootwijk, and L. Leclaire, Basalt basement from the Kerguelen Plateau and the trail of a Dupal plume, Contrib. Mineral. Petrol., 103, 457-469, 1989.

Den, N., J. Ludwig, S. Muruachi, J. Ewing, H. Hotta, N. Edgar, T. Yoshii, T. Asanuma, K. Hagiwara, T. Sato and S. Ando, Seismic refraction measurements in the northwest Pacific basin, J. Geophys. Res., 74, 1,421-1,434, 1969.

Duncan, R.A., and M.A. Richards, Hotspots, mantle plumes, flood basalts, and true polar wander, Rev. Geophys., 29, 31-50, 1991.

Eldholm, O., and J.C. Mutter, Basin structure on the Norwegian margin from analysis of digitally recorded sonobuoys, J. Geophys. Res., 91, 3763-3783, 1986.

Eldholm, O., J. Thiede, E. Taylor, et al., Proc. ODP, Init. Repts, 104, College Station, TX (Ocean Drilling Program), 1987.

Eldholm, O., J. Thiede, E. Taylor, et al., Proc. ODP, Sci. Results, 104, College Station, TX (Ocean Drilling Program), 1989.

Farnetani, C., and M.A. Richards, Numerical investigations of the mantle plume initiation model for flood basalt events, J. Geophys. Res., 99, 13,813-13,833, 1994.

Farnetani, C.G., M.A. Richards, and M.S. Ghiorso, Petrological models of magma evolution and deep crustal structure beneath hotspots and flood basalt provinces, Earth and Planetary Science Letters, 143, 81-94, 1996.

Flovenz, O.G., and Gunnarsson, K., Seismic crustal structure in Iceland and surrounding area, Tectonophysics, 189, 1-17, 1991.

Fokkema, J.T., and Van den Berg, P.M., Removal of surface-related wave phenomena: the marine case, SEG Expanded Abstracts, 1689–1692, 1990.

Forsythe, D.W., Subsurface loading and estimates of the flexural rigidity of continental lithosphere, J. Geophys. Res., 90, 12623-12632, 1985.

Furumoto, A., D. Hussong, J. Campbell, G. Sutton, A. Malahoff, J. Rose, and G. Woollard, Crustal and upper mantle structure of the Solomon Islands as revealed by seismic refraction survey of November-December, 1966, Pac. Sci., 24, 315-322, 1970.

Furumoto, A., J. Webb, M. Odegard, and D. Hussong, Seismic studies on the Ontong Java Plateau, 1970, Tectonophysics, 34, 71-90, 1976.

Ghiorso, M.S. and R.O. Sack, Chemical mass transfer in magmatic processes, IV: A revised and internally consistent thermodynamic model for the interpolation and extrapolation of liquid-solid equilibria in magmatic systems at elevated temperatures and pressures, Contrib. Min. Petrol., 119, 197-212, 1995.

Gladczenko, T.P., M.F. Coffin, and O. Eldholm, Crustal structure of the Ontong Java Plateau: modeling of new gravity and existing seismic data, *Journal of Geophysical Research, 102*, 22711-22729, 1997.

Griffiths, R.W., Thermals in extremely viscous fluids, including the effects of temperature-dependent viscosity, J. Fluid Mech., 166, 115-138, 1986.

Griffiths, R.W., and I.H. Campbell, Stirring and structure in mantle starting plumes, Earth Planet. Sci. Lett., 99, 66-78, 1990.

Hagen, R.A., and Shipboard Scientific Party, Underway geophysics, in Kroenke, L.W., W.H. Berger, T.R. Janacek, et al., Proc. Ocean Drilling Program, Init. Repts., 130, 77-97, 1991.

Hagen, R.A., L.A. Mayer, D.C. Mosher, L.W. Kroenke, T.H. Shipley, and E.L. Winterer, Basement structure of the northern Ontong Java Plateau, in Berger, W.H., L.W. Kroenke, L.A. Mayer, et al., Proc. Ocean Drilling Program, Sci. Results, 130, 23-31, 1993.

Head, J.W., III, and M.F. Coffin, Large igneous provinces: a planetary perspective, in Mahoney, J.J., and M.F. Coffin, eds., Large Igneous Provinces: Continental, Oceanic, and Planetary Flood Volcanism, *Geophysical Monograph 100, American Geophysical Union* (Washington, D.C.), 411-438, 1997.

Hinz, K., J.C. Mutter, C.M. Zehnder and NGT Study Group, Symmetric conjugation of continent-ocean boundary structures along the Norwegian and East Greenland margins, Mar. Petrol. Geol., 3, 166-187, 1987.

Hughes, G., and C. Turner, Upraised Pacific Ocean floor, southern Malaita, Solomon Islands, Geol. Soc. Amer. Bull, 88, 412-424, 1977.

Hussong, D., L. Wipperman, and L. Kroenke, The crustal structure of the Ontong Java and Manihiki oceanic plateaus, J. Geophys. Res., 84, 6,003-6,010, 1979.

Iwabuchi, Y., General Bathymetric Chart of the Oceans (GEBCO), 5.06, Ottawa, 1979.

Kent, R.W., M. Storey, and A.D. Saunders, Large igneous provinces: sites of plume impact or plume incubation, Geology, 20, 891-894, 1992.

King, S.D., Raefsky, A., and Hager, B.H., ConMan: vectorizing a finite element code for incompressible two-dimensional convection in the Earth's mantle, Phys. Earth Planet. Inter., 59, 195-207, 1990.

Kinzler, R.J. and T.L. Grove Primary magmas or mid-ocean ridge basalts 1: Experiments and methods, J. Geophys. Res., 97, 6885-6906, 1992.

Klein, E.M. and C.H. Langmuir, Global corrections of ocean ridge basalt chemistry with axial depth and crustal thickness, J. Geophys. Res., 92, 8089-8115, 1987.

Kroenke, L., Geology of the Ontong Java Plateau, Ph.D. dissertation, University of Hawaii, HIG-72-5, 119 p., 1972.

Kroenke, L., Origin of continents through development and coalescence of oceanic flood basalt plateaus, EOS, 55, 443, 1974.

Kroenke, L., Solomon Islands: San Cristobal to Bougainville and Buka, in Cenozoic tectonic development of the southwest Pacific, edited by L. Kroenke, U.N. ESCAP, CCOP/SOPAC Tech. Bull. 6, 47-61, 1984.

Kroenke, L., and K. Nemoto, Marine geology of the Hess Rise, 2. Basement morphology, sediment thickness, and structural geology, J. Geophys. Res., 87, 9,259-9,278, 1982.

Kroenke, L. and J. Kellog, K. Nemoto, Mid-Pacific mountains revisited, Geo-Marine Letters, 5, 77-81, 1985.

Kroenke, L.W., J.M. Resig, and P.A. Cooper, Tectonics of the southeastern Solomon Islands: formation of the Malaita anticlinorium, in Geology and offshore resources of the Pacific island arcs–central and western Solomon Islands, edited by J.G. Vedder, K.S. Pound, and S.Q. Boundy, Circum-Pacific Council for Energy and Mineral Resources Earth Science Series, 4, Houston, Texas, 109-116, 1986.

Kroenke, L., Berger, W., Janacek, T., et al., Proc. ODP. Init. Repts, 130, College Station, TX (Ocean Drilling Program), 1991.

Kroenke, L.W., et al., Assessing the origins, age and post-emplacement history of the Ontong Java Plateau through basement drilling, Ocean Drilling Program Proposal 448, 1997.

Macdougall, J.D., Continental Flood Basalts, 341pp, Kluwer Academic, Dordrecht, Netherlands, 1988.

Mahoney J., An isotopic survey of Pacific oceanic plateaus: Implications for their nature and origin, in Seamounts, Islands, and Atolls, edited by B. Keating, P. Fryer, R. Batiza, and G.W. Boehlert, Geophys. Monogr. Ser. 43, AGU, Washington, D.C., 1987.

Mahoney J., Deccan Traps, in Continental Flood Basalts, edited by J.D. Macdougall, Kluwer, Boston, 151-194 1988.

Mahoney, J., J. Macdougall, G. Lugmair, and K. Gopalan, Kerguelen hot spot source for Rajmahal traps and Ninetyeast Ridge?, Nature, 303, 385-389, 1983.

Mahoney, J.J., and K.J. Spencer, Isotopic evidence for the origin of the Manihiki and Ontong Java plateaus, Earth Planet. Sci. Lett., 104, 196-210, 1991.

Mahoney, J.J., M. Storey, R.A. Duncan, K.J. Spencer, and M. Pringle, Geochemistry and age of the Ontong Java Plateau, in The Mesozoic Pacific, AGU Monogr. 77, edited by M.S. Pringle, W.W. Sager, W. V. Sliter, and S. Stein, American Geophysical Union, Washington, D.C., 233-261, 1993.

Mayer, L.A., T.H. Shipley, E.L. Winterer, D. Mosher, and R.A. Hagen, Seabeam and seismic reflection surveys on the Ontong Java Plateau, in Kroenke, L.W., W.H. Berger, T.R. Janacek, et al., Proc. Ocean Drilling Program, Init. Repts., 130, 45-75, 1991.

McKenzie, D.P. and M.J. Bickle The volume and composition of melt generated by extension of the lithsophere, J. Petrol., 29, 625-679, 1988.

Morgan, W., Plate motions and deep mantle convection, in Geol. Soc. America Mem., 132, edited by R. Shagam et al., 7-22, 1972.

Morgan, W.J., Convection plumes in the lower mantle, Nature, 230, 42-43, 1971.

Morgan, W.J., Hotspot tracks and the opening of the Atlantic and Indian oceans, in The Sea, 7, edited by C. Emiliani, Wiley, New York, 443-487, 1981.

Mosher, D.C., L.A. Mayer, T.H. Shipley, E.L. Winterer, R.A. Hagen, J.C. Marsters, F. Bassinot, R.H. Wilkens, and M. Lyle, Seismic stratigraphy of the Ontong Java Plateau, in Berger, W.H., L.W. Kroenke, L.A. Mayer, et al., Proc. Ocean Drilling Program, Sci. Results, 130, 33-49, 1993.

Murauchi, S., Ludwig, W.J., Den, N., Hotta, H., Asanuma, T., Yoshii, T., Kubotera, A., and Hagiwara, K., Seismic refraction measurements on the Ontong Java Plateau northeast of New Ireland, J. Geophys. Res., 78, 8653-8663, 1973.

Mutter, C.Z., and Mutter, J.C., Variations in thickness of layer 3 dominate oceanic crustal structure, Earth Planet. Sci. Lett., 117, 295-317, 1993.

Mutter, J., M. Talwani, and P. Stoffa, Evidence for a thick oceanic crust adjacent to the Norwegian margin, J. Geophys. Res., 89, 483-502, 1984.

Nakanishi, M ., and Winterer, E.L., Tectonic events of the Pacific Plate related to formation of Ontong Java Plateau, EOS, 77 (Fall Meeting Supplement), F713, 1996.

Nakanishi, M., K. Tamaki, and K. Kobayashi, Mesozoic magnetic anomaly lineations and seafloor spreading history of the northwestern Pacific, J. Geophys. Res., 89, 15,437-15,462, 1989.

Nakanishi, M., Tamaki, K., and Kobayashi, K., A new Mesozoic isochron chart of the northwestern Pacific Ocean: paleomagnetic and tectonic implications, Geophys. Res. Lett., 19, 693-696, 1992.

Nakanishi, M., K. Tamaki, and K. Kobayashi, Magnetic anomaly lineations from Late Jurassic to Early Cretaceous in the west-central Pacific Ocean, Geophys. J. Int., 109, 701-719, 1992.

Neal, C.R., Mahoney, J.J., Duncan, R.A., Kroenke, L.W., Petterson, M.G., and Jain, J.C., The Ontong Java Plateau, in Mahoney, J.J., and M.F. Coffin, eds., Large Igneous Provinces: Continental, Oceanic, and Planetary Flood Volcanism, *Geophysical Monograph 100, American Geophysical Union* (Washington, D.C.), 183-216, 1997.

Nur, A., and Z. Ben-Avraham, Oceanic plateaus, the fragmentation of continents, and mountain building, J. Geophys. Res., 87, 3,644-3,661, 1982.

Oh, J., Phillips, J.D., Austin, J.A., Jr., and Stoffa, P.L., Deep-penetration seismic reflection images across the southeastern United States continental margin, in Meissner, R., Brown, L, Durbaum, H.-J., Franke, W., Fuchs, K., and Seifert, F., eds., Continental Lithosphere: Deep Seismic Reflections, 22: American Geophysical Union, 225-240, 1991.

Operto, S., Structure et origine du plateau de Kerguelen (Océan Indien): implications géodynamiques, Thèse de l'Université Pierre et Marine Curie, Paris, 292 pp., 1995.

Operto, S., and Charvis, P., Kerguelen Plateau: a volcanic passive margin fragment? Geology, 23, 137-140, 1995.

Operto, S., and P. Charvis, Deep structure of the southern Kerguelen Plateau (southern Indian Ocean) from ocean bottom seismometer wide-angle seismic data, J. Geophys. Res. 101, 25,077-25,103, 1996.

Orcutt, J., L. Dorman, and P. Spudich, Inversion of seismic refraction data, in The Earth's Crust, Geophys. Monogr. Ser., 20, edited by S. Heacock, AGU, Washington, D.C., 371-384, 1977.

Phinney, E., Mann, P., Coffin, M., and Shipley, T., Along-strike variations in the style of oceanic plateau accretion within the Malaita accretionary prism, Solomon Islands, *Eos, Transactions American Geophysical Union, 77 (46)*, F712, 1996.

Planke, S., and O. Eldholm, Seismic response and construction of seaward dipping wedges of flood basalts: Vøring volcanic margin, J. Geophys. Res., 99, 9263-9278, 1994.

Recq, M., and P. Charvis, A seismic refraction survey in the Kerguelen Isles, southern Indian Ocean, Geophys. J. R. Astr. Soc., 84, 529-559, 1986.

Recq, M., D. Brefort, J. Malod, and J. Veinante, The Kerguelan Isles (southern Indian Ocean). New results on deep structure from refraction profiles, Tectonophysics, 182, 227-248, 1990.

Richards, M.A., and R.W. Griffiths, Thermal entrainment by deflected mantle plumes, Nature, 342, 900-902, 1989.

Richards, M.A., Duncan, R.A., and Courtillot, V.E., Flood basalts and hot spot tracks: plume heads and tails, Science, 246, 103-107, 1989.

Richards, M.A., D.L. Jones, R.A. Duncan, and D.J. DePaolo, A mantle plume initiation model for the formation of Wrangellia and other oceanic flood basalt plateaus, Science, 254, 263-267, 1991.

Sager, W.W., and H.-C. Han, Rapid formation of the Shatsky Rise oceanic plateau inferred from its magnetic anomaly, Nature, 364, 610-613, 1993.

Sandwell, D.T., and M.L. Renkin, Compensation of swells and plateaus in the North Pacific: no direct evidence for mantle convection, J. Geophys. Res., 93, 2775-2783, 1988.

Sandwell, D., and K. MacKenzie, Geoid height versus topography for oceanic plateaus and swells, J. Geophys. Res., 94, 7403-7418, 1989.

Sandwell, D.T. & W.H.F. Smith, Marine gravity anomaly from Geosat and ERS-1 satellite altimetry, Journal of Geophysical Research, in press.

Saunders, A.D., T.L Babbs, M.J. Norry, M.G. Petterson, B.A. McGrail, J.J. Mahoney, and C.R. Neal, Depth of emplacement of ocean plateau basaltic lavas, Ontong Java Plateau & Malaita, Solomon Islands: implications for the formation of oceanic LIPs? Eos, 74 (Fall Meeting Supplement), 552, 1993.

Saunders, A.D., J. Tarney, A.C. Kerr, and R.W. Kent, The formation and fate of large oceanic igneous provinces, Lithos, 37, 81-95, 1996.

Sen, M. K., and P. L. Stoffa, Global Optimization Methods in Geophysical Inversion, as part of Advances in Exploration Geophysics series, Elsevier Publishing Co., The Netherlands, 1996.

Sheridan, R.E., D.L. Musser, L. Glover III, M. Talwani, J.I. Ewing, W.S. Holbrook, G.M. Purdy, R. Hawman, and S. Smithson, Deep seismic reflection data of EDGE U.S. mid-Atlantic continental-margin experiment: implications for Appalachian sutures and Mesozoic rifting and magmatic underplating, Geology, 21, 563-567, 1993.

Shipley, T. H., J. Whitman, F. Duennebier, and L. Peterson, Sedimentation, stratigraphy and structural elements of the East Mariana Basin, western Pacific, EPSL, 64, 257-275, 1983.

Shipley, T.H., L.J. Abrams, Y. Lancelot, and R.L. Larson, Late Jurassic-Early Cretaceous oceanic crust and Early Cretaceous volcanic sequences of the Nauru Basin, Western Pacific, in The Mesozoic Pacific, AGU Monogr. 77, edited by M.S. Pringle, W.W. Sager, W. V. Sliter, and S. Stein, American Geophysical Union, Washington, D.C., 103-119, 1993.

Skogseid, J., and O. Eldholm, Vøring Plateau continental margin: Seismic interpretation, stratigraphy and vertical movements, in Eldholm O., J. Thiede, E. Taylor et al., Proc. ODP, Sci. Results, 104, College Station, TX (Ocean Drilling Program), 993-1030, 1989.

Skogseid, J., and O. Eldholm, Early Cenozoic crust at the Norwegian continental margin and the conjugate Jan Mayen Ridge, J. Geophys. Res., 92, 11,471-11,491, 1987.

Sleep, N.H., Hotspots and mantle plumes: some phenomenology, J. Geophys. Res., 95, 6715-6736, 1990.

Sliter, W.V., and R.M. Leckie, Cretaceous planktonic foraminifers and depositional environments from the Ontong Java Plateau with emphasis on sites 803 and 807, in Berger, W.H., L.W. Kroenke, L.A. Mayer, et al., Proc. ODP, Sci. Results, 130, College Station, TX (Ocean Drilling Program, 63-84, 1993.

Stanton, R., and W. Ramsay, Ophiolite basement complex in a fractured, island chain, Santa Isabel, British Solomon Islands, Bull. Aust. Soc. Explor. Geophys., 6, 61-64, 1975.

Stoffa, P.L., W.T. Wood, T.H. Shipley, A. Taira, K. Suyehiro, G.F. Moore, M.A.B. Botelho, H. Tokuyama, and E. Nishiyama, Deep water high-resolution expanding spread and split-spread marine seismic profiles: Acquisition and velocity analysis methods, J. Geophys. Res., 97, 1687–1713, 1992.

Sutton, G., G. Maynard, and D. Hussong, Widespread occurrence of a high-velocity basal crustal layer in the Pacific crust found with repetitive sources and sonobuoys, in The Structure and Physical Properties of the Earth's Crust, Geophys. Monogr. Ser., 14, edited by J. Heacock, 193-209, AGU, Washington, D.C., 1971.

Takahashi, E., 1986, Melting of a dry peridotite KLB-1 up to 14 GPa: Implications on the origin of peridotitic upper mantle, J. Geophys. Res., 91, 9367-9382.

Tarduno, J.A., Vertical and horizontal tectonics of the Cretaceous Ontong Java Plateau, Eos, 73 (Fall Meeting Supplement), 532, 1992.

Tarduno, J.A., W.V. Sliter, L. Kroenke, M. Leckie, H. Mayer, J.J. Mahoney, R. Musgrave, M. Storey, and E.L. Winterer, Rapid formation of the Ontong Java Plateau by Aptian mantle plume volcanism, Science, 254, 399-403, 1991.

Taylor, B., Mesozoic magnetic anomalies in the Lyra Basin, EOS, 59, 320, 1978.

Tejada, M.L.G., Mahoney, J.J., Duncan, R.A., and Hawkins, M.P., Age and geochemistry of basement and alkalic rocks of Malaita and Santa Isabel, Solomon Islands, southern margin of Ontong Java Plateau, Journal of Petrology, 37, 361-394, 1996.

Thiede, J., and O. Eldholm, Speculations about the paleodepth of the Greenland-Scotland Ridge during Late Mesozoic and Cenozoic times, in Structure and Development of the Greenland-Scotland Ridge, edited by M.H.P. Bott, S. Saxov, M. Talwani, and J. Thiede, Plenum, New Yor,, 445-456, 1983.

Thordarson, T., and S. Self, The Laki (Skaftar Fires) and Grimsvotn eruptions in 1783-85, Bull. Volcanol., 55, 233-263, 1993.

Verschuur, D.J., and M.M.N. Kabir, Integration of surface-related and radon based multiple elimination, Proceedings of the EAEG 56th Meeting and Technical Exhibition, Vienna, Austria paper no. H035, 1994.

Verschuur, D.J., A.J. Berkhout, and C.P.A. Wapenaar, Adaptive surface-related multiple elimination, Geophysics, 57, 1166–1177, 1992.

Vogt, P., Subduction and aseismic ridges, Nature, 241, 189-191, 1973.

Watson, S. and D.P. McKenzie, Melt generation by plumes: A study of Hawaiian volcanism, J. Petrol., 12, 501-537, 1991.

Watts, A.B., and U.S. ten Brink, Crustal structure, flexure, and subsidence history of the Hawaiian Islands, J. Geophys. Res., 94, 10473-10500, 1989.

White, R., and D. McKenzie, Magmatism at rift zones: The generation of volcanic continental margins and flood basalts, J. Geophys. Res., 94, 7,685-7,729, 1989.

Whitehead J.A., and D.S. Luther, Dynamics of laboratory diapir and plume models, J. Geophys. Res., 80, 705-717, 1975.

Winterer, E., Anomalies in the tectonic evolution of the Pacific, in The Geophysics of the Pacific Ocean Basin and its Margins, edited by G. Sutton, M. Manghnani, and R. Moberly, 269-278, AGU, Washington, D.C., 1976.

Winterer, E.L., and M. Nakanishi, Evidence for a plume-augmented, abandoned, Early Cretaceous spreading center on Ontong Java Plateau, submitted to *J. Geophys. Res.*

Winterer, E., W. Riedel, et al., Init. Rep. Deep Sea Drilling Proj., 7, Washington, D.C., 1971.

Zehnder, C., and J. Mutter, The continent-ocean transition at (volcanic) passive margins, EOS, 67, 1192, 1986.

Zelt, C.A., and Smith, R.B., Seismic traveltime inversion for 2-D crustal velocity structure, Geophys. J. Int., 108, 16-34, 1992.

Ziolkowski, Anton, Free-surface multiple removal - conjectures and refutations, Proceedings of the European Association of Exploration Geophysicists 56th Annual Meeting and Exposition, Vienna, Austria, paper no. H038, 1994.

Figure 1. R/V *Hakuho Maru* KH98-1 Leg 2 MCS profiles (heavy black lines), OBS locations (triangles), and sonobuoy locations (small black circles) on the OJP (outlined in heavy black) and adjacent Nauru Basin, superimposed on GEBCO contours. DSDP/ODP sites which penetrated igneous basement (filled large circles) and only sediment (open large circles), and existing digital seismic reflection data (dashed lines) are also shown.

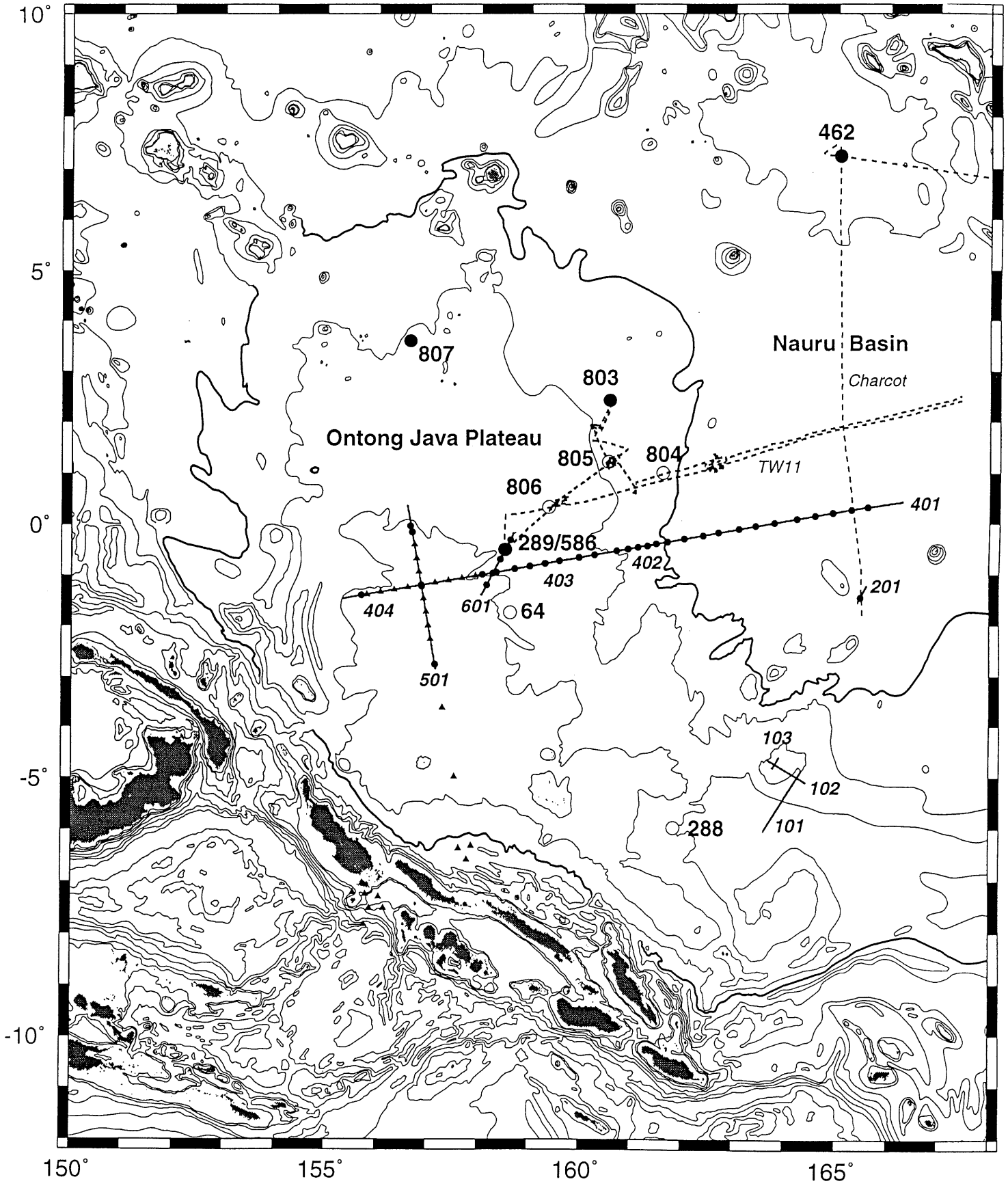

Fig. 1

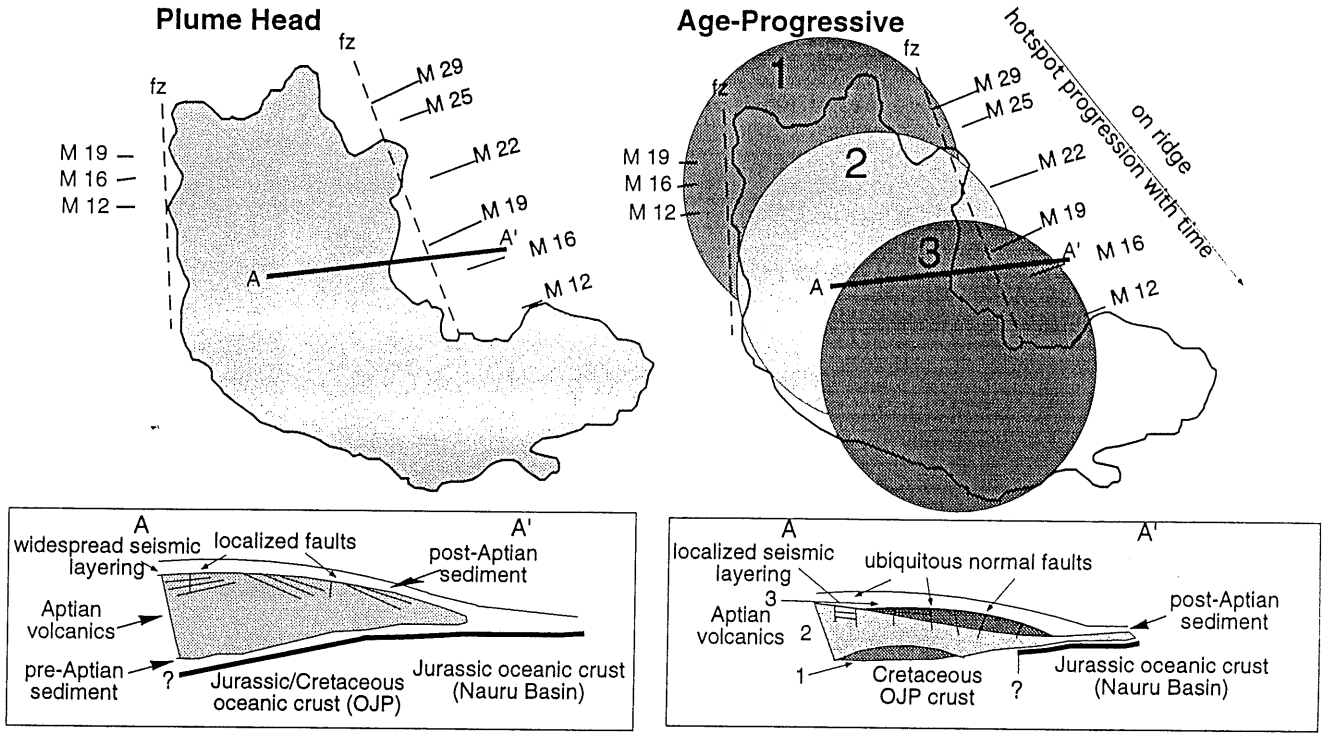

Figure 2. Differences in stratigraphic relationships, crustal structures, and tectonics expected for plume head and age-progressive models of OJP development. The R/V *Hakuho Maru* MCS, sonobuoy, and OBS profiles (see Figs. 1 and 3) should aid in determining which model's predictions (summarized in Table 1) are in better accord with observational data.

Figure 3. Location of OJP-Nauru Basin transect, KH98-1 Leg 2 line 400. Small black circles indicate sonobuoy locations; triangles are OBS locations; large circles are DSDP/ODP sites which penetrated basement (filled) or only sediment (open).

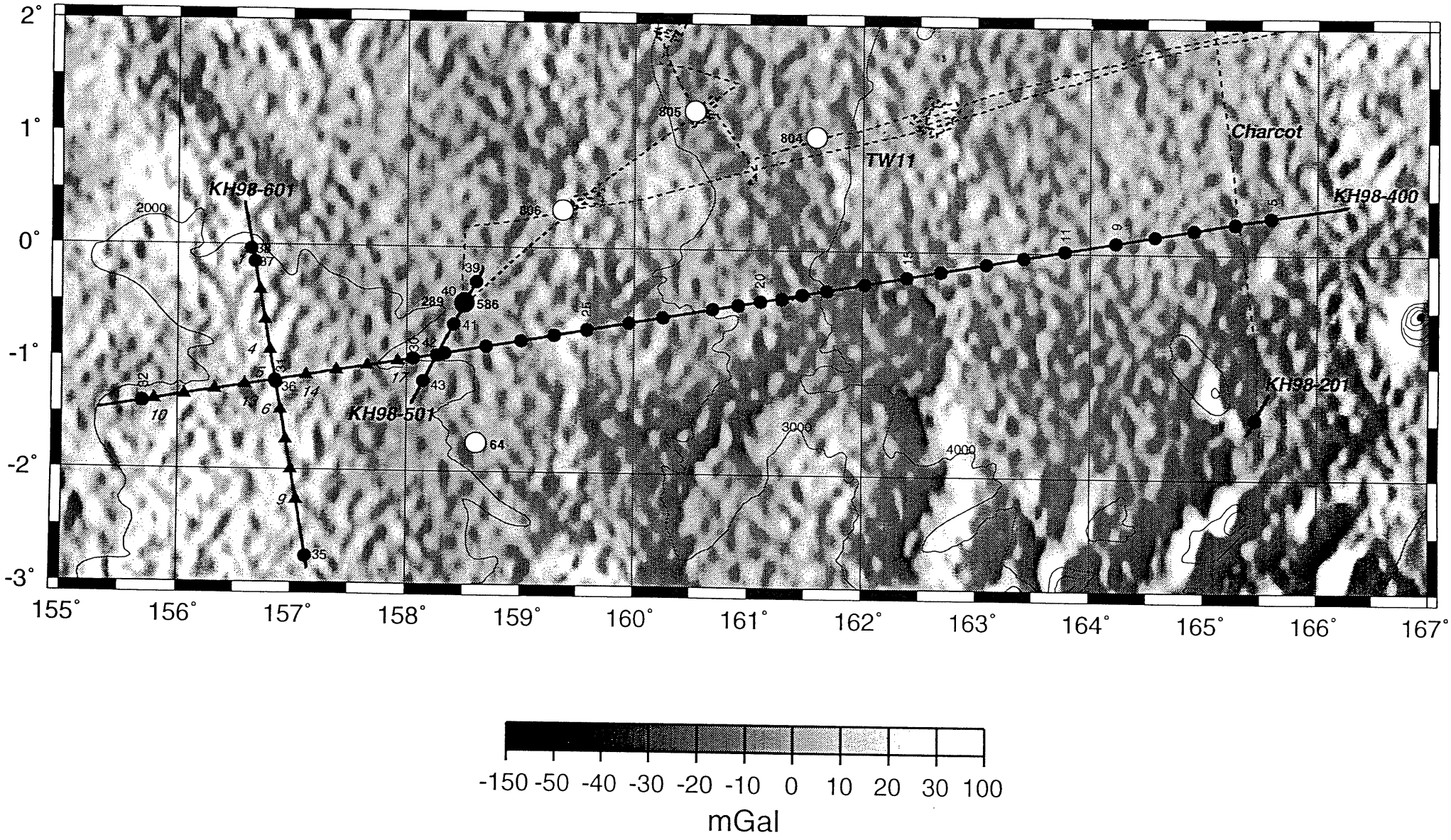

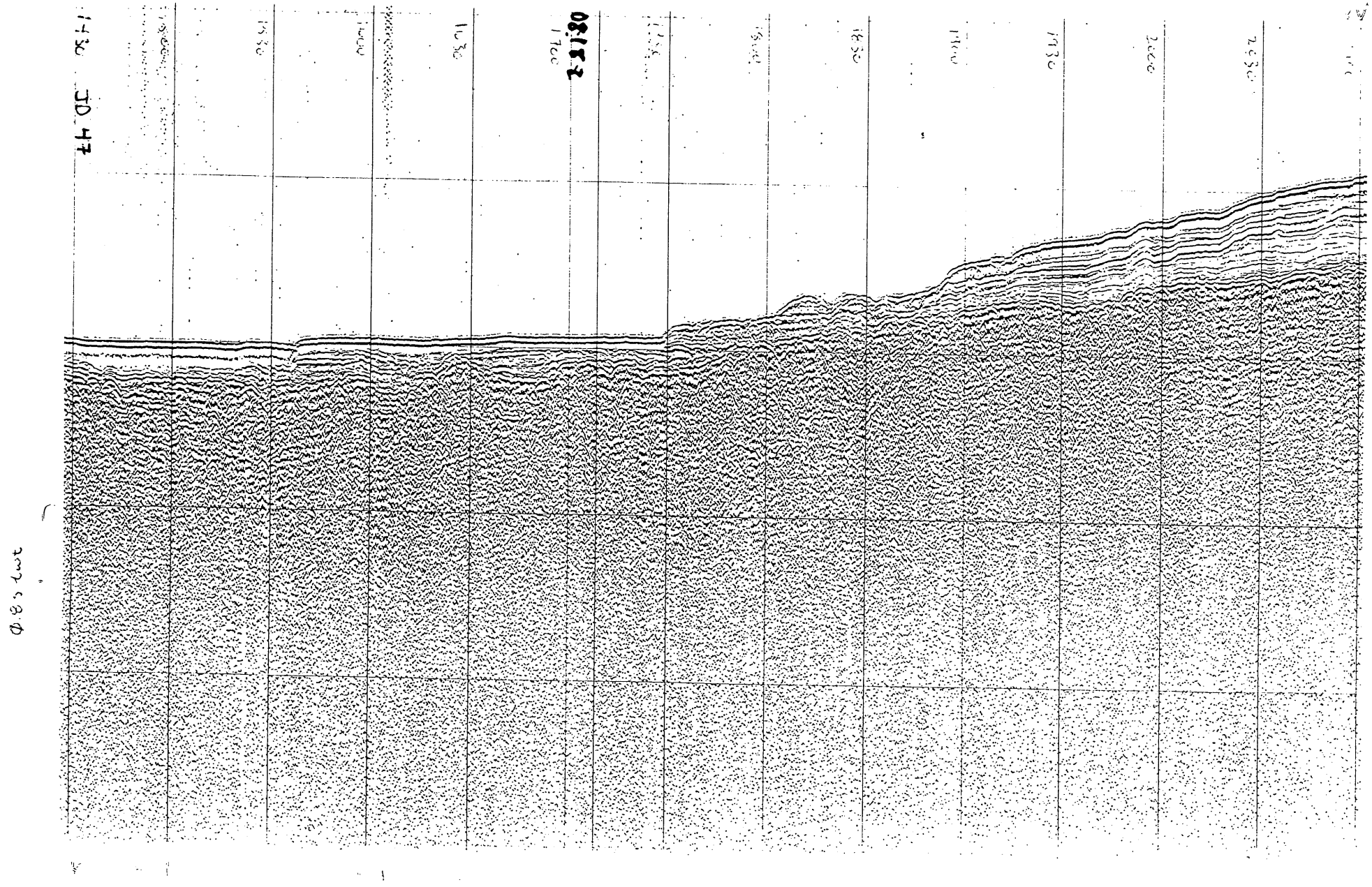

Figure 4. KH98-1 Leg 2 Line 401 segment at the transition between the Nauru Basin and the lower slope domain of OJP's northeastern flank.

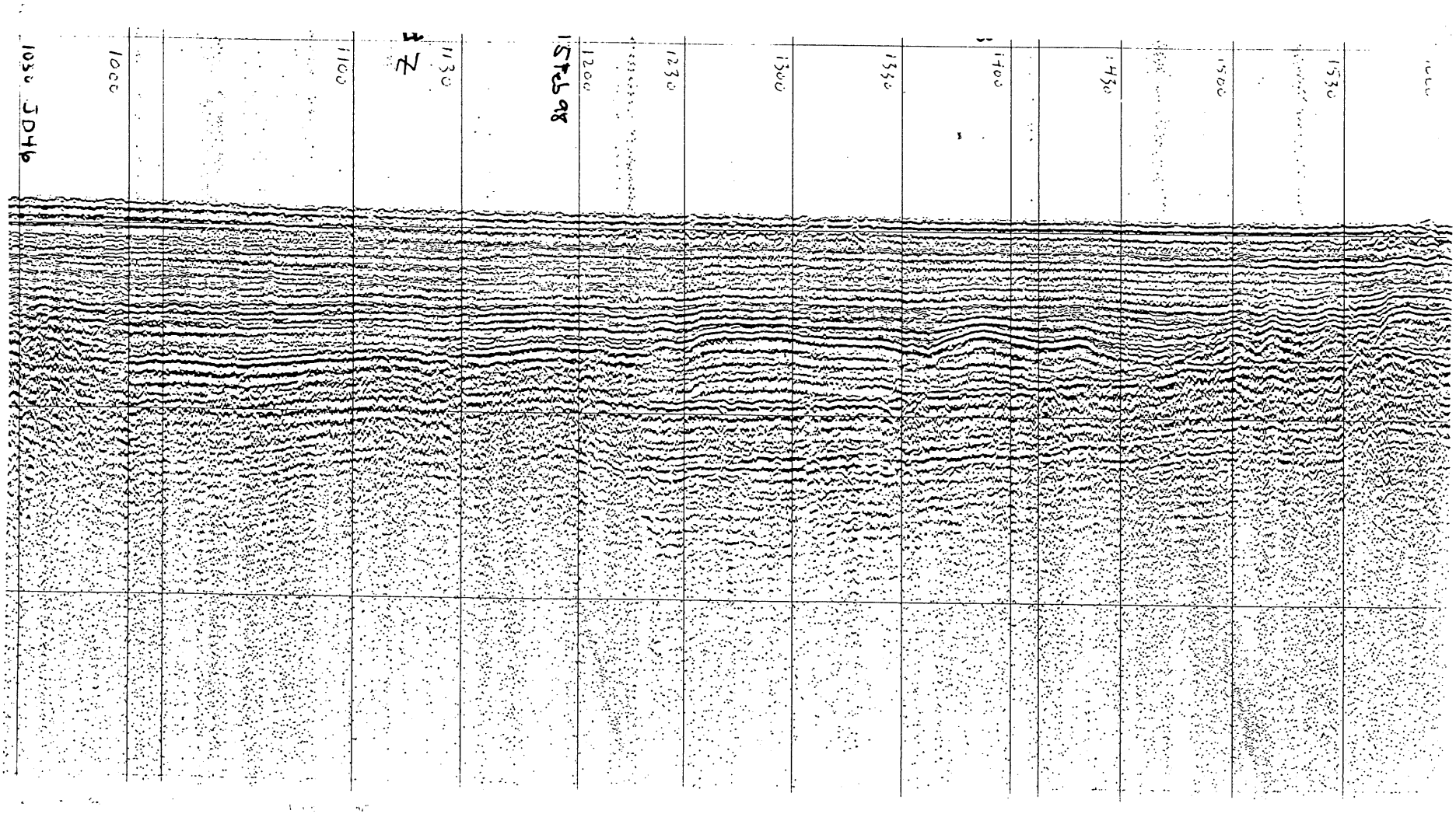

Figure 5. KH98-1 Leg 2 Line 401 segment in the southern Nauru Basin near the intersection with *Charcot* line.

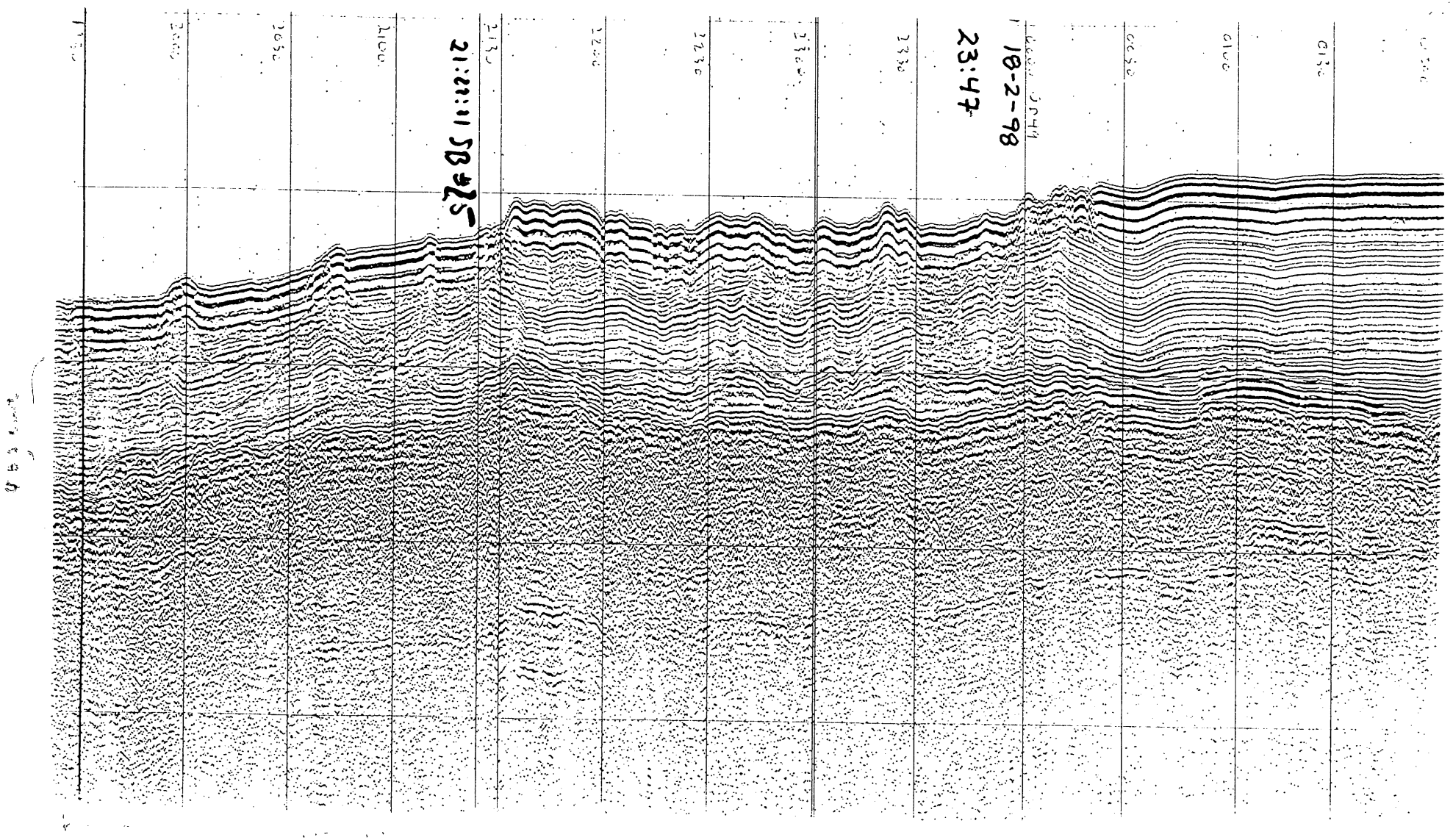

Figure 6. KH98-1 Leg 2 Line 403 segment near the boundary between the upper slope and crestal OJP domains. Note the deformation front at 49.0015.

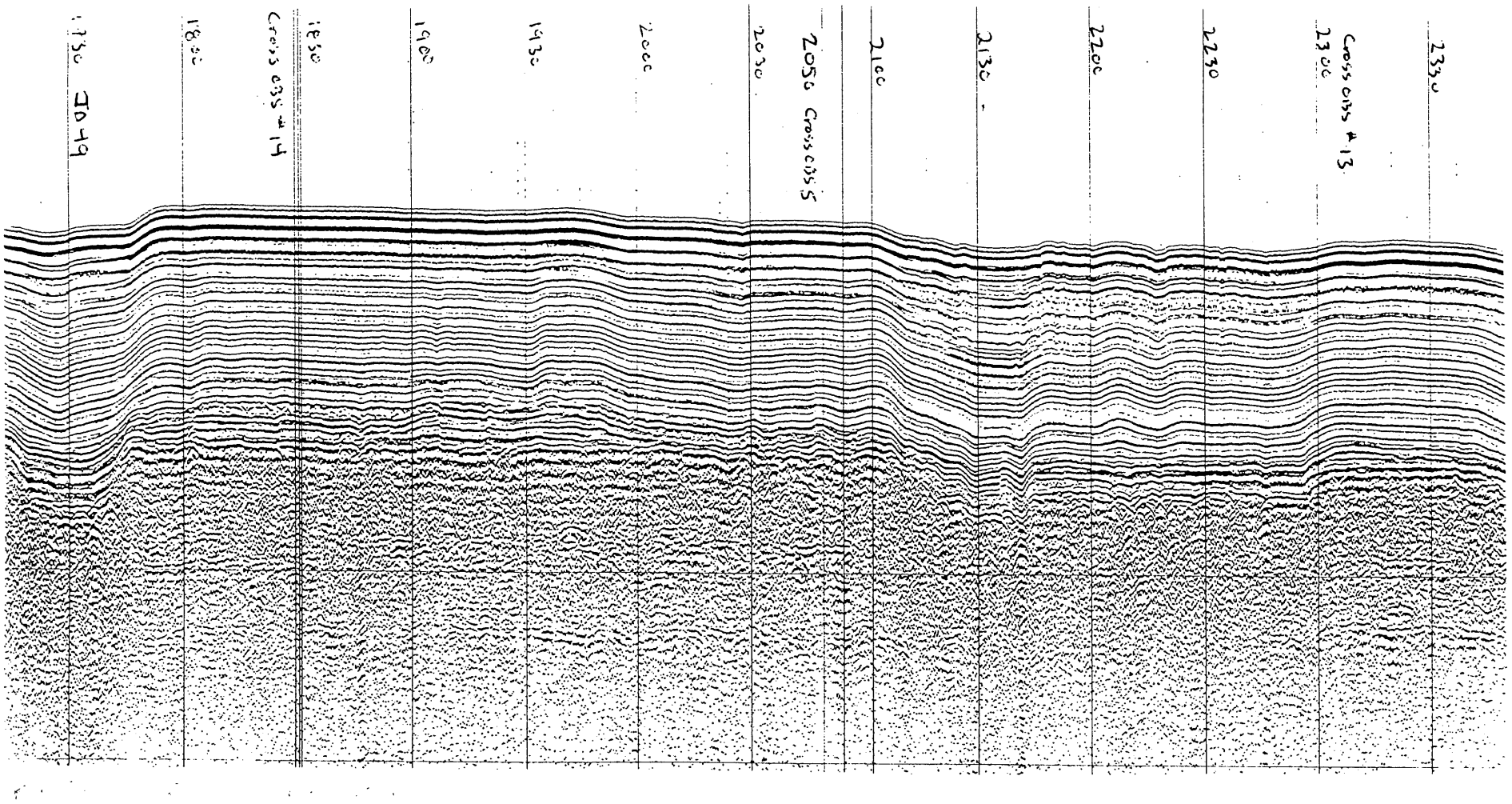

Figure 7. KH98-1 Leg 2 Line 404 segment on OJP's crest. OBS 5 is at the intersection with KH98-1 Leg 2 Line 501. See Figures 3 and 8 for location, and Figure 9 for KH98-1 Leg 2 Line 501.

Figure 8. Location of central OJP profile, KH98-1 Leg 2 Line 501. OBS (wideband, stars; standard, triangles) and sonobuoy (small black circles) locations are shown, as are DSDP sites (large circles: filled, basement; open, sediment only).

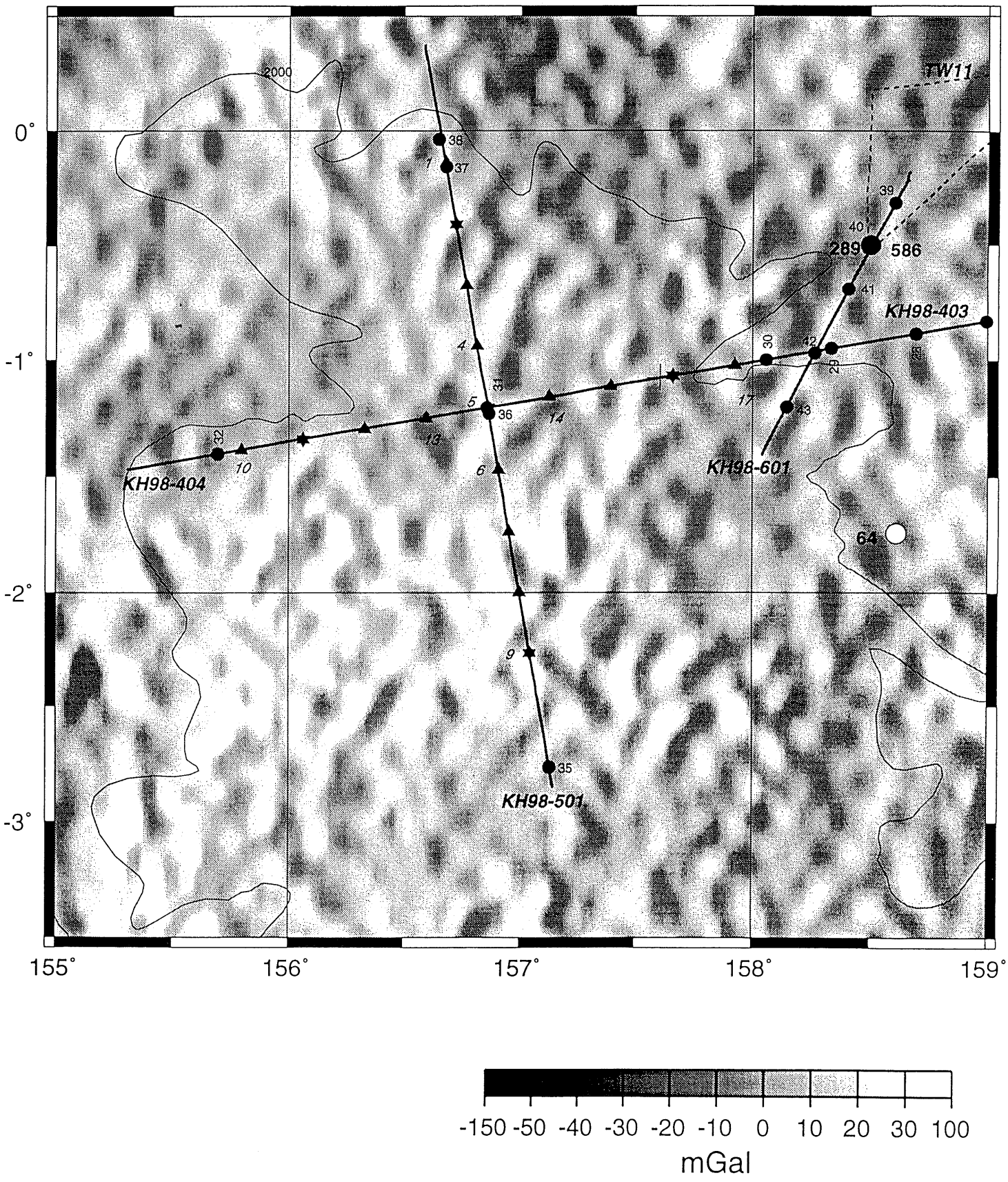

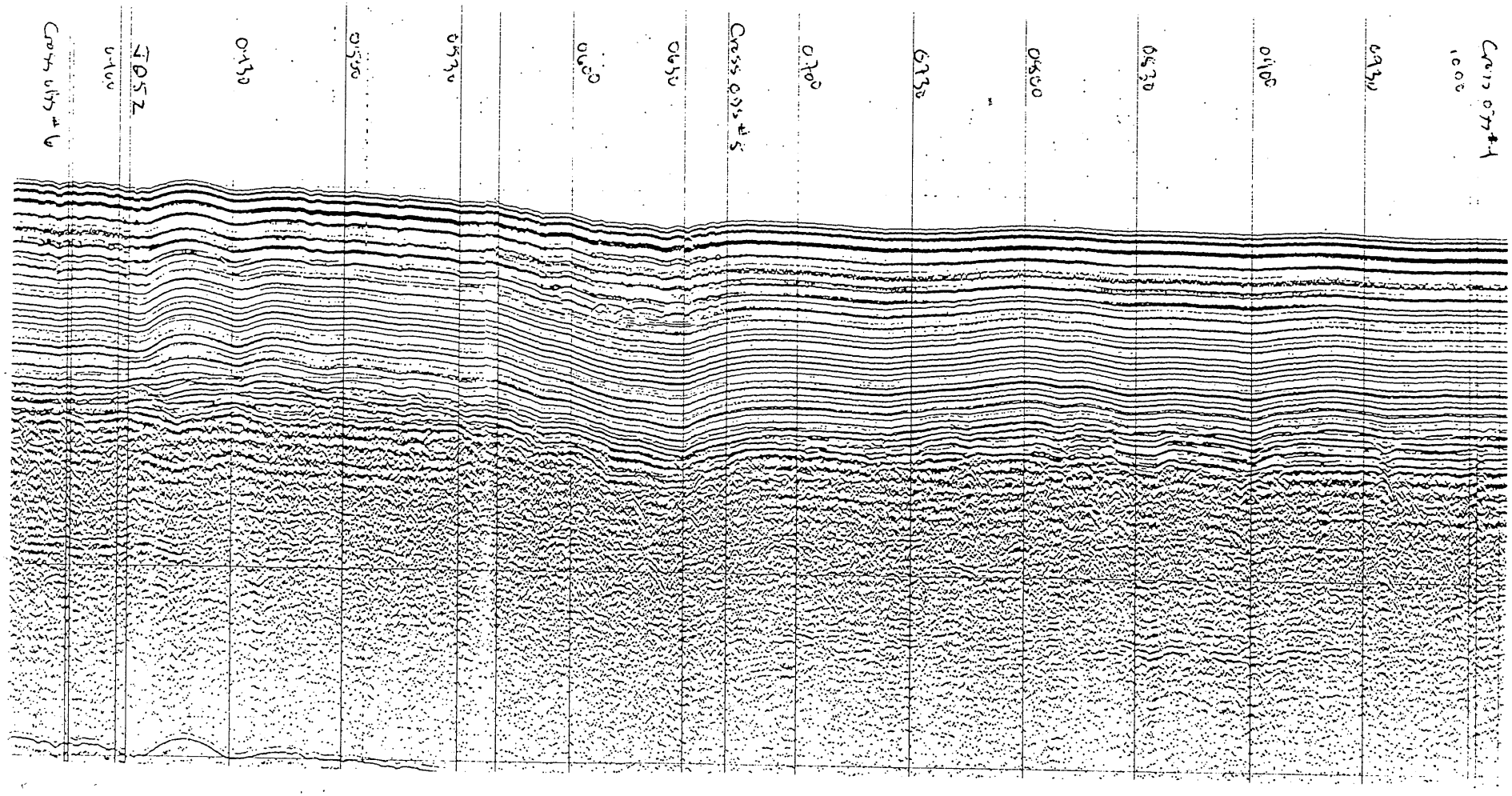

Figure 9. KH98-1 Leg 2 Line 501 segment on OJP's crest. OBS 5 is at the intersection with KH98-1 Leg 2 Line 404 (Fig. 7). See Figures 3 and 8 for location.

Figure 10. Location of DSDP 289-Line 400 tie profile. Sonobuoy (small black circles) and DSDP (large circles: filled, basement; open, sediment only) locations are shown.

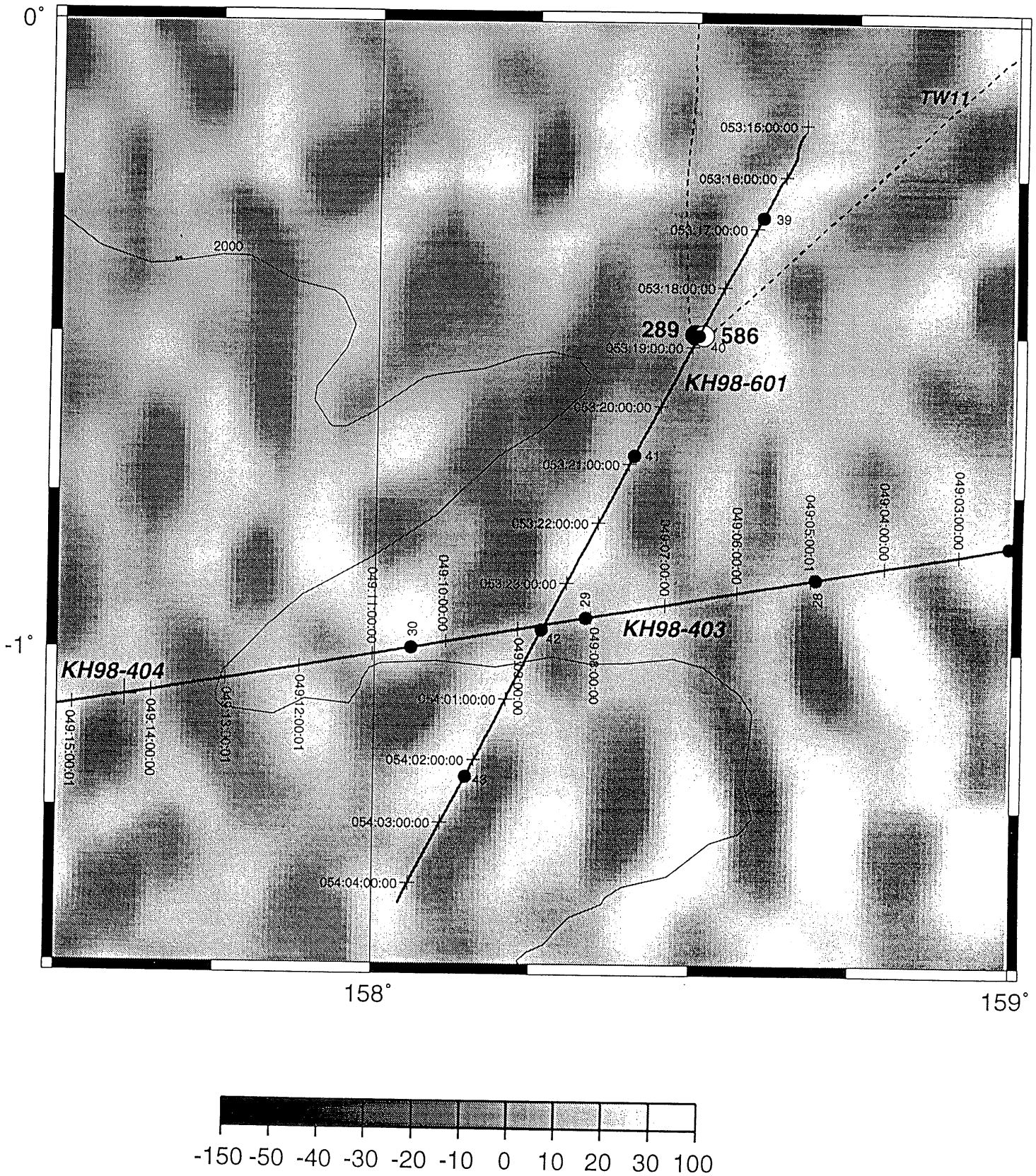

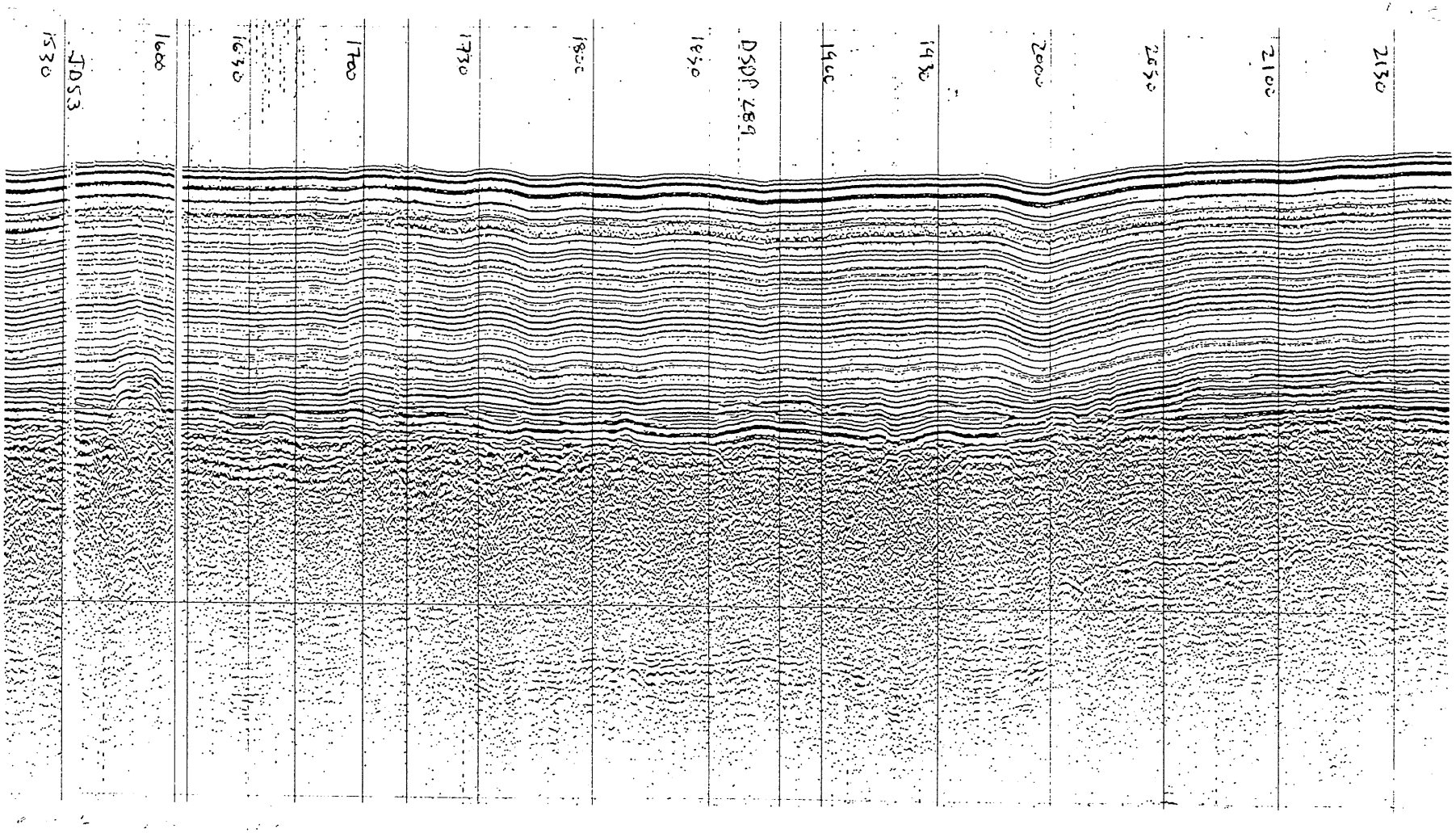

Figure 11. KH98-1 Leg 2 Line 601 segment over DSDP Site 289 (53.1840). See Figures 3, 8, and 10 for location.

Table 1 - Plume Head and Age-Progressive Models: Predictions, State of Previous Data, and Enhancements of KH98-1 Leg 2 Data

Constraint	Plume Head	Age-Progressive	Previous Data	KH98-1 Data
Regional Setting	petrology, geochemistry, and mantle tomography support existence of mantle plumes worldwide, both on- and off-ridge	presence of causative hotspot	some plate reconstructions suggest that the Louisville hotspot generated OJP, via either a plume head or age progression	will put the OJP into proper context relative to flanking Mesozoic oceanic crust of the Nauru Basin
Stratigraphy (MCS, drilling)	OJP built on pre-existing igneous crust; Cretaceous volcanics onlap older sediment and wedge out towards Nauru Basin	no preexisting crust; Cretaceous volcanics continuous with those in Nauru Basin	SCS cannot distinguish intra-basement and basement/sediment relationships	MCS data will image OJP flank/Nauru Basin stratigraphic and structural relationships in the upper crust clearly
	many thick (>10 m) flows, which result in layered reflections in upper 10 km of crust	many thin (~1 m) flows, which result in few layered reflections within upper 10 km of crust	SCS data image only isolated intra-basement events; ~28 m-thick flow at ODP Site 807	MCS data will show presence or absence of layering in upper few km of igneous crust
	localized, non-organized, emplacement-related lithospheric extension (normal faults) - different than Iceland	widespread, organized, mid-ocean ridge-related lithospheric extension—tectonic fabric of normal and transform faults, resembling Iceland	faulting is not resolved in the OJP acoustic basement complex	MCS data will resolve faults, particularly where layering is observed
Crustal Structure (OBS, drilling)	lower crustal body characterized by V_p = 7.0-7.6 km/s	velocities suggestive of expanded oceanic crust; no lower crustal body of V_p = 7.0-7.6 km/s	refraction data support the plume head model (Fig. 2)	OBS data will provide detailed velocity structure to Moho of the thick, central OJP
	thick body of olivine/pyroxene cumulates, with distinctive V_p's and densities; high-velocity mantle	thick sequence of 'oceanic' crust: basalt + gabbro overlying lower velocity mantle	Kerguelen Plateau (KP) results are ambiguous: SKP supports age-progressive model, whereas NKP supports plume head model; no deep samples have been recovered from OJP	will result in siting of OJP basement drilling targets
Geochronology (ODP)	one (e.g., Deccan Traps) or two (as suggested by double plume head model of Bercovici & Mahoney [1994]) age peaks in volcanism	relatively continuous volcanism	basement dates from Malaita and Santa Isabel islands and three shallow ODP drill sites support plume head model	will result in siting of OJP basement drilling targets

3.5 KHZ ECHO SOUNDING

INTRODUCTION

Sub-bottom profiling, using a hull-mounted 3.5 kHz transducer, was undertaken continuously during Leg 2 of the KH98-1 cruise to the Ontong Java Plateau. Excellent analog records were obtained over both the southern (Stewart) and northern arches of the OJP Eastern Salient, across Stewart and the Nauru basins, and well up onto the OJP high plateau (Fig. 1), permitting identification of the acoustic character of bottom and sub-bottom reflectors over most of the region. For the most part, bottom penetration/layering was observed across both the Stewart and northern arches, as well as the intervening Stewart Basin, and layering was particularly well developed across the Nauru Basin.

In general, four types of acoustic horizons (Fig 2) could be distinguished: a stratified layer, a transparent layer, a diffuse layer, and a highly reflective, often impenetrable, opaque layer. The opaque layer was found to be ubiquitous over most of the seafloor of the OJP High Plateau, whereas one or more combinations of the other types were invariably encountered elsewhere. Of particular note is the occurrence of a semi-transparent, diffuse layer found to onlap, cap, and sometimes truncate, underlying stratified horizons in the Stewart and Nauru basins. This layer, particularly widespread in the Nauru Basin, may well have originated as debris flows that emanated from the upper reaches of the Eastern Salient flowing downslope into Stewart Basin and from the High Plateau, coursing northeastward into the Nauru Basin, through the large submarine canyons on the Plateau margin bordering the Basin.

In addition to the ubiquitous opaque layer across the High Plateau, sediment waves (Fig. 3) were also observed over large areas of the plateau crest, particularly in the vicinity of the OBS arrays. The existence of these sedimentary structures suggests the presence of high velocity bottom currents which may have resulted the winnowing of plateau sediment, causing the fine grained fraction (clays and nannofossils) to be removed, leaving the coarse grained fraction (foraminiferal sands) behind, deposited in sediment ridges. This removal of fine-grained sediment and retention of the coarse grained sediment may be the explanation of the pervasive presence of the highly reflective opaque layer acoss the High Plateau.

OBSERVATIONS

EASTERN SALIENT OF THE OJP

12 Feb to 0600Z The slope on southern flank of Stewart Arch is faulted. The seafloor is underlain by an opaque to semi-opaque layer with a few, very faint, reflectors visible in some areas.

0600-0645Z The seafloor over Stewart Arch is underlain by a diffuse, coarsely stratified layer with up to 0.13 sec of penetration. The crest of the arch, 1100m deep, is located at 0641Z.

0645-0836Z The slope on the northern flank of Stewart Arch is steep with numerous, low amplitude, hyperbolic reflectors, a few meters to a few tens of meters high, suggestive of block-faulted terrain. Seafloor is underlain by a diffuse layer up to 0.1 sec thick.

0836-0910Z Rotated fault block (Fig. 4). The seafloor is underlain by a faintly-stratified diffuse layer, up to 0.8 sec thick.

0910-0947Z Steep slope, again with numerous, low-amplitude hyperbolic reflectors, a few meters to a few tens of meters high, that are suggestive of block-faulted terrain. The seafloor is underlain by diffuse layer up to 0.1 sec thick.

0947-1155Z The undulating seafloor of the southern side of Stewart Basin deepens northward from 3415 to 3575m and is underlain by 0.1 sec of stratified sediment.

1155-1420Z The seafloor, gradually shallowing from 3575 to 3530m, is underlain by a diffuse layer (debris flow?) that onlaps adjoining stratified sediments (Fig. 5), 0.06 sec thick on either side.

1420-1600Z Stratified sediments, > 0.2 sec thick, are tilted north and south flanking a 250m high volcaniform peak (Fig. 6) located between 1500 & 1522Z.

1600-2115Z The smooth, broadly-stepped, seafloor of northern side of Stewart Basin is underlain by an undulating stratified layer up to 0.3 sec thick. The seafloor shallows from 3475 to 3298m at the base of the Northern Arch of the Eastern Salient. Seismic line #101 was shot between 1600Z 12 Feb & 1300Z 13 Feb.

2115-2340Z The southern flank of Northern Arch, downfaulted to the south, appears similar to the northern side of Stewart Arch (steep slope with numerous, hyperbolic reflectors suggestive of block-faulted terrain), but with less V.E. and more sediment penetration.

12 Feb 2340-13 Feb 0032Z First crossing of the crest of the Northern Arch (arch crest, 1655m deep, is located at 2356Z). Graben on

crest contains > 0.3 sec of stratified sediment (Fig. 7).

0032-1100Z Traversing the top the of arch. Seafloor is underlain by an undulating and faulted stratified layer, 0.2-0.3 sec thick.

1100-1300Z Second crossing of the crest of the Northern Arch (Fig. 8) Arch crest, 1403m deep, underlain by ~0.27 sec of stratified sediment, is located at 1145Z. Arch flanks are underlain by > 0.3 sec of stratified sediment.

1300-1538Z The seafloor drops from 1817 to 2190m. Sediment penetration nil-- essentially an opaque layer.

1538-2320Z High relief, rugged seafloor, characterized by numerous reflection hyperbolae but is underlain by an essentially smooth basal reflector, < 0.15 sec below seafloor. Troughs and peaks occur at 2900, 2540, 3270, 2750, & 4315m, before dropping to 4460m at the edge of the Nauru Basin.

NAURU BASIN

13 Feb 2320-14 Feb 1100Z The seafloor of the Nauru Basin, rising gently northward from 4460 to 4428m, is underlain by a stratified sediment wedge that gradually thins northward from 0.05 to 0.02 sec (Fig. 9). This wedge is underlain, in turn, by a diffuse layer extending down to ~0.10 sec below the seafloor. An intervening volcaniform ridge, evidenced by a series of reflection hyperbolae rising to 4230m, breaks through the seafloor between 0400 & 0505Z (Fig. 10); the surrounding seafloor being disturbed as far south as 0130Z and as far north as 0505Z. Seismic line #201 was shot between 0430 & 1000Z 14 Feb.

1100-1415Z The Nauru Basin seafloor (4428 to 4368m) is hummocky, underlain by a thin (0.02 sec) stratified layer, perturbed by a series of short-wavelength, low-amplitude reflection hyperbolae, which is underlain in turn by the diffuse layer (Fig. 11).

1415-1645Z The seafloor, gently rising from 4368 to 4357m, is underlain by a thin (0.02 sec) stratified layer, below which a transition occurs in the underlying diffuse layer (Fig. 12). The upper part becomes more transparent (between 0.02-0.04 sec) whereas the lower part initially becomes more opaque and then turns into a thick, well-developed stratified layer (between 0.04-0.14 sec).

14 Feb 1645-15 Feb 0500Z The seafloor (4340-4330m) is underlain by: an upper stratified layer (base <0.015 sec), a transparent layer (base <0.03 sec), and a lower stratified layer (base <0.12 sec). Seismic line #401 was begun at 0400Z 15 Feb.

0500-0745Z The seafloor, gradually deepening from 4330 to 4354m, continues to be underlain by: an upper stratified layer (base <0.015 sec), a transparent layer (base <0.03 sec), and a lower stratified layer (base <0.12 sec).

0745-0800Z A volcaniform ridge, as evidenced by a series reflection hyperbolae, breaks the seafloor and rises to 4170m between 0745 & 0800Z. At 0745Z, the upper stratified layer thins, the underlying transparent layer thickens, and the lower stratified layer wedges out, as the sequence abuts against the eastern flank of the ridge (Fig. 13). Moats are formed on both sides of the ridge with the western moat about 40m deeper than that on the eastern side. On the western flank of the ridge, the entire sequence is deeply incised by an overlapping diffuse layer which appears to truncate the entire section down through the lower stratified layer (Fig. 13).

15 Feb 0800Z-16 Feb 0130Z The seafloor initially rises west of the ridge to 4350m at 0845Z after which it gradually descends to the west becoming increasingly perturbed by a series of short-wavelength, low-amplitude reflection hyperbolae. Westward, the lower stratified layer gradually fades away and the hummocky seafloor, underlain by a thin (0.02 sec) stratified layer, becomes intensely perturbed by the short-wavelength, low-amplitude reflection hyperbolae (Fig. 14) over long low seafloor rises, is underlain in turn by an increasingly thick diffuse layer.

0130-1225Z As the seafloor descends below 4425 it flattens out, loses its hummocky character, and is underlain once again by a normal upper stratified layer, below which lies a semi-transparent layer becoming increasingly diffuse with depth.

1225-1728Z The character of this layered sequence is similar to that crossed earlier to the east. The seafloor, however, beginning to rise in broad gentle steps, signals proximity to the OJP, reaching 4382m at edge of the northeastern margin of the OJP.

1728-1915Z At the edge of the OJP (Fig. 15) an intensely deformed zone is encountered, with no visible coherent reflector present until 1915Z, where the highly stratified, but deeply eroded lower flank of the OJP appears exposed in the section at 4060 m.

OJP HIGH PLATEAU

1915-2130Z An irregular, undulating seafloor, underlain by the well stratified but deeply eroded flank of the OJP is initially observed as the eastern margin is traversed. As the seafloor shallows, however, the underlying deep stratification begins to fade, becoming noticibly faint above 3500m and increasingly fainter with decreasing depth until 2500m is reached (at 2130Z) where the stratified section is entirely replaced by the highly reflective opaque layer (Fig. 2)

15 Feb 2130Z-onward The highly reflective seafloor now visible in the record appears to be ubiquitous over most of the High Plateau. The only seafloor features to break the monotonous presence of this opaque layer are the sediment waves (Fig. 3) first encountered over the crest of the High Plateau

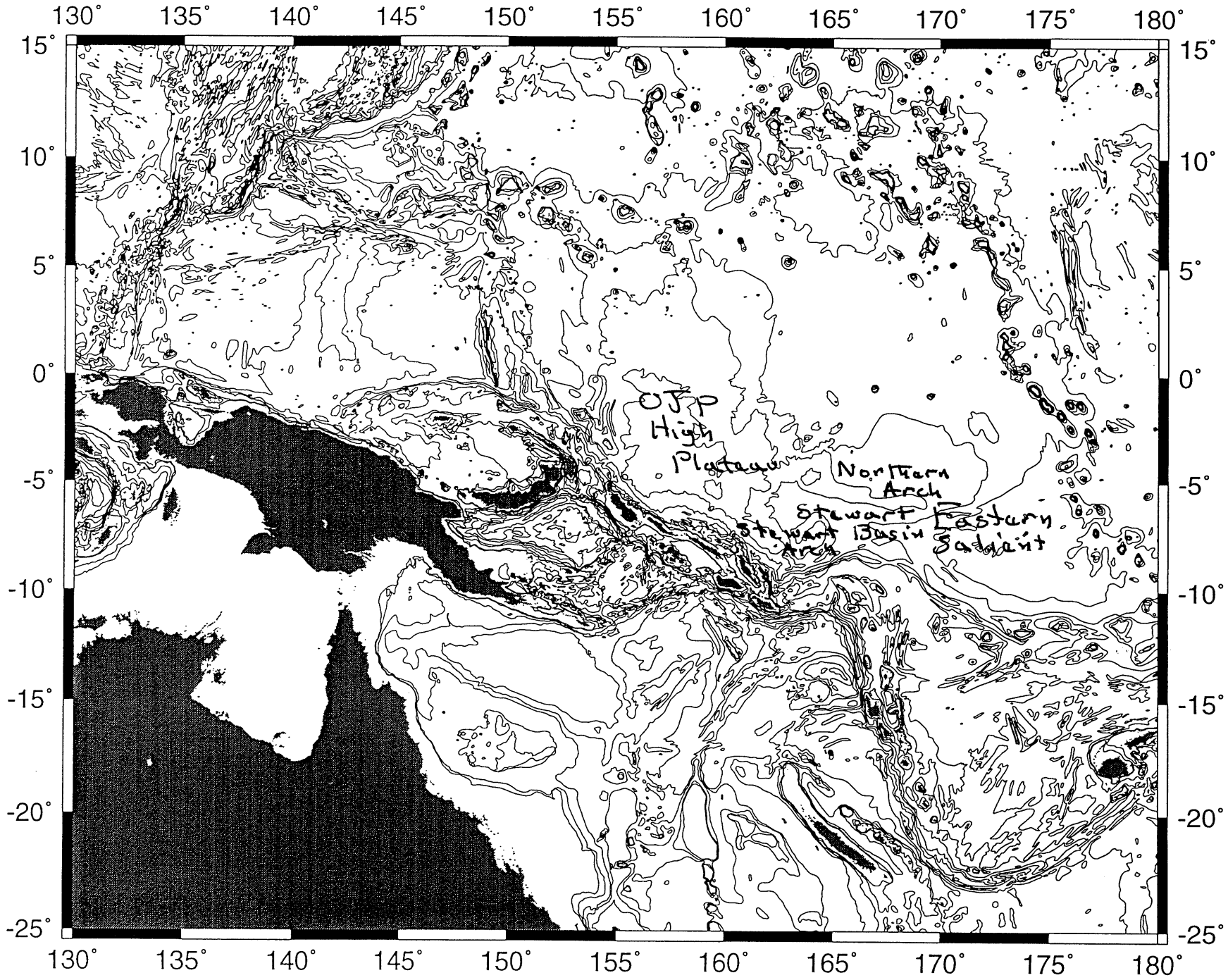
130°
135°
140°
145°
150°
155°
160°
165°
170°
175°
180°
15°
10°
5°
0°
-5°
-10°
-15°
-20°
-25°
OJP
High
Plateau
Northern
Arch
Stewart
Basin
Eastern
Salient
Stewart
Arch

Fig 1

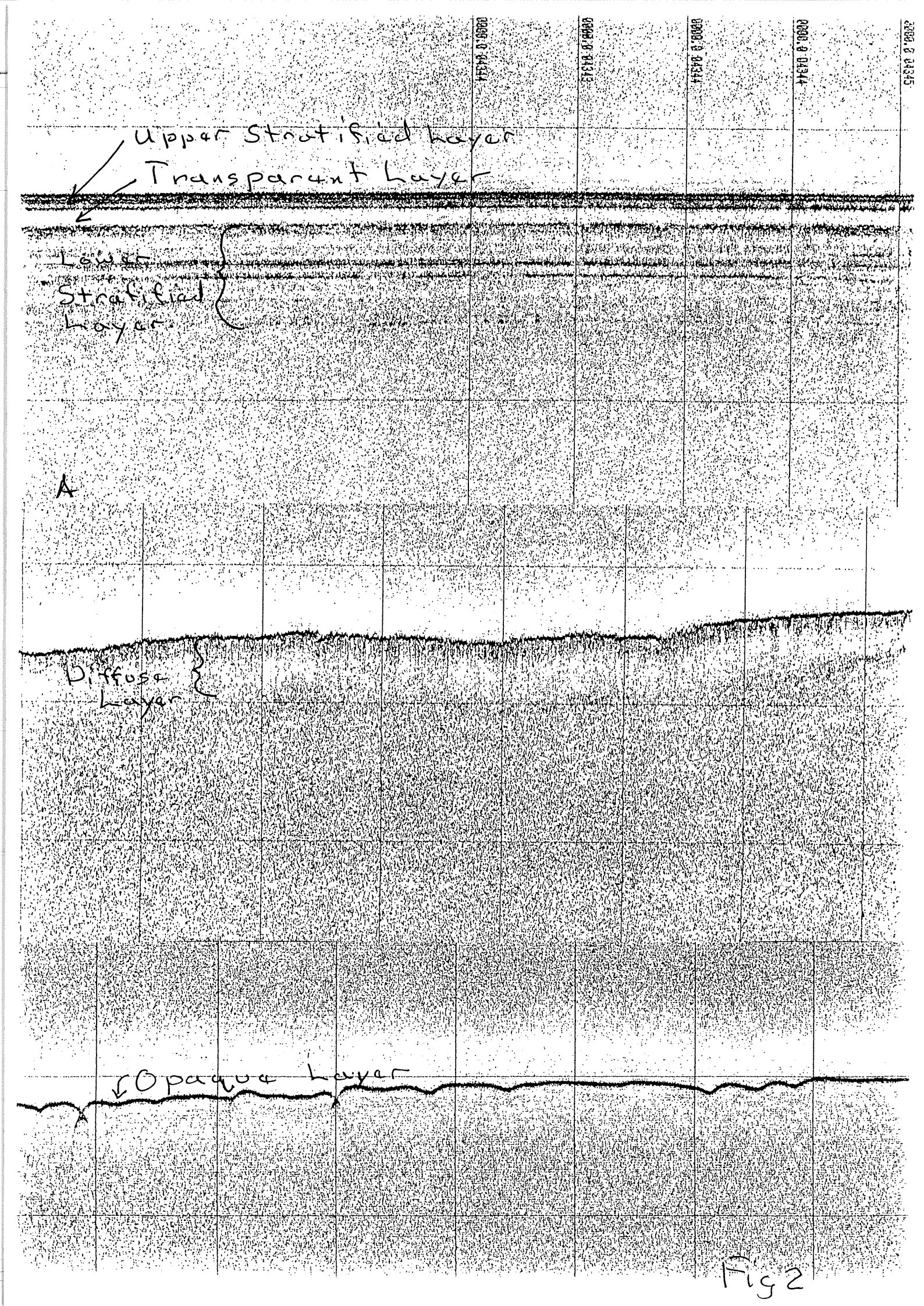
Upper Stratified layer
Transparant Layer
Lower Stratified Layer
A
Diffuse Layer
Opaque Layer

Fig 2

Fig B

Fig 4

Fig 5

Fig 6

Fig 7

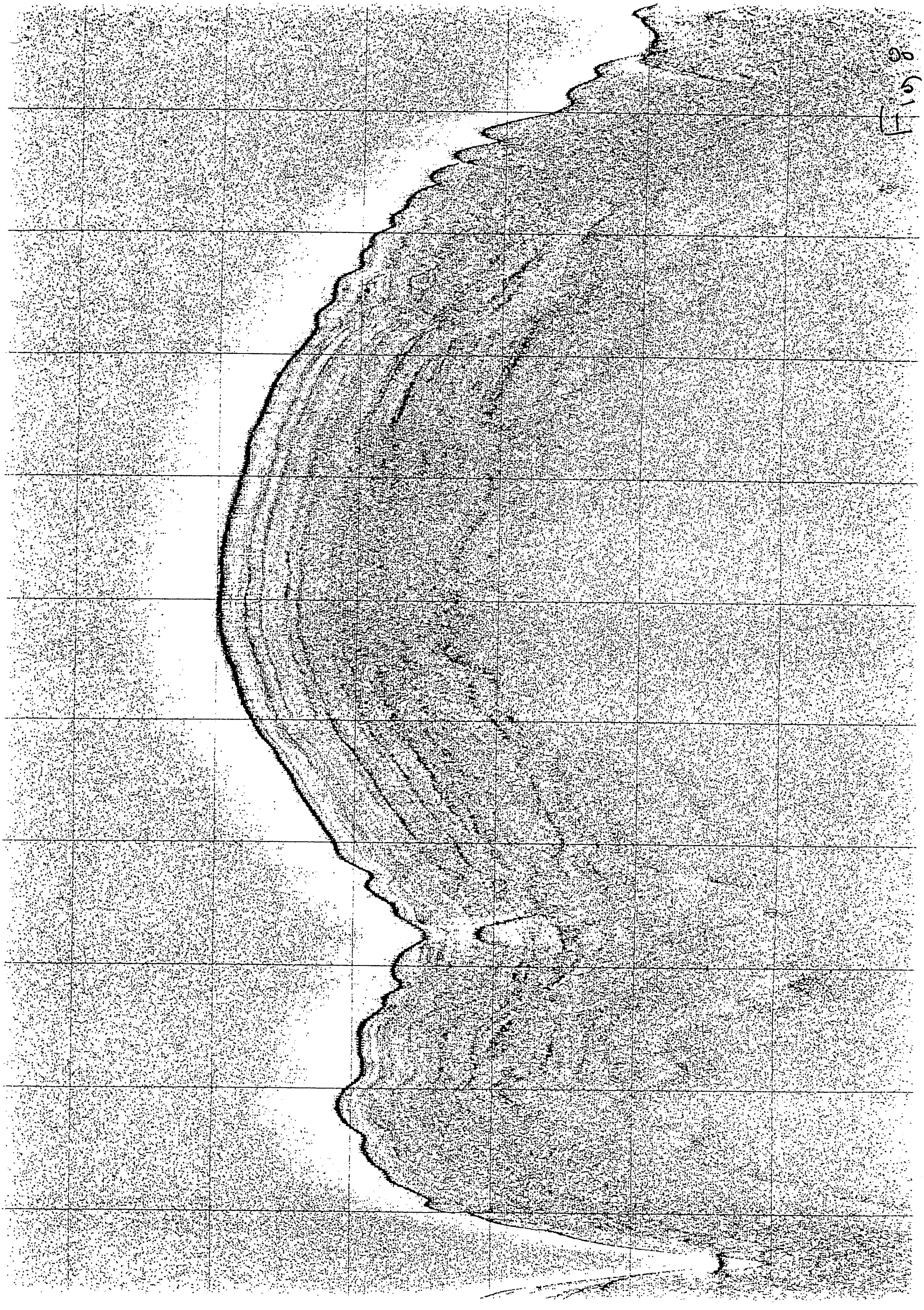

98/02/14 02:30:00 S01 39.5568 E165 20.7227 035.4 008.21 0000.0 04453

98/02/14 02:15:00 S01 39.7763 E165 20.4961 025.3 002.50 0000.0 04455

98/02/14 02:00:00 S01 40.0342 E165 20.0479 024.5 015.46 0000.0 04456

98/02/14 01:45:00 S01 44.2631 E165 18.4322 026.8 014.57 0000.0 04454

98/02/14 01:30:00 S01 47.6868 E163 16.7284 026.3 015.32 0000.0 04457

98/02/14 01:15:00 S01 51.0747 E165 15.0456 025.4 014.80 0000.0 04458

98/02/14 01:00:00 S01 54.4518 E165 13.3691 025.0 014.70 0000.0 04457

98/02/14 00:45:00 S01 57.7876 E165 11.7526 026.8 015.02 0000.0 04459

98/02/14 00:30:00 S02 01.1340 E165 10.0428 025.6 015.42 0000.0 04457

98/02/14 00:15:00 S02 04.4843 E165 08.4621 027.2 015.21 0000.0 04461

98/02/14 00:00:00 S02 07.8202 E165 06.7816 027.4 015.66 0000.0 04464

98/02/13 23:45:00 S02 11.1146 E165 05.0746 025.5 013.22 0000.0 04463

5 of 7

98/02/14 05:00:00 S01 38.2237 E165 24.5666 021.2 004.16 0000.0 04435
98/02/14 04:45:00 S01 38.1631 E165 24.0748 020.5 004.26 0000.0 04435
98/02/14 04:15:00 S01 34.9617 E165 22.7848 045.7 004.20 0000.0 04432
98/02/14 04:00:00 S01 35.5529 E165 23.1786 049.5 003.88 0000.0 04434
98/02/14 03:45:00 S01 36.2112 E165 21.5184 020.9 002.53 0000.0 04447
98/02/14 03:30:00 S01 36.7530 E165 21.1996 030.0 002.52 0000.0 04447
98/02/14 03:15:00 S01 37.2311 E165 20.8978 009.6 002.45 0000.0 04447
98/02/14 03:00:00 S01 37.6998 E165 20.8837 324.1 004.12 0000.0 04450
98/02/14 02:45:00 S01 38.1181 E165 21.0118 020.2 002.34 0000.0 04452
98/02/14 02:30:00 S01 38.6568 E165 20.7227 030.1 002.21 0000.0 04453

98/02/14 13:15:00 S00 38.3631 E165 51.2815 026.1 015.28 0000.0 04399

98/02/14 13:00:00 S00 41.6678 E165 49.6492 026.4 015.23 0000.0 04398

98/02/14 12:45:00 S00 45.1828 E165 47.9961 025.9 015.17 0000.0 04355

98/02/14 12:30:00 S00 48.6918 E165 46.3631 026.7 014.86 0000.0 04413

98/02/14 12:15:00 S00 52.0393 E165 44.7033 026.6 015.75 0000.0 04419

98/02/14 12:00:00 S00 55.4728 E165 42.9588 026.9 015.70 0000.0 04429

98/02/14 11:45:00 S00 58.9875 E165 41.3162 025.5 015.45 0000.0 04423

98/02/14 11:30:00 S01 02.4423 E165 39.5370 025.4 015.25 0000.0 04419

98/02/14 11:15:00 S01 05.8910 E165 37.8723 027.2 014.78 0000.0 04432

98/02/14 11:00:00 S01 09.1480 E165 36.8849 023.1 015.52 0000.0 04428

98/02/14 10:45:00 S01 11.6571 E165 34.7259 002.43 0000.0 04430

98/02/14 10:30:00 S01 12.2630 E165 34.6419 001.4 002.26 0000.0 04430

1-13

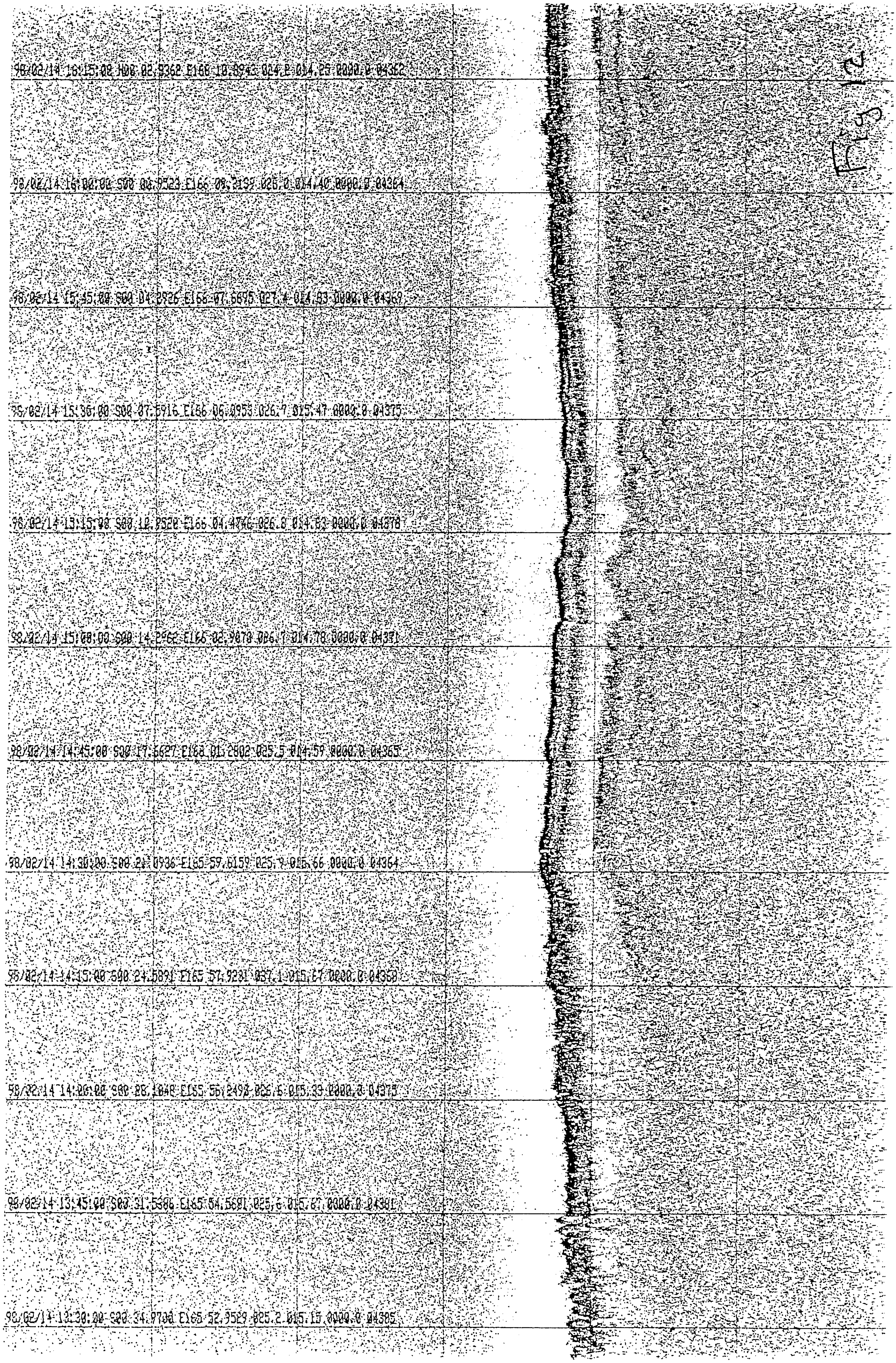

Fig 12

98/02/15 08:45:00 N00 22.5687 E165 52.4943 253.1 007.31 0000.0 04350

98/02/15 08:30:00 N00 22.5284 E165 54.2897 252.1 007.10 0000.0 04351

98/02/15 08:15:00 N00 22.4880 E165 55.0997 254.1 006.87 0000.0 04376

98/02/15 08:00:00 N00 23.1477 E165 57.6110 255.7 007.15 0000.0 04383

98/02/15 07:45:00 N00 23.4270 E165 59.3258 263.0 006.92 0000.0 04351

98/02/15 07:30:00 N00 23.6449 E166 01.0417 264.3 007.25 0000.0 04343

98/02/15 07:15:00 N00 23.8688 E166 02.9241 261.1 006.50 0000.0 04341

98/02/15 07:00:00 N00 24.1221 E166 04.3921 263.6 006.73 0000.0 04333

98/02/15 06:45:00 N00 24.3837 E166 06.0529 261.8 007.25 0000.0 04340

98/02/15 06:30:00 N00 24.6537 E166 07.6928 266.5 006.60 0000.0 04339

98/02/15 06:15:00 N00 24.8481 E166 09.3698 262.1 007.30 0000.0 04340

98/02/15 06:00:00 N00 25.1039 E166 11.0565 261.5 007.14 0000.0 04338

M

17

98/02/15 16:45:00 N00 11.2713 E164 44.6776 257.3 046.54 0000.0 04394

98/02/15 16:30:00 N00 11.5786 E164 46.4313 259.5 047.53 0000.0 04393

98/02/15 16:15:00 N00 11.8566 E164 48.1881 259.6 047.03 0000.0 04378

98/02/15 16:00:00 N00 12.1770 E164 49.9254 261.2 047.10 0000.0 04364

98/02/15 15:45:00 N00 12.4678 E164 51.6467 257.8 047.49 0000.0 04364

98/02/15 15:30:00 N00 12.7736 E164 53.3818 262.1 045.77 0000.0 04387

98/02/15 15:15:00 N00 13.0693 E164 55.0783 264.2 046.83 0000.0 04390

98/02/15 15:00:00 N00 13.3583 E164 56.7693 259.1 046.17 0000.0 04394

98/02/15 14:45:00 N00 13.6262 E164 58.5525 263.0 047.14 0000.0 04385

98/02/15 14:30:00 N00 13.9427 E165 00.2165 263.5 047.09 0000.0 04387

98/02/15 14:15:00 N00 14.2733 E165 02.0465 260.2 047.48 0000.0 04394

98/02/15 14:00:00 N00 14.5812 E165 03.7461 259.6 047.45 0000.0 04391

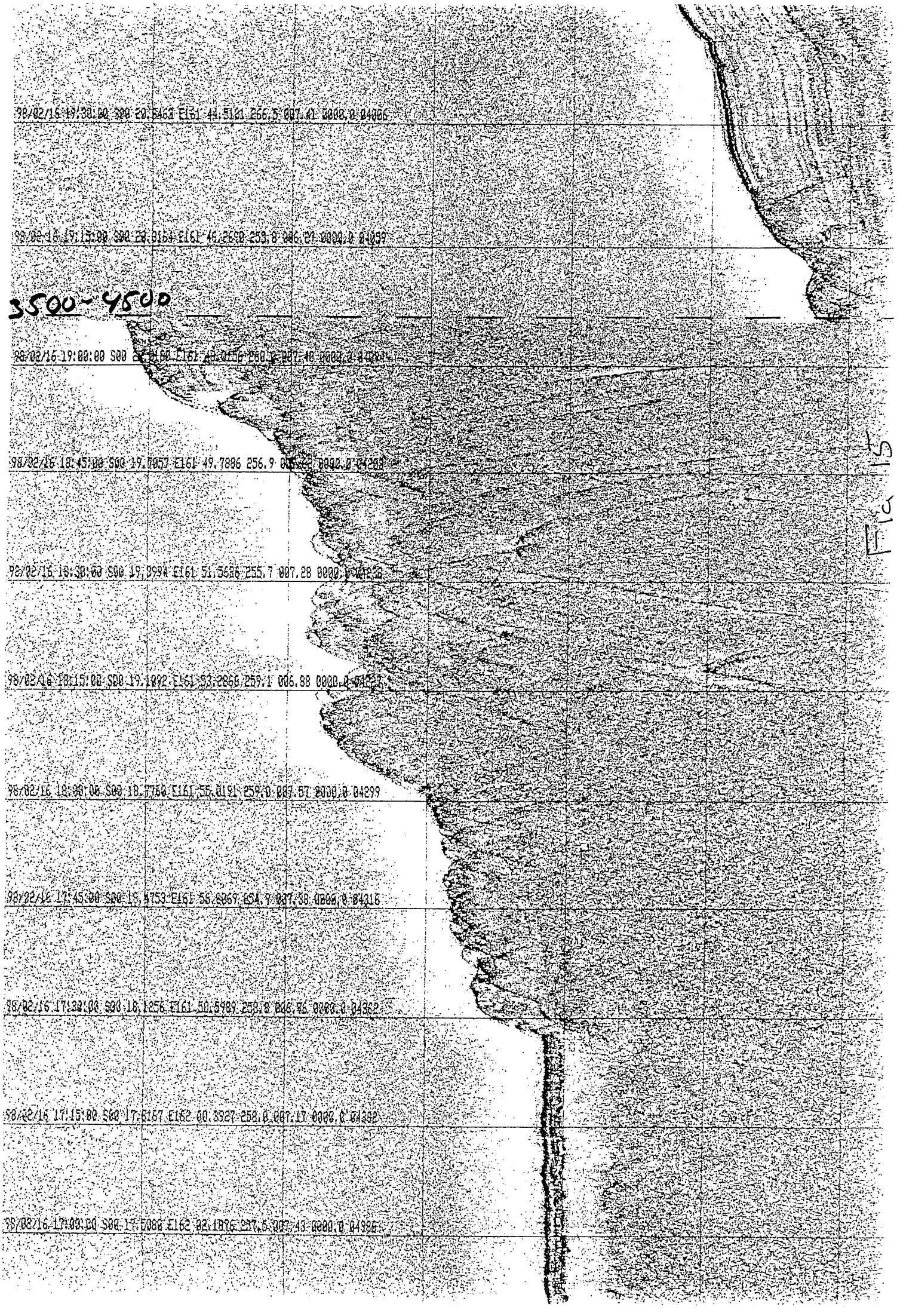
3500~4500

EASTERN SALIENT SURVEY

INTRODUCTION

A high resolution seismic reflection profiling survey across the northern half of the Eastern Salient of the Ontong Java Plateau (OJP) was undertaken early during Leg 2 of the KH98-1 cruise. The objective of this survey was to collect ODP site survey data to enable more precise positioning of proposed basement drill site OJ6 on the crest of the Northern Arch, as well as to obtain additional information on the tectonic setting of the Eastern Salient. Consequently, Line 101 was shot in a northeast direction across the northeastern half of Stewart Basin and over the Northern Arch of the OJP Eastern Salient, roughly perpendicular to the structural trends. After passing east of the Island of Malaita and crossing the North Solomon Trench, and with gravity, magnetic, and 3.5 kHz profiling data being continuously recorded along the track, coarse was set to the northeast at WP1, on the crest of Stewart Arch, for WP2 (Fig 1). At WP2 the high speed 24 channel streamer and one 200 in^3 air gun were deployed. With the air gun firing on a 20 sec rep rate and an 8 sec sweep (0.5 sec delay) being used on the analog monitor record (channel 7), digital recording commenced on Line 101 at 1600Z 12 Feb (JD 143).

OBSERVATIONS

Beginning NE of a small volcaniform ridge, Line 101 was shot in a northeastward direction across the northeastern third of Stewart Basin and over the crest of the Northern Arch (Fig. 2). Between the start of the line and the base of the lower flank of the Northern Arch (1600-2130Z/043), a series of basement ridges were crossed that resembled rotational fault blocks (Fig. 3). The seafloor along this part of the line was underlain by a relatively flat, faint reflector that gradually climbed in the section from a depth of 0.4 below the sea floor at the start of the line to about 0.2 sec in a deformed zone near the base of the southern flank of the arch. Below this faint reflector, about 0.6 sec deep, a highly reflective, undulating horizon also gradually rises in the section to merge with the top of the deformed zone near the base of the arch. Undulations in this reflector are conformable with the crests of the basement ridges. Although considerable relief occurs in the subsurface within the deformed zone (2000-2130Z), with reflectors very difficult to trace in the single channel monitor record, the highly reflective horizon may surface at a small antiform at the base of the lower flank of the arch.

From 2130Z/043-0119Z/044, the line traverses the southern flank and crosses the crest of the Northern Arch, enroute to WP3. The seafloor along this line ranges from 3298m at the base of the southern flank to 1655m at the crest of the arch. Depth to basement, very shallow (<0.2 sec) at times beneath the down-faulted southern flank, is highly variable over the block faulted terrain at the crest of the arch (Fig. 4). The basement reflector, which is overlain by up to 0.7 sec of sediment in a graben on the south side

of the crest and may be overlain by more than 0.8 sec of sediment on the north side of the crest, appears to be less than 0.2 sec deep at the summit of the arch crest. On the northeastern side of the crest, halfway between the summit and WP3, less steeply dipping, overlying reflectors (below ~0.4 sec deep) appear to onlap the more steeply dipping basement reflector.

Although the plan had been to deploy the MCS 48 channel streamer and a large air gun array between WP3 and WP4 to ensure acquisition of adequate basement data along a perpendicular cross line along the arch crest, the shallow depth to basement and clarity of the basement reflector encountered here obviated the additional penetration capabilities of the 48 channel streamer and large gun array. Therefore the survey was extended beyond WP4 with the 24 channel streamer in tow and an additional cross line (Line 103) was planned.

From 0315-0936Z/044, between WP4 and WP5, Line 102 was shot to the northwest along the crest of the Northern Arch. Again the shallow depth (0.64-0.20 sec) and block-faulted nature of basement along this line (which crosses Line 101 at 0458Z) is readily apparent. Basement is clearly visible along the entire length of the line.

From 1116Z-1300Z/044, between WP6 and WP7, line 103 was shot to the northeast across the crest of the Northern Arch (Fig. 5). The seafloor along this line is relatively smooth, shallowing to 1403m at 1145Z near the crossing with Line 102. Basement, moderately block faulted and ranging in depth from 0.36 to 0.24 sec, is, once again, clearly visible along the entire length of the line.

Although the lack of a complete MCS transect of the Eastern Salient inhibits a straight forward interpretation of the regional tectonic setting, considering the rotational block faulting structure that appears to be present in the northeastern half of Stewart Basin, as well as the block faulting observed at the crest of the Northern Arch, it does seem plausible that some type of extensional rifting between Stewart Arch and the Northern Arch has occurred. Final resolution of this problem, however must await additional investigation, particularly results forthcoming from any future ocean drilling legs.

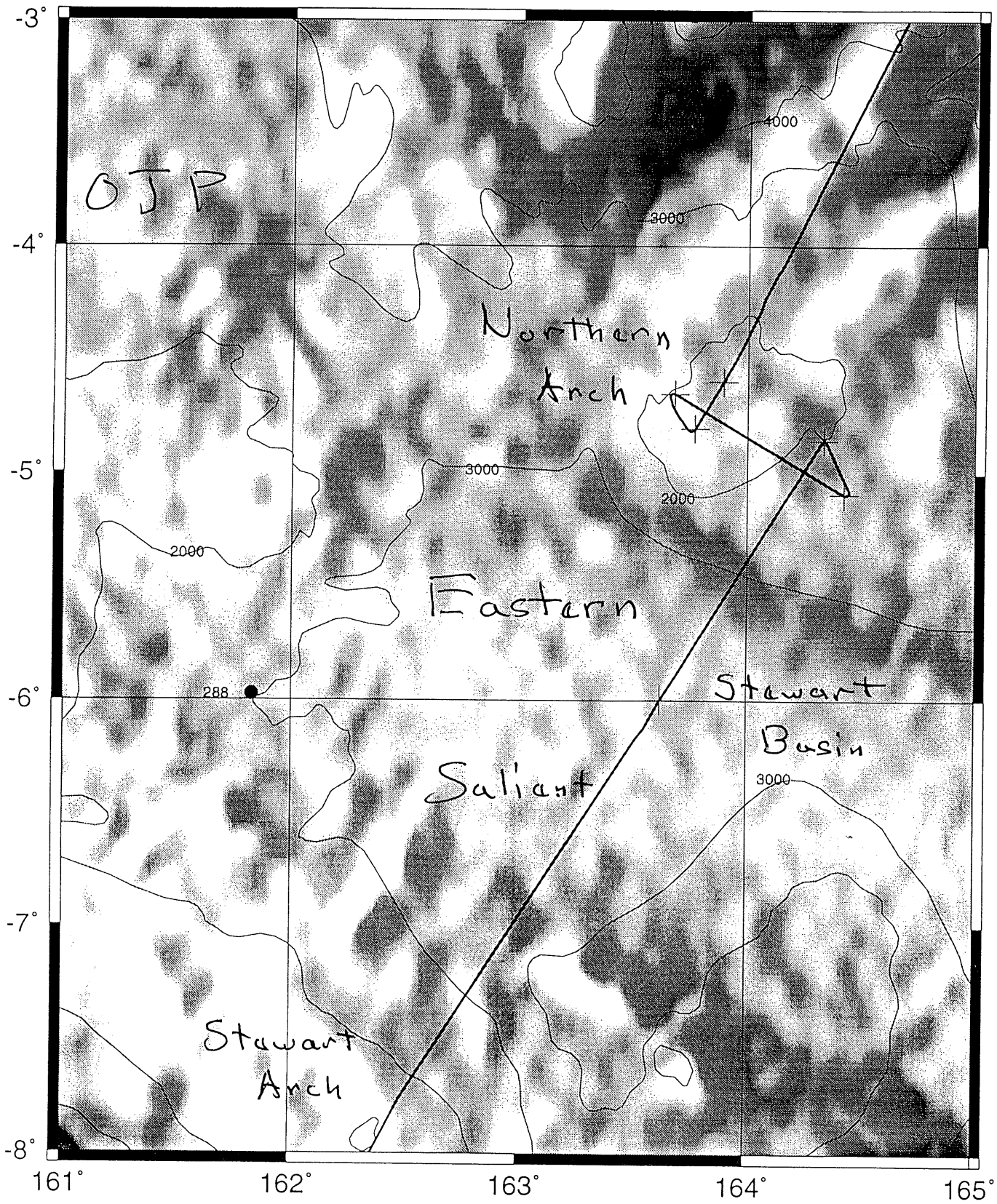

-150 -50 -40 -30 -20 -10 0 10 20 30 100

mGal

Fig 1

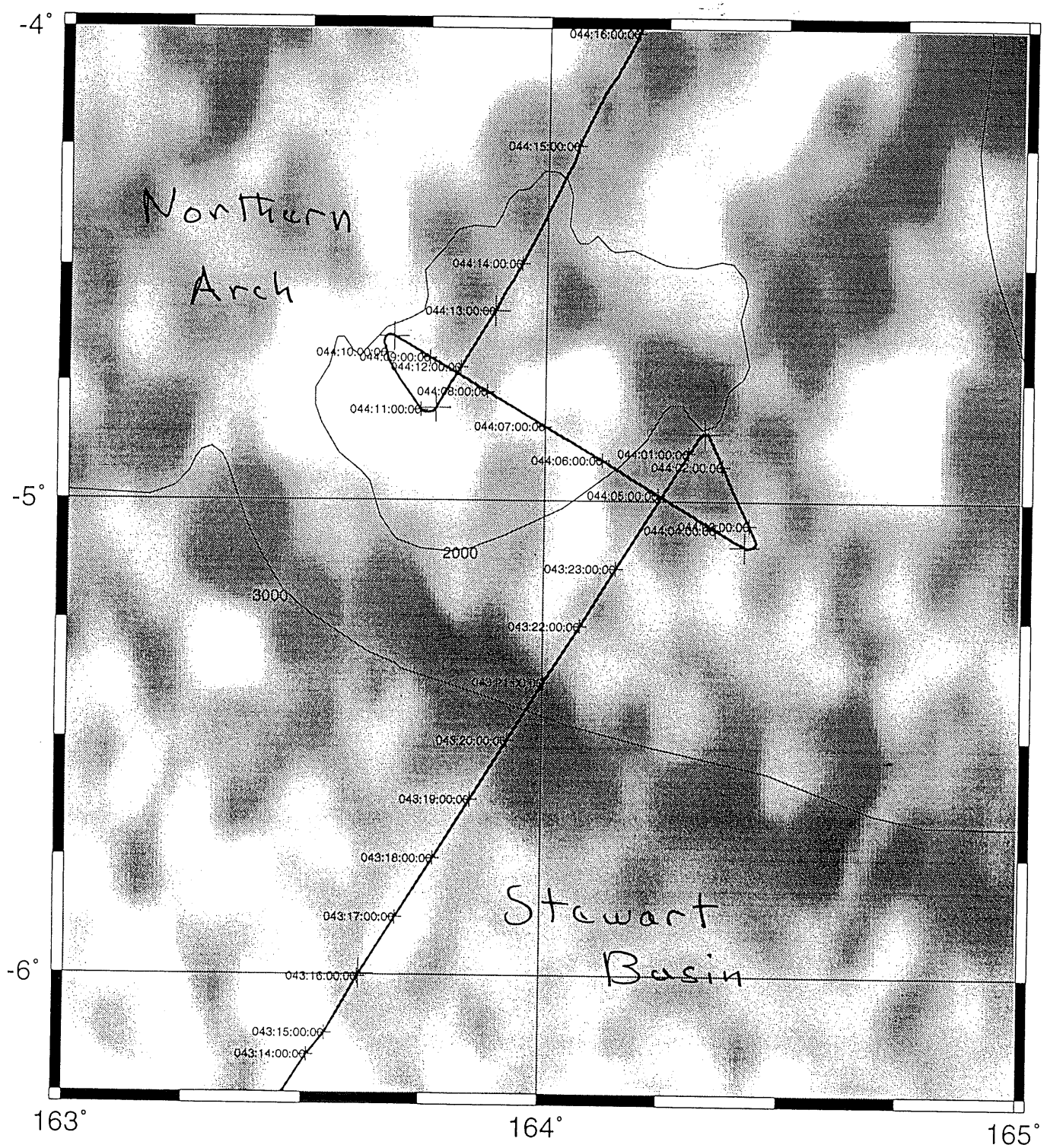
-4°
-5°
-6°
163°
164°
165°
Northern
Arch
Stewart
Basin
2000
3000
044:16:00:00
044:15:00:00
044:14:00:00
044:13:00:00
044:10:00:00
044:09:00:00
044:12:00:00
044:08:00:00
044:11:00:00
044:07:00:00
044:06:00:00
044:01:00:00
044:02:00:00
044:05:00:00
044:04:00:00
043:23:00:00
043:22:00:00
043:19:00:00
043:18:00:00
043:17:00:00
043:16:00:00
043:15:00:00
043:14:00:00

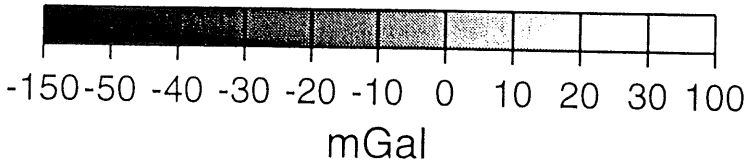
-150 -50 -40 -30 -20 -10 0 10 20 30 100
mGal

Fig 2

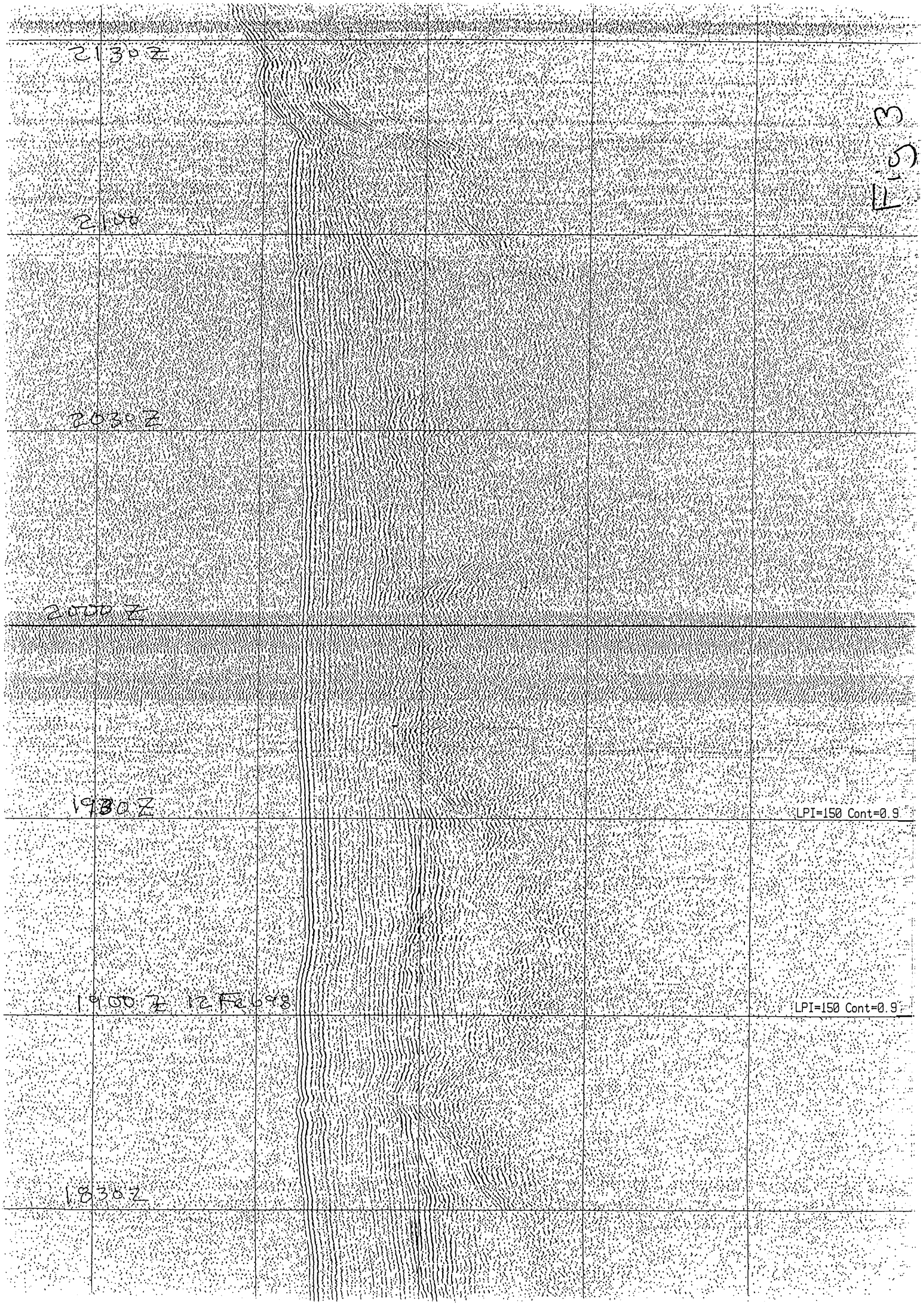
2130Z
2100
2030Z
2000Z
1930Z
LPI=150 Cont=0.9
1900Z 12Feb98
LPI=150 Cont=0.9
1838Z

13/2/98 CC 01:19Z

01:00Z

00:30Z

00:00
13/2/198

T08:14:14 01Jan00 ChA ExTRIG Level= 2.5V, Thr=1.7V Gain=10.0 Scan=8000.000 mS, Delay=0.000 mS

23:30Z

23:00Z

T07 15 34 01Jan00 ChA ExTRIG Level= 2.5V, Thr=1.7V Gain=10.0 Scan=8000.000 mS, Delay=0.000 mS

End of Eastern Salient Site Survey

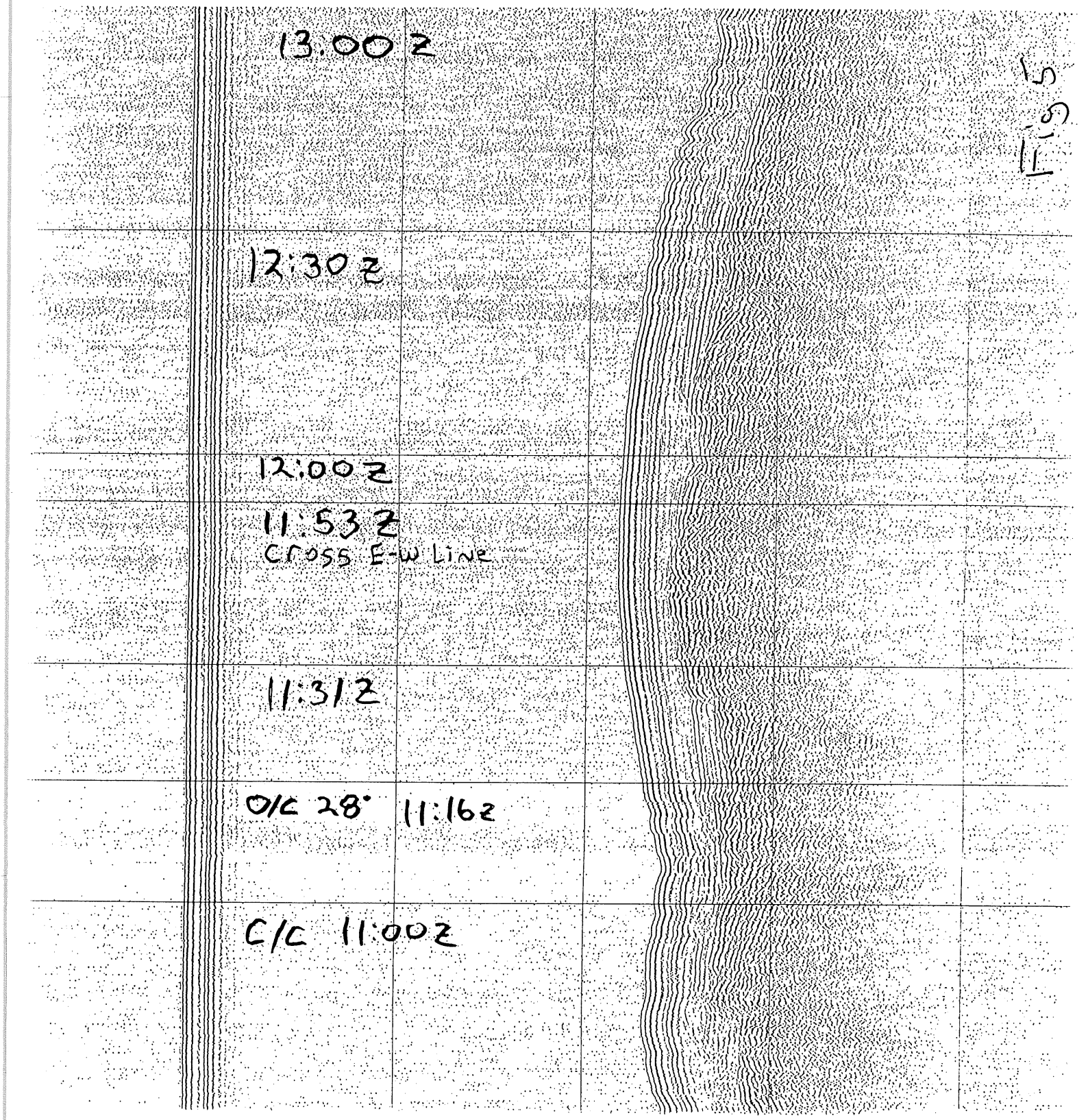

Appendix A. ODP Site OJ3A and OJ3B Summary Forms, and KH98-1 Leg 2 Line 404 (OJ3A) and Line 501 (OJ3B) shipboard brute stacks.

ODP Site Summary Form 6/91

Fill out one form for each proposed site and attach to proposal

Title of Proposal:	Assessing the Origins, Age, and Post-Emplacement History of the Ontong Java Plateau through Basement Drilling
Site-specific Objective(s) (List of general objectives must be inc. in proposal)	basement age, composition, and emplacement environment of thick central plateau

	Proposed Site	Alternate Site
Site Name:	OJ3A	OJ3B
Area:	Central OJP	Central OJP
Lat./Long.:	to be specified	to be specified
Water Depth:	to be specified	to be specified
Sed. Thickness:	pending velocity calculations	pending velocity calculations
Total penetration:	to be calculated	to be calculated

	Sediments	Basement
Penetration:		
Lithology(ies):	carbonate ooze, chert, chalk, limestone	carbonate ooze, chert, chalk, limestone
Coring (check):	1-2-3-***APC*** VPC* ***XCB*** MDCB* PCS ***RCB*** ***Re-entry*** HRGB	
Downhole measurements:	Geophysical tool	

*Systems currently under development

Target(s) (see Proposal Submission Guidelines): ***G***

Site Survey Information (see Proposal Submission Guidelines for details and requirements):

		Check	Details of available data and data that is still to be collected
01	SCS deep penetration		
02	SCS High Resolution		
03	MCS and velocity	x	KH98-1 lines 404 (49.1945) and 501 (51.1930)
04	Seismic grid		
05	Refraction	x	OBS, sonobuoy
06	3.5 or 12 kHz	x	both
07	Swath bathymetry		
08	H.-res side-looking sonar		
09	Photography/video		
10	Heat flow		
11	Magnetics/gravity	x	declassified satellite altimetry data after Sandwell et al. (1994)
12	Coring		
13	Rock sampling		
14	Current meter		
15	Other		

Weather, Ice, Surface Currents: 1.5-2.5 kt west-flowing Equatorial Current

Territorial Jurisdiction:

Other Remarks:

	Name/Address	Phone/FAX/Email
Contact Proponent:	Millard F. Coffin Institute for Geophysics The University of Texas at Austin 4412 Spicewood Springs Rd., # 600 Austin, TX 78759-8500	ph. +1-512-471-0429 fax +1-512-475-6338 email: mikec@utig.ig.utexas.edu

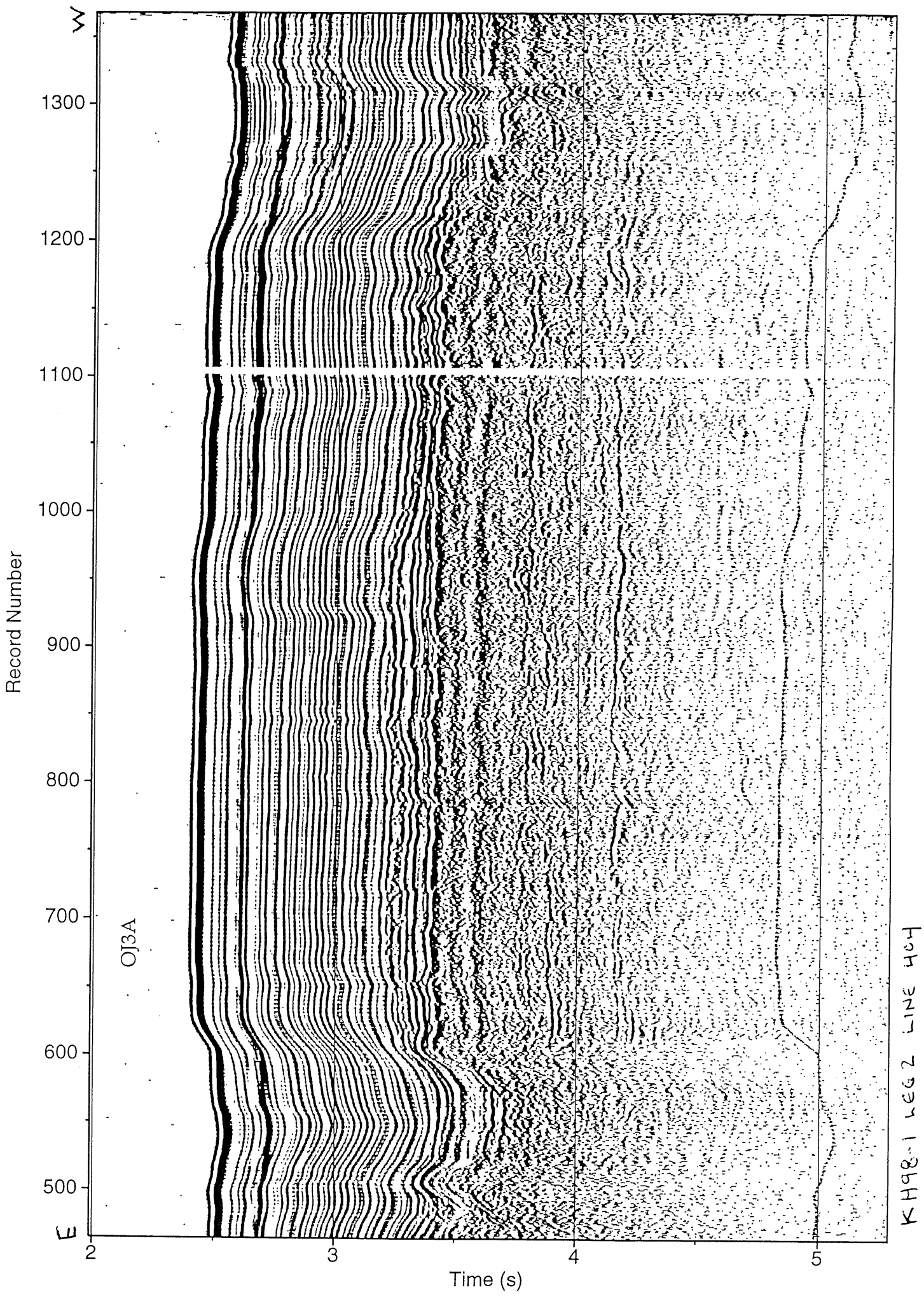
- File gather.segy -
W
1300
1200
1100
1000
900
800
700
600
500
E
Record Number
OJ3A
2
3
4
5
Time (s)
KH98-1 LEG 2 LINE 4C4

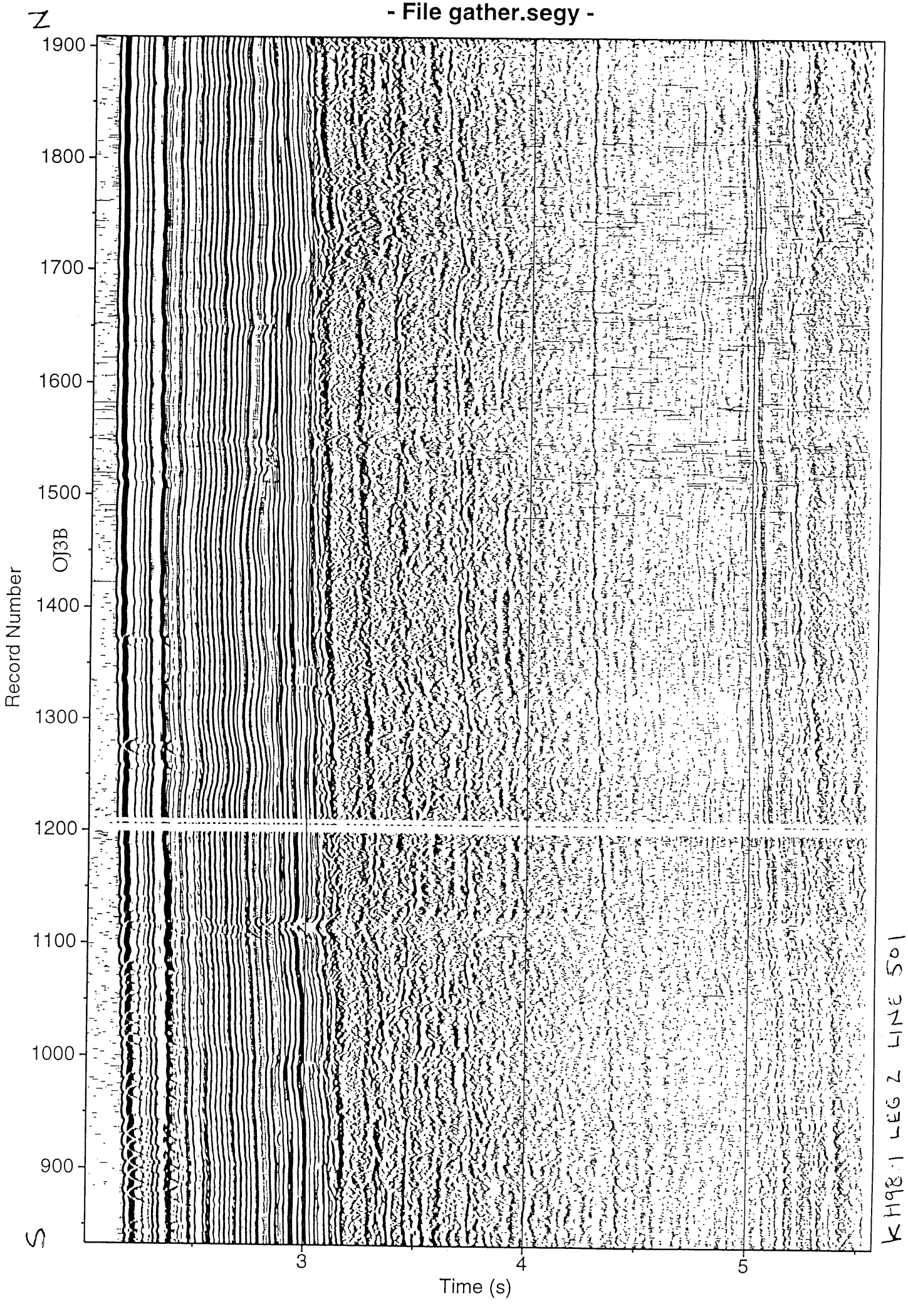
- File gather.segy -
N
S
1900
1800
1700
1600
1500
1400
1300
1200
1100
1000
900
Record Number
OJ3B
3
4
5
Time (s)
KH98-1 LEG 2 LINE 501

Appendix B. ODP Site OJ11A and OJ11B Summary Forms, and KH98-1 Leg 2 Line 401 shipboard brute stacks.

ODP Site Summary Form 6/91

Fill out one form for each proposed site and attach to proposal

Title of Proposal:	Assessing the Origins, Age, and Post-Emplacement History of the Ontong Java Plateau through Basement Drilling
Site-specific Objective(s) (List of general objectives must be inc. in proposal)	basement age, composition and emplacement environment on NE flank of OJP

	Proposed Site	Alternate Site
Site Name:	OJ11B	OJ11C
Area:	OJP's NE Flank	OJP's NE Flank
Lat./Long.:	to be specified	to be specified
Water Depth:	to be specified	to be specified
Sed. Thickness:	pending velocity calculations	pending velocity calculations
Total penetration:	to be calculated	to be calculated

	Sediments	Basement
Penetration:		
Lithology(ies):	chalk, chert, limestone	chalk, chert, limestone
Coring (check):	1-2-3-*APC* VPC* *XCB* MDCB* PCS *RCB* *Re-entry* HRGB	
Downhole measurements:	Geophysical tool	

*Systems currently under development

Target(s) (see Proposal Submission Guidelines): *G*

Site Survey Information (see Proposal Submission Guidelines for details and requirements):

		Check	Details of available data and data that is still to be collected
01	SCS deep penetration		
02	SCS High Resolution		
03	MCS and velocity	x	KH98-1 line 402 (47.1915)
04	Seismic grid		
05	Refraction	x	sonobuoys
06	3.5 or 12 kHz	x	both
07	Swath bathymetry		
08	H.-res side-looking sonar		
09	Photography/video		
10	Heat flow		
11	Magnetics/gravity	x	declassified satellite altimetry data after Sandwell et al. (1994)
12	Coring		
13	Rock sampling		
14	Current meter		
15	Other		

Weather, Ice, Surface Currents: 1.5-2.5 kt west-flowing Equatorial Current

Territorial Jurisdiction:

Other Remarks:

	Name/Address	Phone/FAX/Email
Contact Proponent:	Millard F. Coffin Institute for Geophysics The University of Texas at Austin 4412 Spicewood Springs Rd., # 600 Austin, TX 78759-8500	ph. +1-512-471-0429 fax +1-512-475-6338 email: mikec@utig.ig.utexas.edu

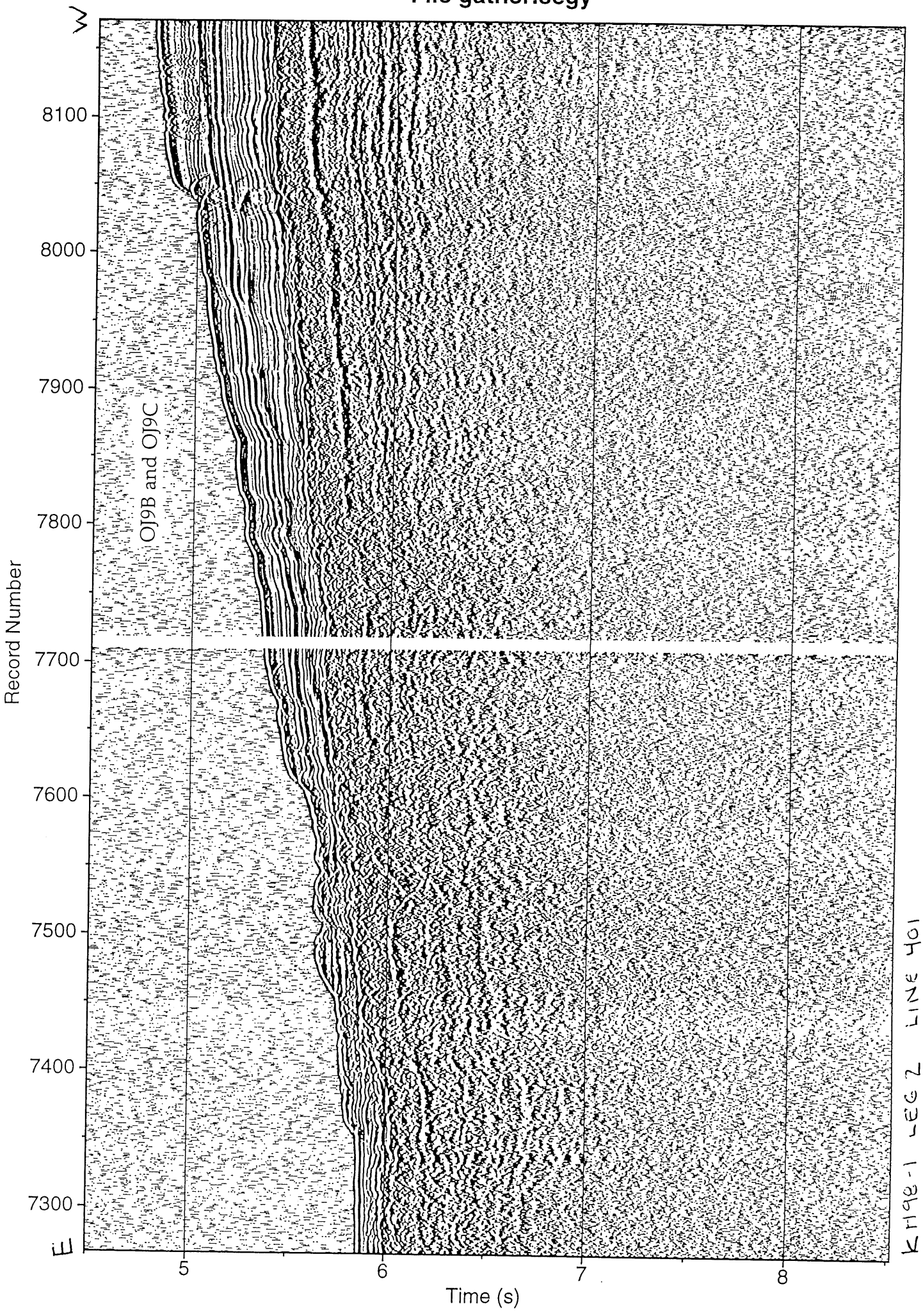
- File gather.segy -
W
8100
8000
7900
7800
7700
7600
7500
7400
7300
E
Record Number
OJ9B and OJ9C
5
6
7
8
Time (s)
KH98-1 LEG 2 LINE 401

Appendix C. ODP Site OJ9B and OJ9C Summary Forms, and KH98-1 Leg 2 Line 401 (OJ9B), Line 201 (OJ9C), and *Charcot* seismic lines. The KH98-1 Leg 2 seismic data are neartrace shipboard monitors, and the *Charcot* data are stacked.

ODP Site Summary Form 6/91

Fill out one form for each proposed site and attach to proposal

Title of Proposal:	Assessing the Origins, Age, and Post-Emplacement History of the Ontong Java Plateau through Basement Drilling
Site-specific Objective(s) (List of general objectives must be inc. in proposal)	A reference site on abyssal seafloor adjacent to the Ontong Java Plateau 1) Obtain a complete sedimentary record over Earliest Cretaceous oceanic crust to reconstruct the vertical tectonic and volcanic history of the adjacent Ontong Java Plateau 2) Study the environmental effects of the ≈90 and ≈122 Ma Ontong Java volcanic events 3) Examine the evolution of the composition of Pacific oceanic crust

	Proposed Site	Alternate Site
Site Name:	OJ9B	OJ9C
Area:	Southern Nauru Basin	Southern Nauru Basin
Lat./Long.:	0.2866°N/165.3022°E	1.4219°S/165.4691°E
Water Depth:	4396	4442 m
Sed. Thickness:	1000	800 m
Total penetration:	1100	900 m

	Sediments	Basement
Penetration:	1000 m / 800 m	100 m
Lithology(ies):	biogenic ooze, clan, chalk, chert, limestone, volcaniclastics	basalt
Coring (check):	1-2-3-***APC*** VPC* ***XCB*** MDCB* PCS ***RCB*** ***Re-entry*** HRCB	
Downhole measurements:	Quad0Combo, Geochemical, FMS, GHMT	

*Systems currently under development

Target(s) (see Proposal Submission Guidelines): *G*

Site Survey Information (see Proposal Submission Guidelines for details and requirements):

		Check	Details of available data and data that is still to be collected
01	SCS deep penetration		OJ9B: Intersection of KH98-1 line 401 (1352) and Charcot (SP4698) OJ9C: Intersection of KH98-1 line 201 (0650) and *Charcot* (SP906) (See Shipley et al., 1993, for details of Charcot MCS)
02	SCS High Resolution		
03	MCS and velocity	x	
04	Seismic grid		
05	Refraction	x	sonobuoys
06	3.5 or 12 kHz	x	both
07	Swath bathymetry		SeaBeam
08	H.-res side-looking sonar		
09	Photography/video		
10	Heat flow		
11	Magnetics/gravity	x	declassified satellite altimetry data after Sandwell & Smith (1997) shipboard gravity and magnetics - KH98-1
12	Coring		
13	Rock sampling		
14	Current meter		
15	Other		

Weather, Ice, Surface Currents: Calm

Territorial Jurisdiction: Republic of Nauru

Other Remarks: None

	Name/Address	Phone/FAX/Email
Contact Proponent:	Loren Kroenke/John Mahoney	ph. +1-808-956-7845 fax +1-808-956-2538 email: kroenke@soest.hawaii.edu

Nauru Basin - KH98-1 Leg 2 MCS Line 401, Near Channel Record

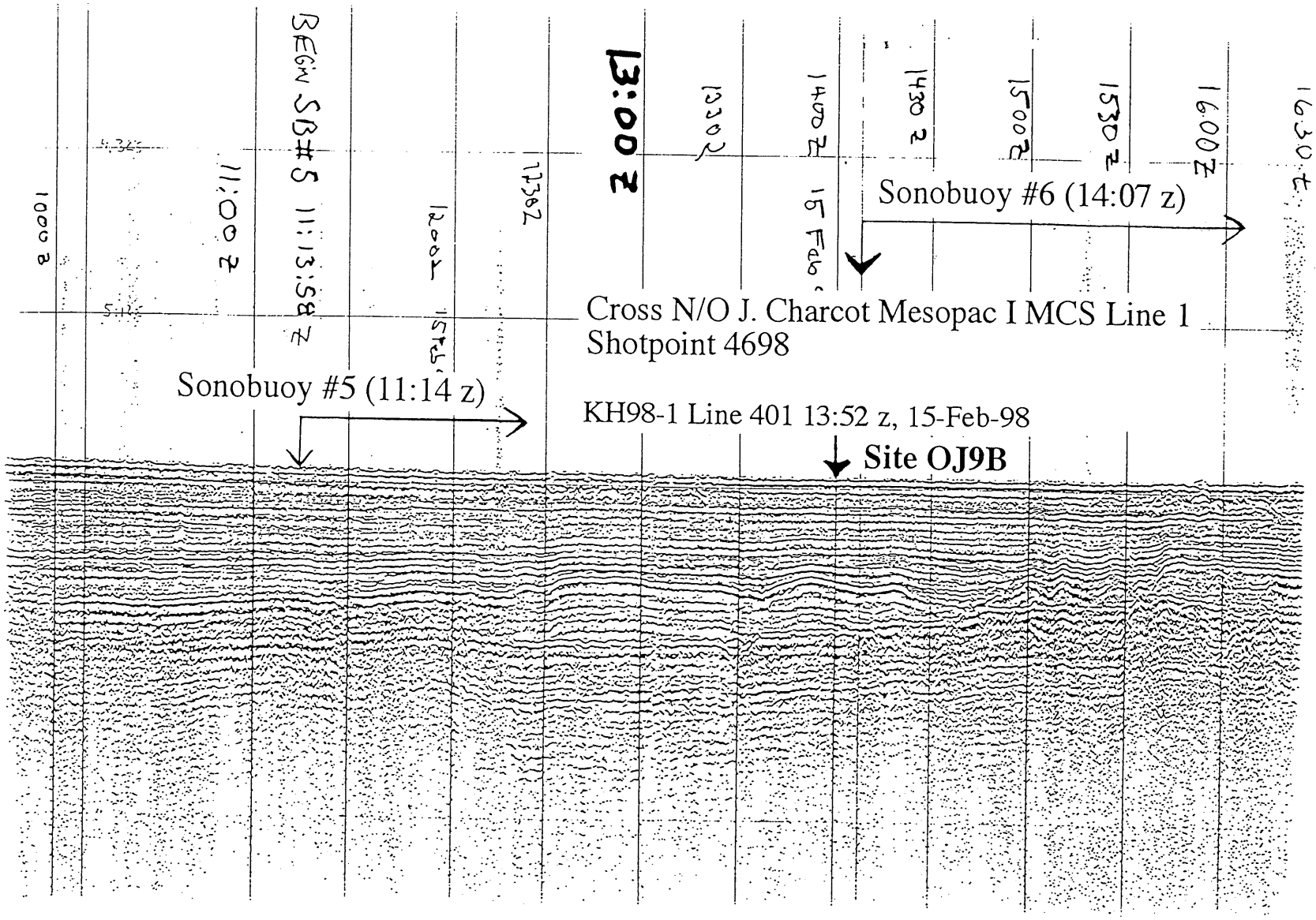

Nauru Basin - N/O J. Charcot Mesopac I MCS Line 1

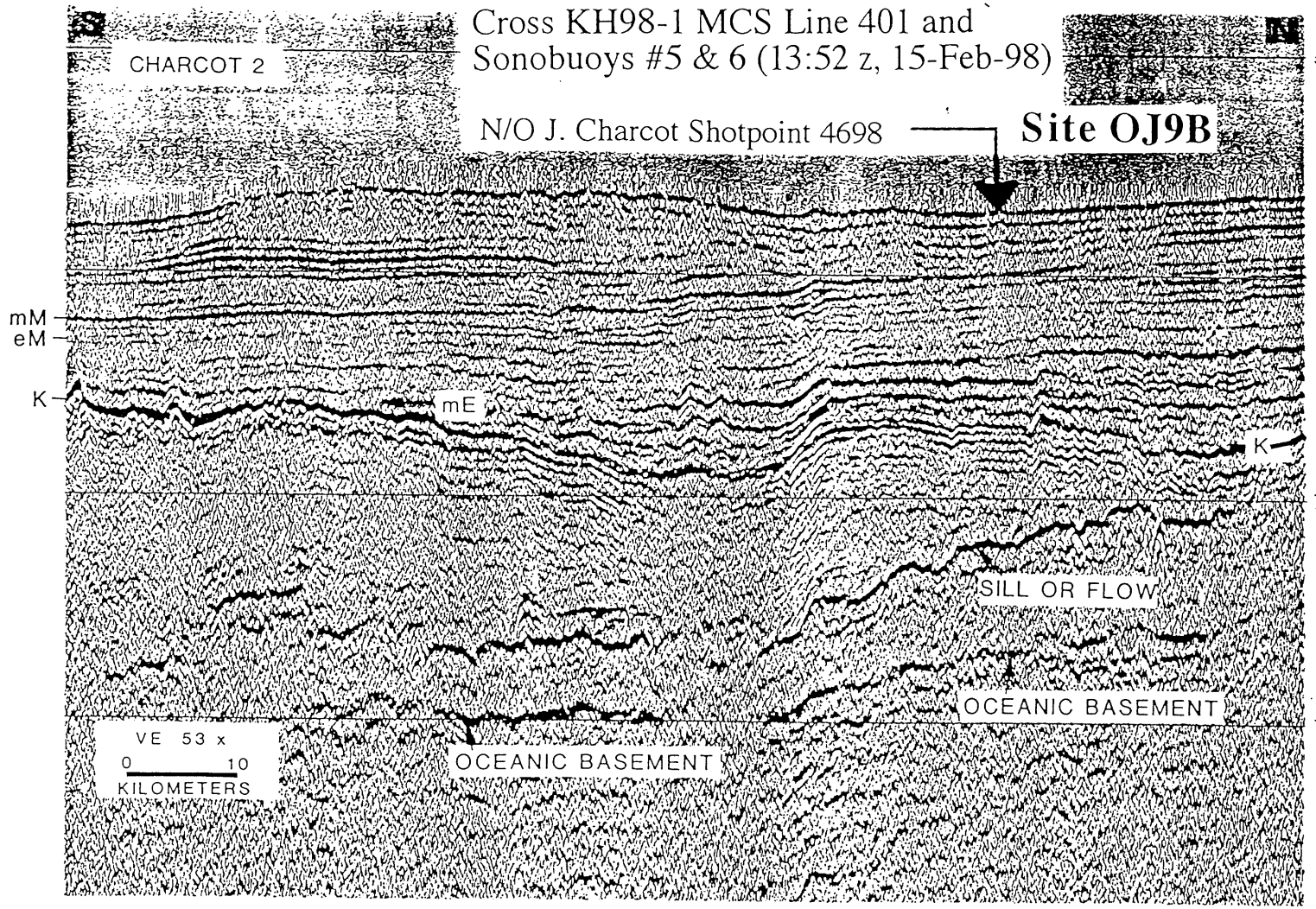

Fig. 11. Oceanic basement is visible in the center of this section. Overlying high amplitude event on the right side is interpreted as a flow (or perhaps sill). The section beneath the flow (?) contains few coherent reflections, probably due to scattering associated with the surface of the unit. The overlying section shows onlap onto the dipping event. Higher in the section the middle Eocene cherts and sediments pinch out against K. Location is shown in Figure 2.

Shipley et al., 1993

Nauru Basin - KH98-1 Leg 2 MCS Line 201, Near Channel Record

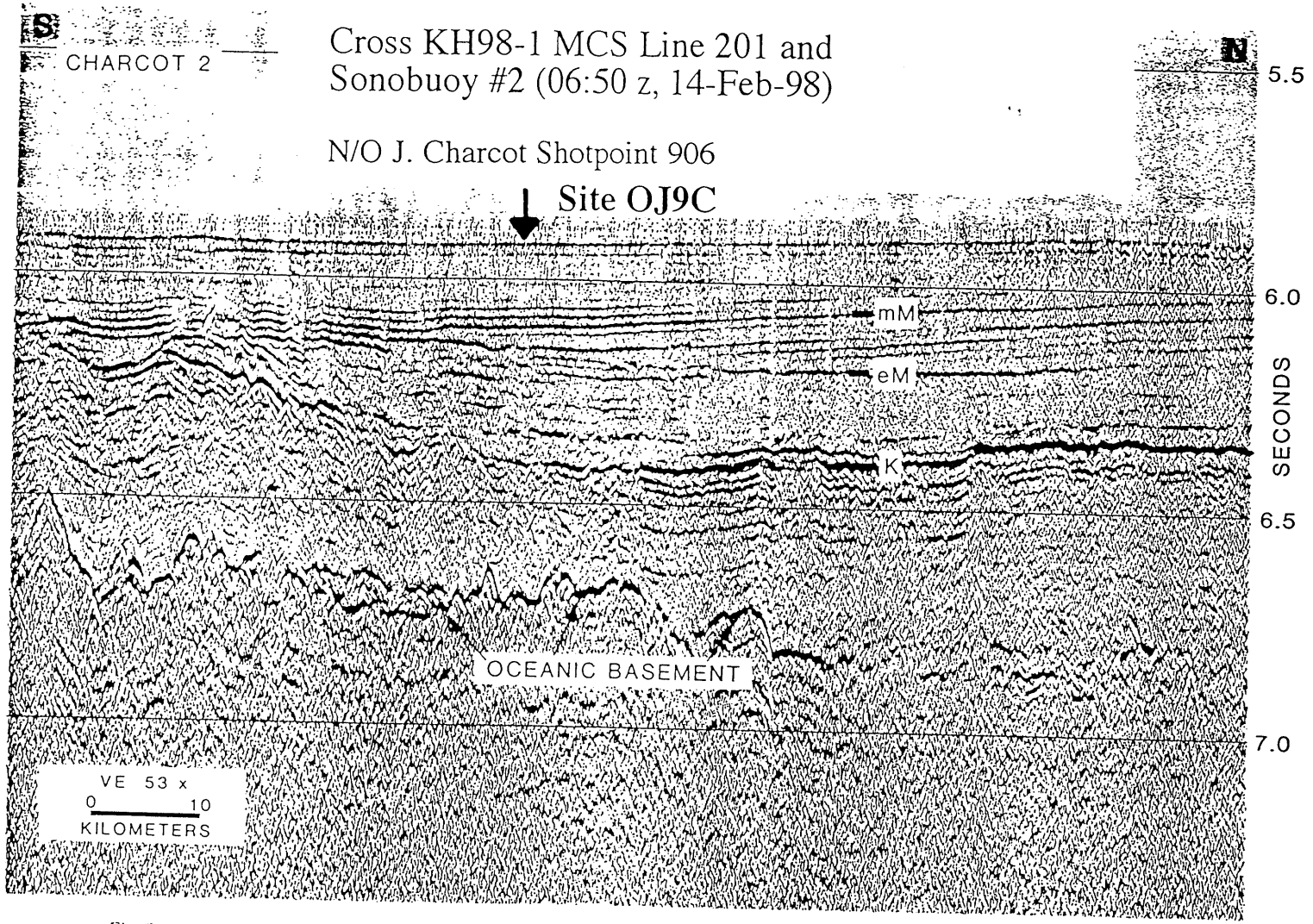

Fig. 8. Section at southernmost end of the *Charcot* line showing rough oceanic basement. Well-defined stratigraphy is evident between basement and the surface correlated with Cretaceous volcanics. The reduced reflectivity of K suggests that is not volcanic rock but a time-equivalent surface, perhaps volcanoclastic (?). Note downlap occurs onto the early Miocene surface. Processing information and the initial reports on this data are presented in Froger [1989; Froger and Lancelot, 1990]. The data were stacked 24-fold and subsequently deconvolved and filtered preserving original relative amplitude information that is important in identifying volcanics and cherts. Location is shown in Figure 2.

Shipley et al., 1993

ODP Site Summary Form 6/91

Fill out one form for each proposed site and attach to proposal

Title of Proposal:	Assessing the Origins, Age, and Post-Emplacement History of the Ontong Java Plateau through Basement Drilling
Site-specific Objective(s) (List of general objectives must be inc. in proposal)	A Reference Site on abyssal seafloor adjacent to the Ontong-Java Plateau 1) Obtain a complete sedimentary record over Cretaceous/Jurassic oceanic crust (M-17) to reconstruct the vertical tectonic and volcanic history of the adjacent Ontong-Java Plateau 2) Study the environmental effects of the ~90 and~122 Ma Ontong-Java volcanic events 3) Examine the evolution of the composition of Pacific oceanic crust

	Proposed Site	Alternate Site
Site Name:	OJ9B	OJ9C
Area:	Southern Nauru Basin	
Lat./Long.:	0.2866 N 165.3022 E	
Water Depth:	4396 m	
Sed. Thickness:	1000 m	
Total penetration:	1100 m	

	Sediments	Basement
Penetration:	1000 m	100 m
Lithology(ies):	Bio. Ooze, clay, chalk, chert, limestone Volcanoclastics	Basalt
Coring (check):	1-2-3-APC VPC* XCB MDCB* PCS RCB X Re-entry X HRGB	
Downhole measurements:	Quad-Combo, Geochemical, FMS, GHMT	

*Systems currently under development

Target(s) (see Proposal Submission Guidelines): *G*

Site Survey Information (see Proposal Submission Guidelines for details and requirements):

		Check	Details of available data and data that is still to be collected
01	SCS deep penetration		
02	SCS High Resolution		
03	MCS and velocity	x	Intersection of KH98-1 line 401 (1352 z) and Charcot Line (sp 4698)
04	Seismic grid		(See Shipley et al., 1993 for details of Charcot MCS)
05	Refraction	x	sonobuoys
06	3.5 or 12 kHz	x	both
07	Swath bathymetry	x	SeaBeam
08	H.-res side-looking sonar		
09	Photography/video		
10	Heat flow		
11	Magnetics/gravity	x	declassified satellite altimetry data after Sandwell & Smith (1997)
12	Coring		Shipboard Gravity and Magnetics - KH98-1
13	Rock sampling		
14	Current meter		
15	Other		

Weather, Ice, Surface Currents: Calm

Territorial Jurisdiction: Republic of Nauru

Other Remarks: None

	Name/Address	Phone/FAX/Email
Contact Proponent	Loren Kroenke/ J. Mahoney	(808) 956-7845/ (808) 956-2538 kroenke@soest.hawaii.edu

Nauru Basin - KH98-1 Leg 2 MCS Line 401, Near Channel Record

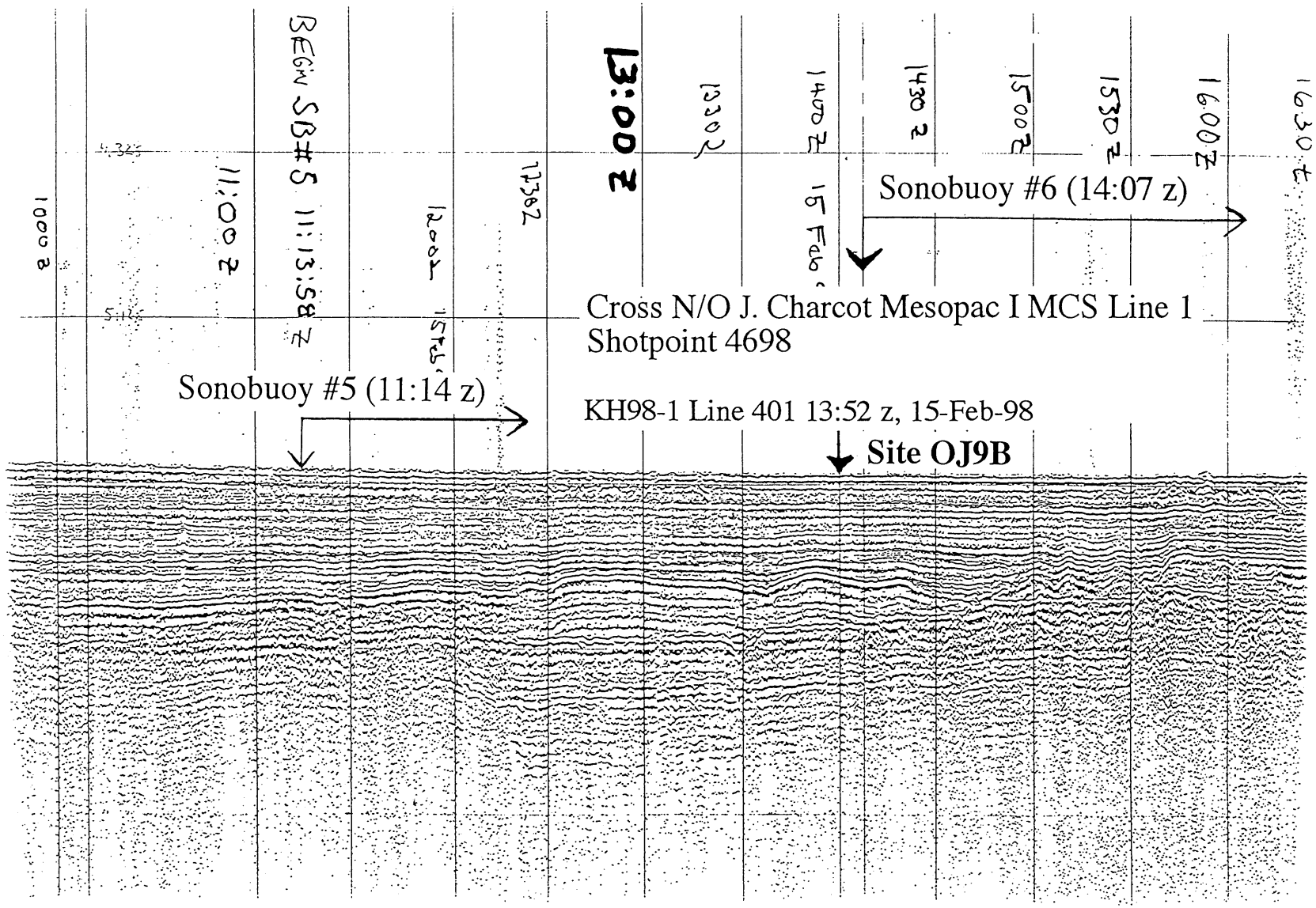

Nauru Basin - N/O J. Charcot Mesopac I MCS Line 1

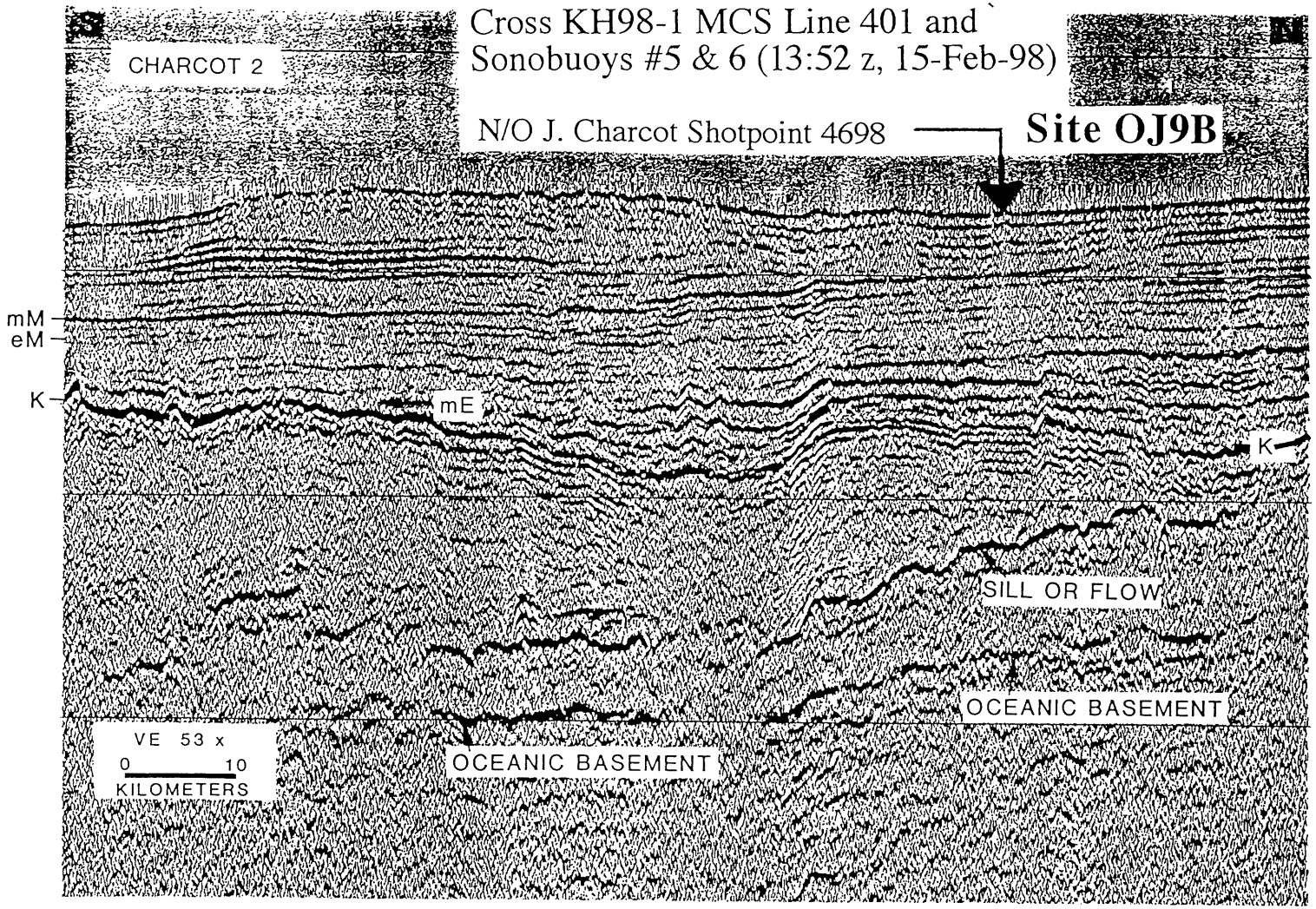

Fig. 11. Oceanic basement is visible in the center of this section. Overlying high amplitude event on the right side is interpreted as a flow (or perhaps sill). The section beneath the flow (?) contains few coherent reflections, probably due to scattering associated with the surface of the unit. The overlying section shows onlap onto the dipping event. Higher in the section the middle Eocene cherts and sediments pinch out against K. Location is shown in Figure 2.

Shipley et al., 1993

ODP Site Summary Form 6/91

Fill out one form for each proposed site and attach to proposal

Title of Proposal:	Assessing the Origins, Age, and Post-Emplacement History of the Ontong Java Plateau through Basement Drilling
Site-specific Objective(s) (List of general objectives must be inc. in proposal)	A Reference Site on abyssal seafloor adjacent to the Ontong-Java Plateau 1) Obtain a complete sedimentary record over Earliest Cretaceous oceanic crust to reconstruct the vertical tectonic and volcanic history of the adjacent Ontong-Java Plateau 2) Study the environmental effects of the ~90 and~122 Ma Ontong-Java volcanic events 3) Examine the evolution of the composition of Pacific oceanic crust

	Proposed Site	Alternate Site
Site Name:	OJ9B	OJ9C
Area:		Southern Nauru Basin
Lat./Long.:		1.4219 S 165.4691 E
Water Depth:		4442 m
Sed. Thickness:		800 m
Total penetration:		900 m

	Sediments	Basement
Penetration:	800 m	100 m
Lithology(ies):	Bio. Ooze, clay, chalk, chert, limestone Volcanoclastics	Basalt
Coring (check):	1-2-3-APC VPC* XCB MDCB* PCS RCB X Re-entry X HRGB	
Downhole measurements:	Quad-Combo, Geochemical, FMS, GHMT	

*Systems currently under development

Target(s) (see Proposal Submission Guidelines): *G*

Site Survey Information (see Proposal Submission Guidelines for details and requirements):

		Check	Details of available data and data that is still to be collected
01	SCS deep penetration		
02	SCS High Resolution		
03	MCS and velocity	x	Intersection of KH98-1 line 201 (0650 z) and Charcot Line (sp 906)
04	Seismic grid		(See Shipley et al., 1993 for details of Charcot MCS)
05	Refraction	x	sonobuoys
06	3.5 or 12 kHz	x	both
07	Swath bathymetry	x	SeaBeam
08	H.-res side-looking sonar		
09	Photography/video		
10	Heat flow		
11	Magnetics/gravity	x	declassified satellite altimetry data after Sandwell & Smith (1997)
12	Coring		Shipboard Gravity and Magnetics - KH98-1
13	Rock sampling		
14	Current meter		
15	Other		

Weather, Ice, Surface Currents: Calm

Territorial Jurisdiction: Republic of Nauru

Other Remarks: None

	Name/Address	Phone/FAX/Email
Contact Proponent	Loren Kroenke/ J. Mahoney	(808) 956-7845/ (808) 956-2538 kroenke@soest.hawaii.edu

Nauru Basin - KH98-1 Leg 2 MCS Line 201, Near Channel Record

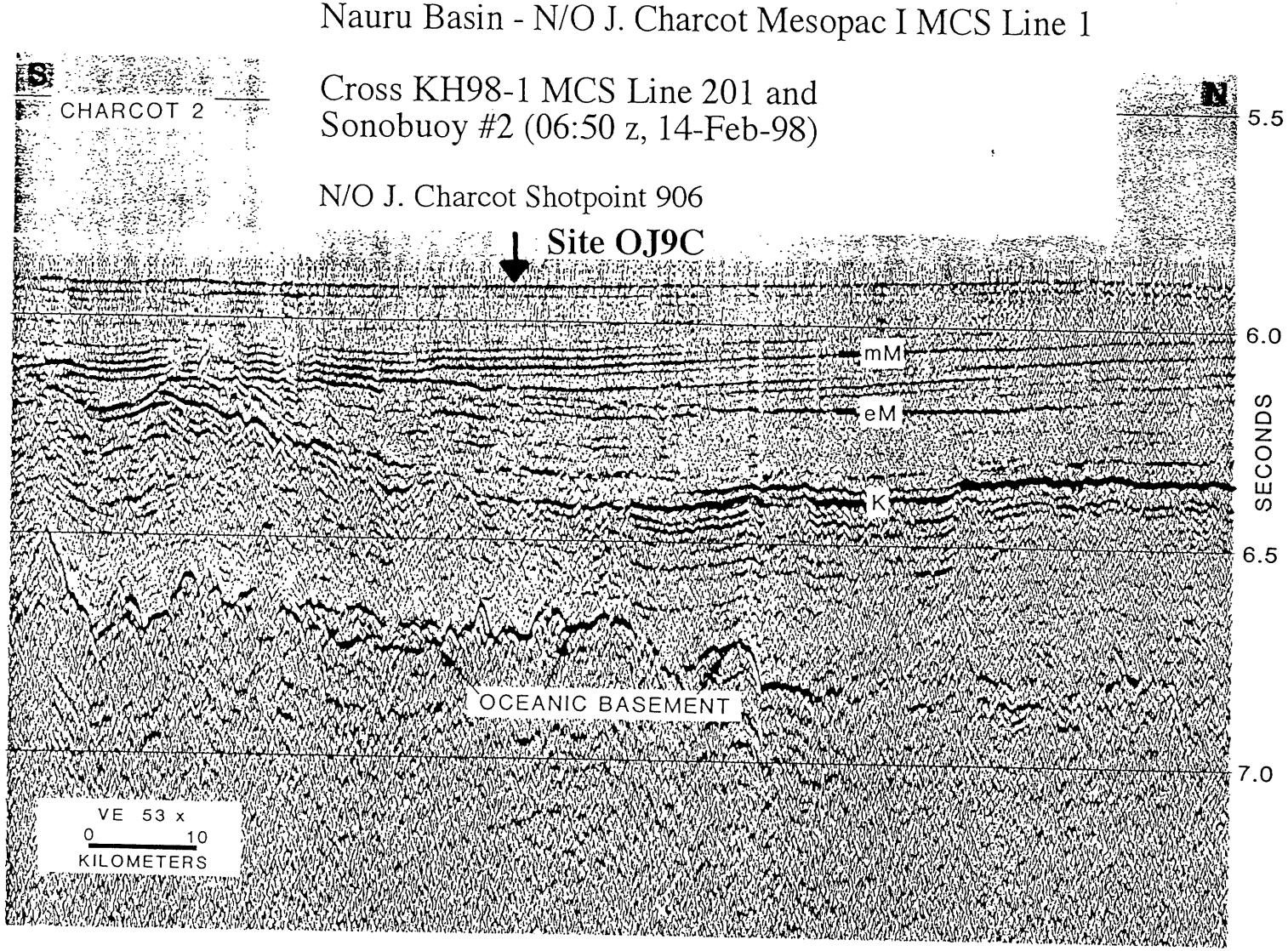

Fig. 8. Section at southernmost end of the *Charcot* line showing rough oceanic basement. Well-defined stratigraphy is evident between basement and the surface correlated with Cretaceous volcanics. The reduced reflectivity of K suggests that is not volcanic rock but a time-equivalent surface, perhaps volcanoclastic (?). Note downlap occurs onto the early Miocene surface. Processing information and the initial reports on this data are presented in Froger [1989; Froger and Lancelot, 1990]. The data were stacked 24-fold and subsequently deconvolved and filtered preserving original relative amplitude information that is important in identifying volcanics and cherts. Location is shown in Figure 2.

Shipley et al., 1993

ODP Site Summary Form 6/91

Fill out one form for each proposed site and attach to proposal

Title of Proposal:	Assessing the Origins, Age, and Post-Emplacement History of the Ontong Java Plateau through Basement Drilling
Site-specific Objective(s) (List of general objectives must be inc. in proposal)	basement age, composition and emplacement environment of previously unsampled Eastern Salient of OJP

	Proposed Site	Alternate Site
Site Name:	OJ6A	OJ6B
Area:	OJP's Eastern Salient	OJP's Eastern Salient
Lat./Long.:	5°03.0875, 164°12.494 E	
Water Depth:	1690 m	
Sed. Thickness:	310 m (0.345)	
Total penetration:	460 m	

	Sediments	Basement
Penetration:	310 m	150 m
Lithology(ies):	ooze/chalk/Ls	Basalt

Coring (check): 1-2-3-*APC* VPC* *XCB* MDCB* PCS *RCB*✓ Re-entry✓ HRGB

Downhole measurements: Geophysical tool

*Systems currently under development

Target(s) (see Proposal Submission Guidelines): *G*

Site Survey Information (see Proposal Submission Guidelines for details and requirements):

		Check	Details of available data and data that is still to be collected
01	SCS deep penetration		
02	SCS High Resolution		
03	MCS and velocity	x	KH98-1 lines 101, 102, 103
04	Seismic grid		
05	Refraction	x	sonobuoy
06	3.5 or 12 kHz	x	both
07	Swath bathymetry		
08	H.-res side-looking sonar		
09	Photography/video		
10	Heat flow		
11	Magnetics/gravity	x	declassified satellite altimetry data after Sandwell et al. (1994)
12	Coring		
13	Rock sampling		
14	Current meter		
15	Other		

Weather, Ice, Surface Currents: 1.5-2.5 kt west-flowing Equatorial Current

Territorial Jurisdiction:

Other Remarks:

	Name/Address	Phone/FAX/Email
Contact Proponent:	L.W. Kroenke / J. Mahoney	(808) 956-7845 (808) 956-5154 kroenke@soest.hawaii.edu

Nauru Basin - KH98-1 Leg 2 MCS Line 201, Near Channel Record
Sonobuoy #2
Cross N/O J. Charcot Mesopac I MCS Line 1
Shotpoint 906
KH98-1 Line 201 06:50 z, 14-Feb-98
1000 z
0730 z
0900 z
0830 z
0800 z
0730 z
0700 z
06:30 z
06:00
05:30 z
14 Feb
05:01 z
14 32 02Jan00 ChA ExTRIG Level= 2.5V Thr=1.7V Gain=3.2 Scan=8000.000 mS Delay=4000.000 mS
4-12 Sec
Begin MCS 24 Channel Line 201 14 Fe
KH98-1 Leg 2 1st Crossing

Nauru Basin - N/O J. Charcot Mesopac I MCS Line 1

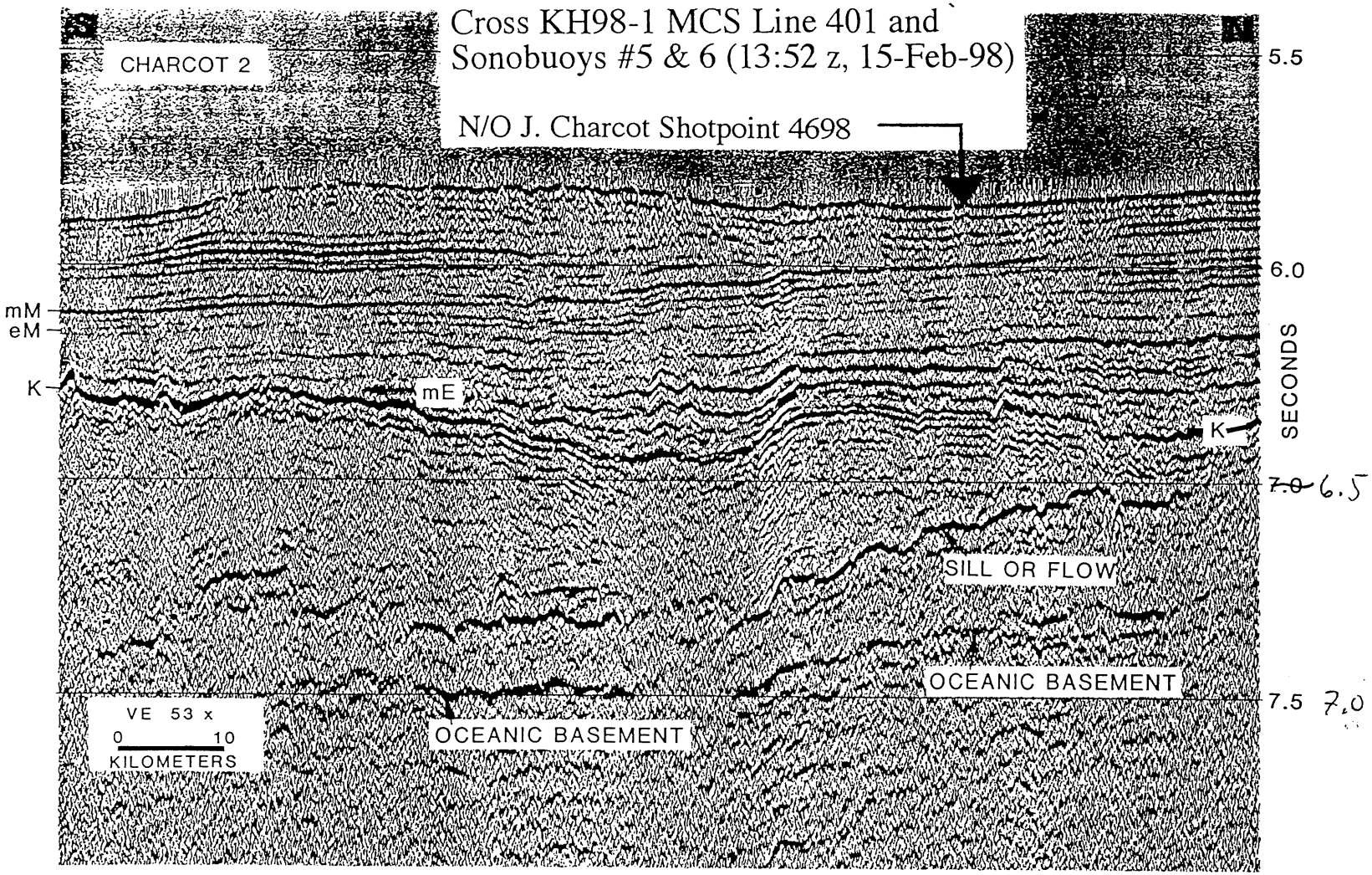

Fig. 11. Oceanic basement is visible in the center of this section. Overlying high amplitude event on the right side is interpreted as a flow (or perhaps sill). The section beneath the flow (?) contains few coherent reflections, probably due to scattering associated with the surface of the unit. The overlying section shows onlap onto the dipping event. Higher in the section the middle Eocene cherts and sediments pinch out against K. Location is shown in Figure 2.

Shipley et al., 1993

Nauru Basin - KH98-1 Leg 2 MCS Line 401, Near Channel Record

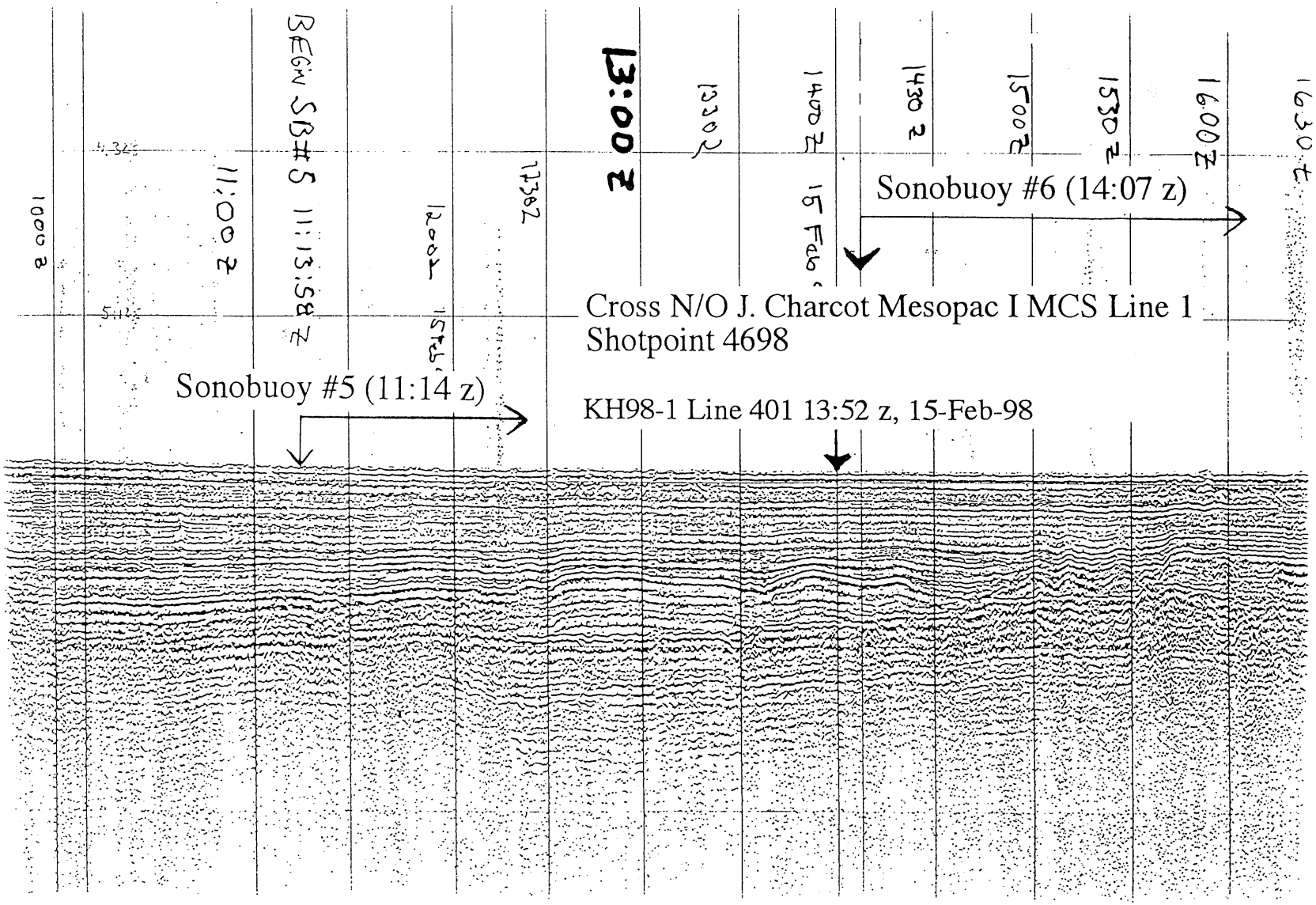

KH98-1 CRUISE REPORT: NAURU BASIN SEISMIC INVESTIGATION WITH MCS REFLECTION AND SONOBUOY REFRACTION

R. L. Larson, University of Rhode Island
L. J. Abrams, University of North Carolina at Wilmington

INTRODUCTION

The Nauru Basin was formed originally by sea floor spreading in the Late Jurassic and Early Cretaceous (magnetic lineations M11-M29 or 133-155 Ma) from the Pacific-Phoenix ridge system (Larson, 1976; Nakanishi et al., 1992), which extended east to the present location of the Nova-Canton Trough and an unknown distance to the west. Spreading occurred at whole rates varying from 6-10 cm/yr. The basin subsequently was overprinted by volcanism associated with the formation of the Ontong Java plateau (samples currently range in age from 110 to 124 Ma). The basin was investigated with two MCS seismic lines and 13 sonobuoys, 9 of which were successful. Both seismic lines are in the southern part (Early Cretaceous) of Nauru Basin.

SEISMIC LINE #201

The first seismic line, #201 was shot on a NE course from 0430z/14 to 1000z/14 about 190 km southwest of Nauru Island and just southeast of a small seamount. No correlatable magnetic lineations are present at this location. The intent was to cross a north-south MCS seismic line previously acquired on the N/O Jean Charcot (Shipley, et al., 1993, fig. 8) in an area where original volcanic basement might be seismically visible. The crossing was made at 0650z/14 and shot point #906 on the Charcot line (see figures) . The 24-channel hydrophone streamer, 1-17 liter and 2-20 liter airguns were utilized for this line. Sonobuoy #1 was deployed at 0559z and almost immediately failed due to the hyprophone wire being cut by the MCS cable. Sonobuoy #2 was deployed at 0615z and operated satisfactorily. A definite, high velocity, refracted arrival was recorded on this buoy.

The principal observations from the MCS analogue moniter record are that a maximum of 0.8 sec. of flat-lying, layered sediments overlie a generally flat, but not smooth basement reflector. This basement reflector does not have the "ringing" character observed over DSDP Site 462 in the northern Nauru Basin. This combination of observations and the observation of sonobuoy refractions suggest that basement here is different from that at DSDP 462 (mid-Cretaceous volcanics at least 600 m deep). A more definitive conclusion between the possibilities of original sea floor spreading basement and mid-Cretaceous volcanic overprint will have to await a modeling analysis of the sonobuoy data.

A reflector at 0.48 sec. sub-bottom is probably mid Eocene chert (reflector "K" of Shipley, et al., 1993). A high-amplitude, flat reflector appears at about that depth between 0910z-1000z that may be a volcanic sill. It terminates abruptly at 0910z, reinforcing the sill interpretation.

SEISMIC LINE #401

The second seismic line, #401 was shot on a course heading of 260 degrees and extends over the crest of the Ontong Java Plateau. Only the eastern portion of that line, which extends over the Nauru Basin, is described here. The Nauru Basin is defined for the purpose of this report as the area of almost completely flat-lying sea floor lying below approximately 4,400 m and east of the Ontong Java Plateau. On line #401 this extends from 0330z/15 to 1230z/16. The first part of this profile, up to 0030z/16, is essentially coincident with and subparallel to magnetic lineation M17 (140-143 Ma). The intent of

this line was to cross the Charcot MCS line a second time in another area where original volcanic basement might be seismically visible and where Shipley et al. (1993) interpreted a cross-cutting reflector deep in the sedimentary section as a volcanic flow or sill (fig. 11, Shipley, et al., 1993). The crossing with the Charcot line was made at 1352z/15 and shot point #4698 on the Charcot line (see figures). Both crossings (lines 201 and 401) produced records that are very similar to the Charcot line at the crossing points. The 48-channel hydrophone streamer, 1-17 liter and 1-20 liter airguns were deployed for this portion of line #401.

Sonobuoys 3-13 were deployed regularly along this portion of line #401. Sonobuoy 3's antenna did not deploy, sonobuoy 4's cable was cut by the MCS hydrophone streamer, and sonobuoy 10's hydrophone failed. The other sonobuoys all operated satisfactorily. Sonobuoy 6 definitely recorded a refracted arrival and sonobuoy 5 probably did as well. No refractions were observed on the analogue moniter records of any of the other buoys.

The principal observations from the MCS analogue moniter record are the following. From 0330z/15 to 1000z/15 are 0.4-0.5 sec. of layered, gently undulating sediments overlying a basement reflector that has low amplitude bumps to the east and flattens westward. Due to the proximity to Nauru Island, this basement reflector is probably associated with the formation of that island and is not original sea floor spreading basement.

From 1000z/15 to 1600z/15 is a potential seismic window to the original Earliest Cretaceous basement created by sea floor spreading at M17 time. As much as 1.1 sec. of flat-lying and cross-cutting reflectors overlie a sometimes bumpy, sometimes flat but tilted basement reflector. The uppermost 0.5 sec. of sediments are flat-lying and probably post-middle-Eocene chert, probably carbonate turbidites from the Ontong Java Plateau and Nauru Island. Underlying these reflectors is a distorted, high amplitude reflector that Shipley et al. (1993) interpreted as middle-Eocene chert on the Charcot MCS profile. These reflectors and those beneath them onlap or are cut by a dipping (down to the south and east) reflector that Shipley et al. (1993) interpreted as a volcanic sill or flow, possibly from the Ontong Java Plateau eruption episode. Approximately the same onlap, cross-cutting relationships are present on both the Charcot and KH98-1 profiles. Sonobuoys 5 and 6 were collected over this sequence and the observation of refractions on at least one of those buoys may be significant and indicative of refractions from Earliest Cretaceous basement.

From 1600z/15 to 1230z/16 basement is generally observed as a series of "ringing" reflectors that are relatively flat-lying but discontinuous along the profile. These basement reflectors are almost certainly mid-Cretaceous basalts emplaced during or after the Ontong Java Plateau volcanic episode. Magnetic lineation M17 can be correlated west to 0030z/16 where it tails off into low-amplitude, non-diagnostic anomalies. The uppermost sediments are partially opaque (grey) but unlayered from 1600z/15 to 0100z/16 and more transparent to the west. These uppermost sediments thin from 0.4 sec. in the east to 0.2 sec. in the west and the transparent sediments onlap the opaque sediments at the boundary. These sediments give the subtle appearence of having been transported down Ontong Java Plateau from the west and preferentially accumulated in the area of partially opaque material. They are underlain by a flat-lying, high-amplitude reflector that is probably middle-Eocene chert and prehaps by some underlying Late Cretaceous volcaniclastics. Although sonobuoys 7-13 were deployed regularly along this portion of the profile, no refractions were observed on the analogue moniter records.

REFERENCES

Larson, R.L., 1976, Late Jurassic and Early Cretaceous evolution of the western Central Pacific Ocean. Jour. Geomag. and Geoelectric., 28: 219-236.

Nakanishi, M., Tamaki, K., and Kobayashi, K., 1992, Magnetic anomaly lineations from Late Jurassic to Early Cretaceous in the west-central Pacific Ocean. Geophys. Jour. Int., 109: 701-719.

Shipley, T.S., Abrams, L.J., Lancelot, Y., and Larson, R.L., 1993, Late Jurassic-Early Cretaceous oceanic crust and Early Cretaceous volcanic sequences in the Nauru Basin, western Pacific. In Pringle, M. et al., Eds., The Mesozoic Pacific: Geology, tectonics and volcanism, AGU Mono. 77, 103-119.

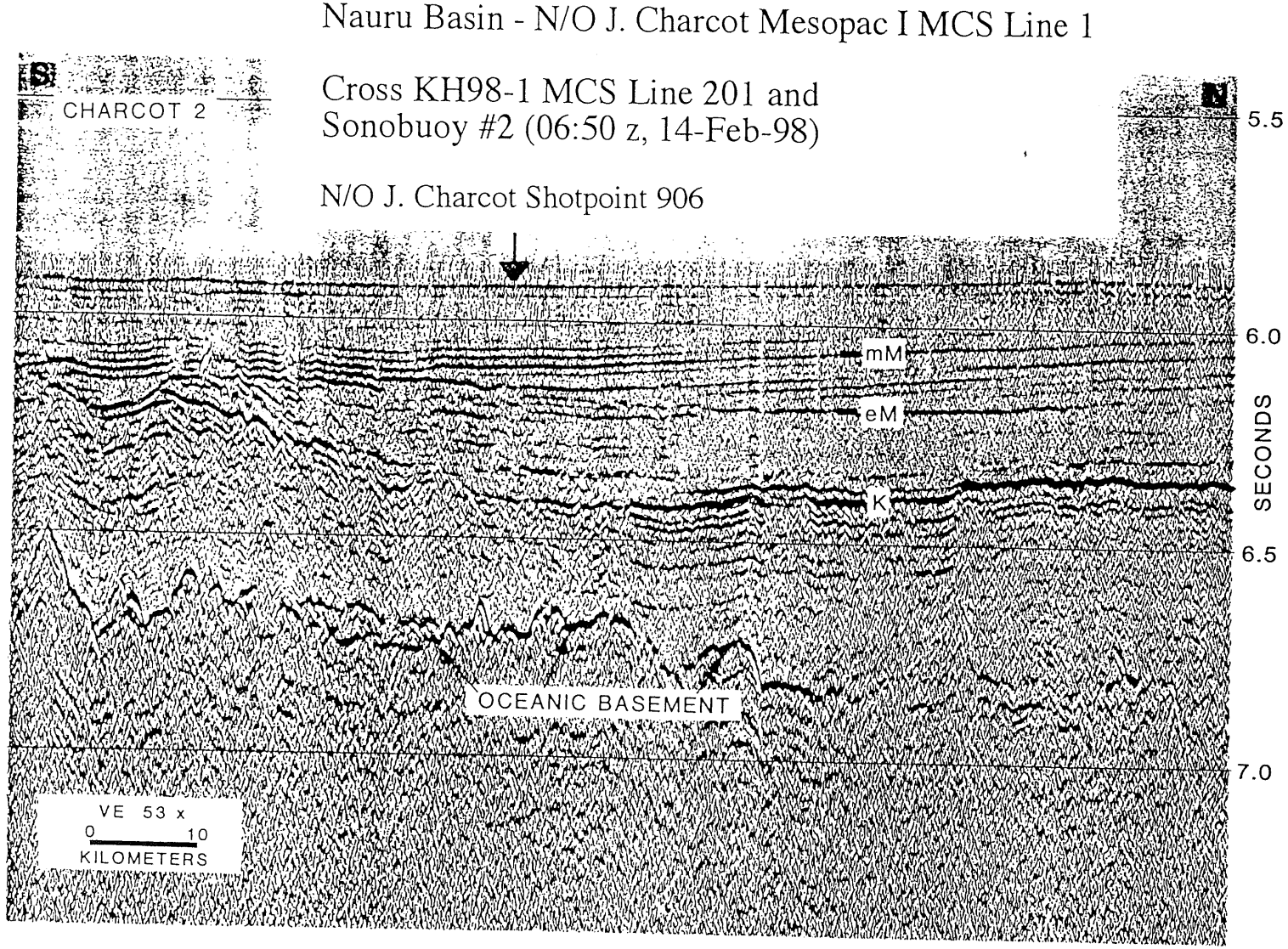

Fig. 8. Section at southernmost end of the *Charcot* line showing rough oceanic basement. Well-defined stratigraphy is evident between basement and the surface correlated with Cretaceous volcanics. The reduced reflectivity of K suggests that is not volcanic rock but a time-equivalent surface, perhaps volcanoclastic (?). Note downlap occurs onto the early Miocene surface. Processing information and the initial reports on this data are presented in Froger [1989; Froger and Lancelot, 1990]. The data were stacked 24-fold and subsequently deconvolved and filtered preserving original relative amplitude information that is important in identifying volcanics and cherts. Location is shown in Figure 2.

Shipley et al., 1993

A Study of the Crust and Upper-Mantle Structure of OJP using OBSs

* Kimihiro Mochizuki[1,2], Eiichiro Araki[1,2,3], Shinji Yoneshima[1,2] (ORI)
Masano Shinohara[2], Seiichi Miura[2], Yasuhira Aoyagi[2], Hiromasa Nishisaka[1], Manabu Mochida[1], Takashi Yoshizawa[1], Takeshi Sato[2] (Chiba University)
Minoru Nishino[2] (Tohoku University)

OBS types

Twenty-nine free-fall pop-up ocean bottom seismometers (OBSs) of six different types were collected from Tohoku University (THK), Chiba University (CHU), Earthquake Research Institute of the University of Tokyo (ERI), and Ocean Research Institute of the University of Tokyo (ORI): nine OBSs are from THK, 3 OBSs are from ERI, and the other 17 OBSs are assemblage of parts from CHU and ORI. There are two types of recorders equipped in the THK OBSs: hard-disk type and digital-audio-tape (DAT) type. Four hard-disk OBSs are equipped with four hard-disks in themselves, and the other five DAT OBSs have a digital audio tape (DAT) recorder. Their seismometer comprises 3 component velocity sensors mounted on gimbals whose characteristic frequency is 4.5 Hz. Three ERI OBSs are of the same type, and store data on a 2-Gbyte Magneto-Optical disk. They have 3 component 2 Hz velocity sensors mounted on gimbals. There are three types of ORI-CHU type OBSs. Although all of their data- storage medium is a DAT tape, seven of them are implemented with a data compression function whereas the other 10 recorders are without data-compression functionality. Two types of sensors are used for ORI-CHU OBSs: twelve OBSs have 4.5 Hz 3 component velocity sensors mounted on gimbals, and the other five OBSs have a 3 component broad band seismometer (PMD 2023). Detailed OBS specifications are summarized in Table 1 where OBS-to-station assignments are also shown.

ERI OBSs have a different outer shape, whereas THK and ORI-CHU OBSs look the same. A set of red-colored synthetic floats are attached to the yellow outer plastic sphere, which is placed on a base frame (See photographs on the next page).

---

* Numerical numbers on a shoulder of each author's name shows author's participating Leg numbers.

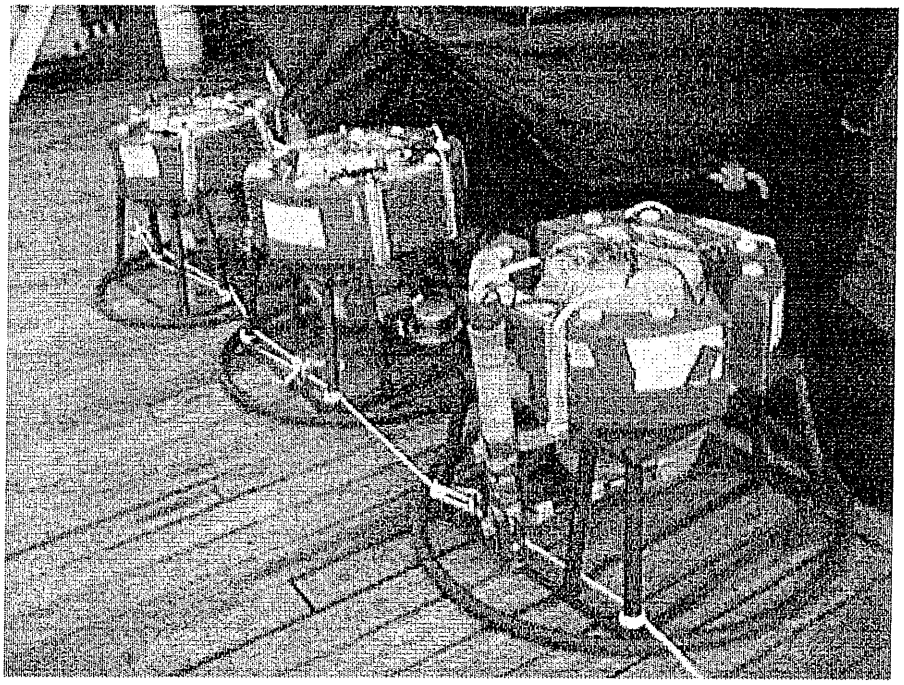

Figure 2 ERI OBS. A set of synthetic floats are attached to the yellow plastic outer shell, and it is placed on a metal frame.

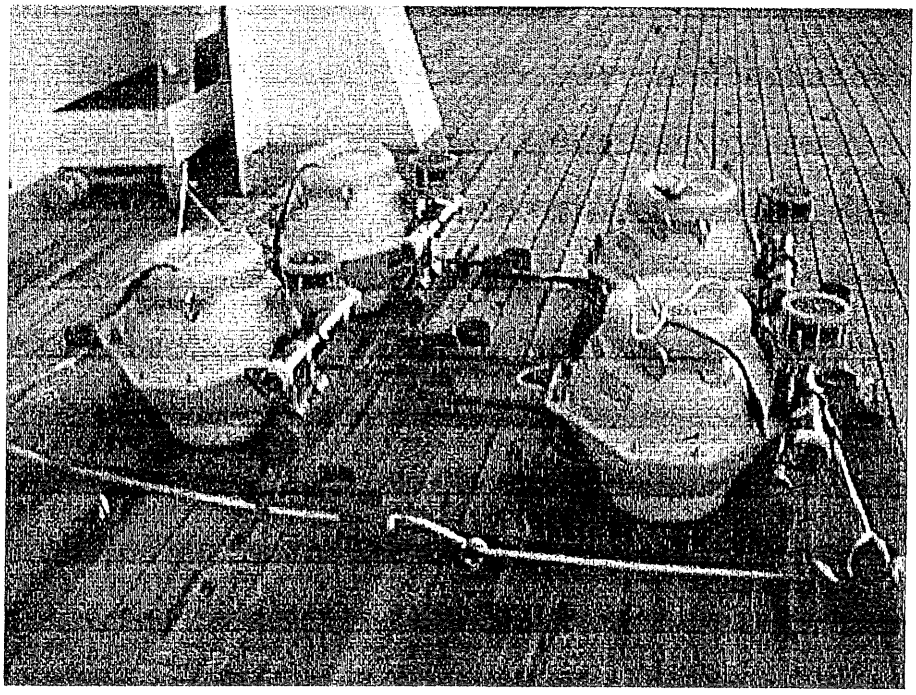

Figure 1 ORI-CHU and THK OBS

Study Objectives

Natural earthquake observation and a crustal structure experiment using newly developed Broad-Band type OBSs

A new type of OBS has been developed with a broad-band three-component sensor unit (PMD 2023) whose frequency band spans from 20 s to 20 Hz. Tiltmeter and thermometer units were also equipped in the OBS, and its data will be stored for the first approximately 20 minutes after the system starts recording.

A prototype of this broad-band OBS had been deployed off the Shikoku Island, Japan, for about a month in April through May, 1997, and continuously recorded both natural earthquakes and airgun shots. The recorded data were in good quality, and the waves generated by airgun shooting had sharp onsets and they were easily identified. However, because it was the first deployment and not enough knowledge had been accumulated by then, the amplifier gains were not suitably adjusted. The OBS system noise exceeded the seafloor ambient noise level at the frequencies higher than around 10 Hz.

We conducted preparatory observation at one of the very quiet earthquake observatories on land (Tsukuba Earthquake Observatory, Earthquake Research Institute, University of Tokyo) from late December, 1997, until early January, 1998, so as to gain information on sensor's characteristics and to determine amplifier's proper gain level. Three broad-band seismometers were deployed. We put a PMD 2023 sensor unit directly on a foundation which was isolated from the surrounding buildings. A Guralp CMG-3 three component sensor unit which was mounted in a glass sphere was covered with a plastic outer shell, and was placed on the foundation. Another PMD 2023 sensor unit was placed in a glass-sphere with batteries and a recorder, and the sphere was covered by a set of plastic hard shells in order to simulate the actual observation environment, and the whole system was placed on the same foundation. The data from those three sets of sensor units were compared, and the amplifier's gain level was determined.

Six of broad-band OBSs were deployed in Leg 1: one of them was deployed southwest of the East Mariana Basin, and the other five were deployed within the cross lines (see below the subsection, "Seismic experiment using OBSs and airgun sources").

Broad-band OBS observation southwest of the East Mariana Basin

One of the newly developed broad-band OBSs was deployed at the southwest tip of the East Mariana Basin (Station EMB). The station is surrounded by seismically active trenches and troughs so that it is expected to observe a large number of earthquakes from a wide range of back-azimuths. By analyzing waveforms of those earthquakes, heterogeneity of crustal and upper-mantle velocity structure of the surrounding area will be studied.

The crustal and upper-mantle structure of the surrounding area will be compared with that of the Ontong-Java Plateau, and their similarities and dissimilarities will be discussed.

The seafloor ambient noise will also be recorded, and a spectrum analysis will be applied. Comparison of the seafloor noise spectrum with that of the land stations recorded at Tsukuba Earthquake Observatory prior to the cruise will make possible a discussion on OBS's state of observation.

Seismic experiment on the Ontong-Java Plateau using OBSs and airgun sources

A topographic high is located in the northern part of the Ontong-Java Plateau. Its topographic feature suggests an arrival of the head of a mantle swell at the high. Geomorphological structure is fairly smooth, and laterally homogeneous velocity structure is expected beneath the plateau, which may be well represented by 1-D structure for the first approximation. Although not extensive gravity anomalies are associated with the topographic high, its variation ranges 30 mgals in the experiment region with the largest positive anomaly located at the center of the high.

Seventeen OBSs (station OJC 1 ~ 17) were planned to be deployed along a pair of cross lines on the northern gentle slope of the Ontong-Java Plateau. The southern end of the experiment lines is located at the topographic high mentioned above. Each line spans approximately 240 km. One of the line (EW line) is tangent to the bathymetric contour, and the other line (NS line) runs perpendicular to it. EW line is also aligned with the long range MCS experiment line scheduled in Leg 2. OBSs are expected to record large offset airgun shots, and it will help understand velocity variation along depth within the uppermantle beneath the Pacific Plate oceanic crust. By including MCS reflection data, the marginal structure of the Ontong-Java Plateau will be determined.

Each OBS is approximately 15 miles apart from one another (see Table 1 for exact locations). Five stations among the seventeen OBSs (the end point but one on both sides of each line, and the center) are the broad-band OBSs described in the

prior section. Four airguns with two 20-liter and two 17-liter chambers are planned to be used to generate seismic waves. The crustal thickness of the Ontong-Java Plateau was derived to be about 35 km by previous studies. With this experiment configuration, it is expected to derive a crustal structure model down to the Moho discontinuity. Fifty to eighty kilometer long Moho discontinuity will be resolved.

An OBS deployment of the southern end station failed because of an accident with a release hook by which the OBS was lifted. A detailed description of the accident will be included in a later section.

Observation of earthquake activity north of the Choiseul Island

A thrust fault was identified on a couple of 1995 Ewing lines. Three OBSs (station NC 1 ~ 3) will be deployed north of the Choiseul Island in order to detect probable micro-earthquake activity occurring along the thrust fault. Refer also to the report, "Cruise report on North Solomon trench survey, KH98-1-Leg 1" by Paul Mann et al.

Observation of earthquake activity south of the Bouginville Island

Six OBSs of THK type (station SB 1 ~ 6) were deployed south of the Bouginville Island, where extensive earthquake activity along the New Briton Trench from the west terminates to the east. As will be shown, the earthquake activity ranges from shallow depths to a depth around 500 km with various magnitues. Precise determination of those earthquakes will give a clear picture of the surface of the subducting slab.

Seafloor topography in the region was unexpectedly rough, and consisted of peaks, valleys and cliffs. It was required to give up the designed OBS locations, and better places were sought by observing the 3.5 kHz echo sounder.

Observation of natural earthquakes by a large array across the Ontong-Java Plateau

Two OBSs (station OJL 1 and 2) were deployed between the OJC and NC sites with an equal separation distance. OJL stations and NC site are aligned to the extension of NS line of the OJC site so that they construct a large OBS array across the Ontong-Java Plateau. By observing ray parameters of in-coming seismic waves, a velocity structure down to the upper mantle beneath the Ontong-Java Plateau will be obtained.

Extensive earthquake activity for a wide range of depths occur beneath the SB

site south of the Bouginville Island. Propagation paths of those earthquakes occurring at various depths to each OBS constituting the large array will vary through the crust and upper mantle. Derivation of velocity structure down to the upper mantle will be made possible by observing the earthquakes whose hypocentral locations are precisely determined by the SB stations.

As is mentioned, five OBSs among the OJC stations are broad band type and constructs a smaller array by themselves. A waveform analysis may also be applied to the data from those OBSs.